

**EVALUATION OF GRAPHENE OXIDE AND REDUCED
GRAPHENE OXIDE FOR THE REMOVAL OF SELECTED
HALOGENATED PHENOLS FROM WATER**

Thesis

Submitted in partial fulfilment of the requirement for the degree of

DOCTOR OF PHILOSOPHY

By

S. HEPSIBA NIRUBA CATHERINE

Reg.No.155106CV15F03



**DEPARTMENT OF CIVIL ENGINEERING
NATIONAL INSTITUTE OF TECHNOLOGY
KARNATAKA**

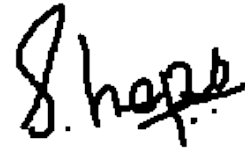
SURATHKAL, MANGALORE – 575025

June 2020

DECLARATION

By the Ph.D. Research Scholar

I hereby *declare* that the Research Thesis entitled “**EVALUATION OF GRAPHENE OXIDE AND REDUCED GRAPHENE OXIDE FOR THE REMOVAL OF SELECTED HALOGENATED PHENOLS FROM WATER**” which is being submitted to the *National Institute of Technology Karnataka, Surathkal* in the partial fulfilment of the requirement for the award of the Degree of **Doctor of Philosophy in Civil Engineering** is a *bonafide report of the research work carried out by me*. The materials contained in this Research Thesis has not been submitted to any other University or Institution for the award of any degree.



S. HEPSIBA NIRUBA CATHERINE

Register No: **155106CV15F03**

Department of Civil Engineering

Place: Mangalore

Date: 09.06.2020

CERTIFICATE

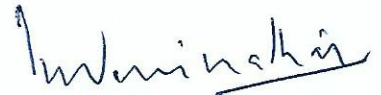
This is to certify that the Research Thesis entitled “**Evaluation of Graphene Oxide and Reduced Graphene Oxide for the Removal of Selected Halogenated Phenols from Water**” submitted by **S. HEPSIBA NIRUBA CATHERINE** (Register Number: **155106 CV15F03**) as the record of the research work carried out by her, is *accepted as the Research Thesis submission* in partial fulfilment of the requirements for the award of degree of *Doctor of Philosophy*.



(Dr. Basavaraju Manu)

Associate Professor and Research Guide

Department of Civil Engineering



Chairman- DRPC

Department of Civil Engineering

Chairman (DRPC)

Department of Civil Engineering
National Institute of Technology Karnataka, Surathkal
Mangalore - 575 025, Karnataka, INDIA

ACKNOWLEDGEMENT

I acknowledge my thanks to NITK, Surathkal for providing the fellowship and financial support necessary for the completion of my doctoral work.

I would like to express my deep sense of gratitude to my research supervisors, Dr. B. Manu, Associate Professor, Department of Civil Engineering, NITK, Surathkal for giving me an opportunity to pursue my research work under their valuable guidance. My sincere gratitude to my RPAC members, Dr. Hari Mahalingam, Department of Chemical Engineering and Dr. B.M Sunil Department of Civil Engineering, for their timely assessment and evaluation of my research progress. Their valuable inputs at all stages of my work have contributed immensely in giving the final shape to my research work.

I would to express my sincere thanks to Prof. Yang hsin Shih, National Taiwan university, Taiwan and Prof. Ruey-an Doong, National Tsing Hua University, Hsinchu Taiwan for their constant support, encouragement and through guidance throughout my experimental work at department of Agricultural chemistry and their kind help in providing the facilities.

I thank the present Head of the Department, Prof. Swaminadhan and former Heads of the Department, Varghese George, K. N. Lokesh, and Prof. Reddy for providing the necessary facilities. I am also thankful to Prof. Shrihari, Dr. Devatha C.P, Dr. Arun Kumar Thalla for their constant moral support and encouragement. I extend my heartfelt gratitude to all the staff members of the Department of Civil Engineering, NITK.

My Special Thanks to Mr. Manohar Shanbhogue and Mr. Shresta Kumar for all the direct and indirect help offered time and again. It would not have been the same without your support. I am grateful to all non-teaching staff of Department of Civil Engineering, inclusive of the lab staff for their timely co-operation and constant support.

I truly appreciate the all-inclusive support extended by my friends Sangeetha, Padmapriya, Dr. Arun Kumar, Dr. Sanjeev Sangami, Dr. Reka Rao, Bhaskar, Mahesh, Ms. Uma, Pavithra, Poojitha, Loshini, Lillian and all others for giving me fun filled, cherishable memories and for being there through all thick and thin.

I would like to express my sincere thanks to my brother Kirubanidhi Jebabalan, Research scholar, Coimbatore Institute of Technology, Coimbatore, for his selfless advice and support to join as a research scholar in NITK and support throughout my life. I would also like to thank my husband Shanmugam. M Research Scholar National Tsing Hua University, Hsinchu Taiwan for his encouragement and continuous support during my research especially during my stay in Taiwan.

I would like to thank God for giving me the strength, knowledge, ability and opportunity to undertake this research study and to persevere and complete it satisfactorily.

Last but not least, I would like to thank my father Mr. T. Sundararajan and mother Mrs. S. Rajeswari for their massive love and support throughout my life. Without them, achieving this goal would not have been possible.

Finally, I extend my gratitude to all those who have contributed directly or indirectly towards the completion of this work.

Thank you.

Hepsiba Niruba Catherine.S

ABSTRACT

Carbon-based materials especially graphene nanocomposites (GNS) have attracted wide attention in recent years. In this study, graphene oxide (GO) and reduced graphene oxide (rGO) were prepared by Improved Hummers method having high suspension stability in water. Both GO and rGO were investigated for the adsorption of halogenated compounds from water, its stability at the GNS-water interface and its effective application in the debromination of brominated flame retardant. Emerging contaminants (ECs) are compounds of emerging concern that are of raising concern in the past 20 years. ECs such as bisphenol A (BPA), 4-nonylphenol (4-NP) and tetrabromobisphenol A (TBBPA) pose threat to both humans and the ecosystem. GNS including GO and rGO are also considered as EC due to its potential hazard. The adsorption of organic contaminants such as the phenolic ECs on GNS affects the stability at the GNS-water interface and the fate of organic contaminants, thus causing further environmental risk. Various spectroscopic tools such as SEM, TEM, XRD, Raman, FTIR, and XPS were used to characterize the nanomaterial synthesized. The obtained results confirmed that the size of GO and rGO were with a surface area of 2.02 and 227.32 m²/g. The XRD analysis shows that the values of diffraction peak 2θ were 10.01 and 26.09 confining to the synthesized GO and rGO. Later both GO and rGO were used to study the adsorption behaviour of some ECs and common phenolic compounds that include 4-chlorophenol, 2,4-dichlorophenol, 2,4,6-trichlorophenol and phenol considering its stability in water interface were studied. The adsorption capacity of GNS with phenol, TBBPA, and BPA was examined for its thermodynamic equilibrium at different temperatures. The adsorption equilibrium was reached less than 10 h and was fitted using both Langmuir and Freundlich isotherms. The kinetics and isotherms models of the sorption of aromatic compounds on GNS were investigated at ambient conditions. It was also demonstrated that GO and rGO that varied in C/O ratio is identified as an efficient approach for debromination of TBBPA. A pathway of TBBPA, tri-BBPA, di-BBPA, mono-BBPA, and BPA was thus proposed for TBBPA degradation. Debromination was observed by using metal-free carbon-based nanomaterial. The structural defects of GBMs, act as active sites responsible for catalytic performance. Furthermore, ESR analysis provided insights into the evolution of reactive oxygen species (ROS) such as superoxide radical (O⁻²·) and singlet oxygen (¹O₂) during the debromination

process. Therefore, these active species were identified to be the primary radicals generated onto the surface of GBMs, which results in the formation of less brominated BPA. Finally, reuse of the adsorbents for all the pollutants were investigated, and we observed that adsorbent reusability was >93% of its activity up to 5 cycles. These novel findings unveil the crucial role of oxygen functional groups on GBMs surface for the catalytic degradation of TBBPA. These findings emphasize that when carbon-based materials are used for sorption studies of halogenated compounds more attention should be considered on estimating the adsorption capacity in addition to the degradation.

KEYWORDS: Emerging contaminants, graphene oxide, reduced graphene oxide, adsorption mechanism, electrostatic attraction, hydrogen-bonding, stability, debromination

TABLE OF CONTENTS

CONTENTS	i
LIST OF FIGURES	iv
LIST OF TABLES	vi
NOMENCLATURE	vii
CHAPTER 1	1
INTRODUCTION	1
1.1 Introduction and Motivation.....	1
1.2 Primary Objectives	4
1.3 Organization of Thesis	4
CHAPTER 2	6
LITERATURE REVIEW	6
2.1 Engineered Nanomaterial's (ENM).....	6
2.2 Graphene-Based Nanomaterials (GNS).....	7
2.3 Emerging Contaminants (ECs).....	9
2.4 Stability of Graphene-Based Materials.....	10
2.5 Adsorbents for Removal of Emerging Contaminants.....	13
2.5. 1 Carbon nanotubes (CNTs).....	13
2.5.2 Graphene	14
2.6 Adsorption Mechanism	15
2.7 Debromination of TBBPA.....	17
2.8 Risk of Environmental nanomaterials(ENM) and its applications in water treatments	19
2.9 Summary of Literature	19
2.10 Scope of Study.....	20
CHAPTER 3	22
METHODOLOGY	22
3.1 General	22

3.2 Materials.....	23
3.3 Characterization of Graphene Oxide.....	23
3.3.1 Fourier Transform Infrared Spectroscopy (FTIR).....	23
3.3.2 X-Ray Diffraction (XRD).....	24
3.3.3 X-ray Photoelectron Spectroscopy (XPS).....	24
3.3.4 Identification of Bromide Ion.....	24
3.4 Synthesis of Graphene Oxide (GO) and Reduced Graphene oxide (rGO).....	25
3.5 Experimental Methodology.....	26
3.5.1 Adsorption experiments.....	26
3.5.2 Thermodynamic Studies.....	28
3.5.3 Debromination and regeneration experiments.....	28
3.5.4 Data Analysis.....	30
CHAPTER 4.....	32
RESULTS AND DISCUSSION.....	32
4.1 General.....	32
4.2 Interaction of Graphene nanoflakes with emerging contaminants and some common phenolic compounds in a water matrix.....	32
4.2.1 Characterization of Graphene nanoflakes.....	32
4.2.2 Kinetics of phenolic contaminants on graphene oxide.....	35
4.2.3 Adsorption isotherms of phenolic compounds onto graphene oxide.....	36
4.2.4 Adsorption mechanism of phenolic compounds onto graphene oxide.....	39
4.3 Reactivity of Graphene Oxide and Reduced Graphene Oxide toward Tetrabromobisphenol A, Bisphenol A, and Phenol from Water.....	43
4.3.1 Characterization of GNS.....	43
4.3.1 Adsorption kinetics of TBBPA, BPA, and phenol on GNS.....	45
4.3.2 Adsorption isotherms of TBBPA, BPA, and phenol on GNS.....	46
4.3.3 Effect of temperature on adsorption isotherms.....	47
4.3.4 Possible Adsorption mechanism.....	51
4.4 Investigate the debromination of TBBPA by graphene-based materials.....	52
4.4.1 Removal of TBBPA by GO and rGO.....	52
4.4.2 Products and pathways of TBBPA transformation by GO and rGO.....	56
4.4.3 Time dependent quantification of by-products.....	58
4.4.4 Plausible mechanism for the debromination activity.....	60

4.4.5 Reusability of recycled GBMs nanoparticles	64
CHAPTER 5	66
SUMMARY AND CONCLUSIONS	66
5.1 Summary	66
5.2 Conclusions	66
5.2.1 Interaction of GO NPs with emerging contaminants and some common phenolic compounds in a water matrix	66
5.2.2 The reactivity of Graphene Oxide and Reduced Graphene Oxide toward Tetrabromobisphenol A, Bisphenol A, and Phenol from Water.	67
5.2.3 Investigate the debromination of TBBPA by graphene-based materials.....	68
5.3 Scope for Future Research.....	69
REFERENCES.....	70
APPENDIX.....	78
PUBLICATIONS BASED ON PRESENT WORK	83
RESUME.....	85

LIST OF FIGURES

Figure.NO	PG.NO
1.1 Removal of Emerging contaminants using GNS	3
2. 1: General applications of nanomaterials.....	7
2. 2: Different types of carbonaceous materials.....	8
2. 3: Structure of graphite, graphene oxide (GO) and reduced graphene oxide (rGO).....	9
2. 4: Various sources for the release of emerging contaminants into the environment.....	10
2. 5: The stability of GNS in aqueous solution.....	13
3. 1: Synthesis of GO and rGO.....	26
3.2 Schematic of work performed.....	29
4. 1: (a) SEM and (b) TEM of GO. (c) XRD, (d) FTIR, and (e) Raman spectra of graphite and GO (f) carbon (C1s) peaks of GO and Oxygen(O1s) peaks (g) Zeta potential of GO samples as a function of pH (h) Sedimentation curve after adsorption of BPA on GO, insert a photograph of aqueous dispersion of GO.	34
4. 2: (a) Adsorption kinetics of 4-chlorophenol, 2,4-dichlorophenol, 2,4,6-trichlorophenol (b) phenol, BPA, 4-nonylphenol and TBBPA on GO.....	35
4. 3: Adsorption isotherms of (a) 4-CP, (b) 2,4-DCP, (c) 2,4,6-TCP, (d) phenol, (e) 4-NP (f) BPA and (g) TBBPA on GO. The dotted line represents the Freundlich model and the dashed line represents the Langmuir model	38
4. 4: FTIR spectra after adsorption of (a) 4-Chlorophenol, 2,4-dichlorophenol and 2,4,6-trichlorophenol and (b) bisphenol-A, phenol, TBBPA and 4-nonylphenol on GO.....	40
4. 5: (a) The effect of pH on adsorption isotherms of 2,4,6-TCP (b) The effect of pH on adsorption isotherms of TBBPA on GO.....	42
4. 6: (a) SEM and (b) TEM of rGO. (c) SEM and (d) TEM of GO.....	44
4. 7: (a) XRD of graphite, rGO and GO, (b) FTIR, (c) Raman spectra and (d) Zeta potentials of GO and rGO	44
4. 8: (a) Adsorption kinetics of phenol, BPA and TBBPA on GO and (b) that of phenol, BPA and TBBPA on rGO.....	46

4. 9: Adsorption isotherms of (a) phenol, (b) BPA (c) TBBPA on GO and (d) phenol, (e) BPA, (f) TBBPA on rGO under different temperature conditions.....	47
4. 10: Plots of $\ln K$ versus $1/T$ for adsorption of (a) phenol, (b) BPA and (c) TBBPA on GO and rGO.....	50
4. 11: Adsorption kinetics of TBBPA on rGO and GO.....	52
4. 12: Adsorption isotherms of TBBPA on (a) GO and (b) rGO under different temperature conditions	54
4. 13: (a) HPLC analysis of the appearance of TBBPA its intermediate products and the final product (b) Proposed primary debromination pathway of TBBPA using GO and rGO.....	57
4. 14: TBBPA degradation (a) using graphite, GO and rGO and intermediates m/z profile from LC-MS (b) Mono-BBPA (c) Di-BBPA, and (d) Tri-BBPA.	59
4. 15: (a) Time-dependent profile of TBBPA degradation and (b) evolution of bromide ion concentration, at pH 5.5, GO and (c) and (d) for rGO, dose 15 ppm, 10 ppm TBBPA	61
4. 16: ESR signal using DMPO as a spin duct for (a) rGO, (b) GO; FFA analysis with time for (c) GBMs; Total phenols concentration for (d) GBMs.....	63
4. 17: Degradation and adsorption of TBBPA reacted with (a) GO and (b) rGO	64
4. 18: Cycling experiments with recycled graphene based nanoparticles.	65

LIST OF TABLES

Table NO	PG.NO
2. 1: Adsorption of Emerging contaminants using Graphene based materials.....	16
2. 2: Debromination of TBBPA using metal based nanomaterials.....	18
3.1: Molecular structure and chemical properties of phenolic compounds.....	22
3.2 Reaction conditions for the removal of emerging contaminants using GBMs.....	27
3.3: HPLC Conditions of phenolic compounds.....	28
4. 1: kinetics constant for adsorption of PCs on GO.....	36
4. 2: Isotherm constants for adsorption of PCs on GO.....	37
4.3: Selected physicochemical properties of carbonaceous materials.....	45
4.4: Isotherm constants for adsorption of phenol, BPA and TBBPA on GNS.....	49
4.5: Adsorption thermodynamic parameters for phenol, BPA and TBBPA on rGO and GO...50	
4.6: Kinetics constant for adsorption of TBBPA on rGO and GO.....	53
4.7: Isotherm constants for adsorption of TBBPA on rGO and Rgo.....	55
4.8: Adsorption thermodynamic parameters for TBBPA on rGO and GO.....	56
4. 9: Distribution of the intermediates and the final products at a reaction time of 240min...58	

NOMENCLATURE

Emerging contaminants	ECs
Graphene oxide	GO
Reduced graphene oxide Graphene	rGO
Graphene nanomaterials	GNs
Tetrabromobisphenol A	TBBPA
Tri-bromobisphenol A	Tri-BBPA
Di-bromobisphenol A	Di-BBPA
Mono-bromobisphenol A	Mono-BBPA
Bisphenol A	BPA
4-nonylphenol	4-NP
4-cholorophenol	4-CP
2,4-dicholorophenol	2,4-DCP
2,4,6-tricholorophenol	2,4,6-TCP
Adsorption capacity	qe
Equilibrium concentration	Ce
Electron donor acceptor	EDA
Pi-pi	$\pi - \pi$
Dissociation constant	pKa
Fourier Transform Infrared Spectroscopy	FTIR

X-ray Photoelectron Spectroscopy	XPS
X-Ray Diffraction	XRD
High Performance Liquid Chromatography	HPLC
Gas Chromatography Mass Spectrometry	GCMS
Octanol-water Partition Coefficient	K _{ow}
Coefficient of Determination	R ²
Specific Surface Area	SSA

CHAPTER 1

INTRODUCTION

1.1 Introduction and Motivation

Water is the most important component for all living beings on the planet. Emerging contaminants (ECs) are found in surface water, groundwater, drinking water, and water treatment plant discharge (Gogoi et al., 2018; Terzić et al., 2008). They are persistent in the environment ranging from mg/L to ng/L pose a severe risk to human health and ecosystem (Kozlov et al., 2012; Ratola et al., 2012). In surface water both organic and inorganic contaminants are regulated by the legislation defined by the European Commission (European Commission, 2008), mostly targeting the industrial and agricultural chemicals. Later in 2012, the legislation broadened to incorporate a greater number of chemicals including some ECs (European Commission, 2012). Recent studies on wastewater have gained attention towards the occurrence of newly identified compounds, the presence of ECs in the environment is mainly due to the discharge from the treated wastewater (Richardson et al., 2018). ECs are a new class of identified compounds that have been investigated in the past 20 years, mainly contain pharmaceuticals, surfactants, flame retardants, hormones, and engineered nanomaterials, which are widely detected in many environmental media due to rapid industrialization and urbanization. These compounds raise public concerns as they are toxic, have no regulatory standards and also inflict long-lasting effects on humans and the environment (Zhu et al., 2017). These chemicals present in the environment are of more concern as they do not appear individually but mostly as a complex leading to a synergistic effect (Jackson et al., 2013). Various ECs have been detected in water supplies that have adverse effects on humans, leading to long term stability in drinking water supplies. Their harmful effect on both humans and the aquatic system is an issue of concern among scientists and the general public.

Nanomaterials are considered to be on the cutting edge of material science research and have applied in various fields including life science, energy, environmental applications, and used in our everyday life. Due to the rapid development of nanotechnology,

nanoscale carbon-based materials such as graphene have increased the attention among worldwide (Ramesha et al., 2011). Natural carbon-based nanoparticles occur in negligible quantities than the artificially synthesized. It is estimated that the worldwide production of metal oxide and carbon nanotubes (CNTs) to be between 100 and 1000t/year. Nanoparticles are used in various fields in electronics, computers, and more than 1800 consumer products. The estimated increase in the global market for graphene-based products is projected to increase by around 51.7% in five years.

Graphene nanomaterials (GNS) has gained recent attention among researchers, due to its significant electronic, mechanical and chemical properties. The large scale usage and production of GNS have unavoidably lead to the release into the environment, posing a potential threat to health and also increasing the possible interaction with the contaminants at the GNS-water interface is crucial to evaluate its impact in the environment (Chowdhury et al., 2015b; Johra et al., 2014). Graphene nanomaterials (GNS) and their derivate reveal excellent performance in the environmental contaminant removal of dyes, organic, inorganic pollutants and heavy metal, due to the large theoretical surface area, fast electron transfer and the presence of functional group (Jiang et al., 2018; Wu et al., 2014; Yang et al., 2011). Graphene oxide (GO) and its reduced form (rGO), important classification of GNS has the potential in elimination of organic compounds containing benzene ring due to strong interaction with π - π system, high affinity of PAHs to graphene material was also dominated by π - π stacking (Chowdhury et al. 2015; Wang et al. 2014a). GNS a derivative of graphite that contains oxygen-bearing functional groups embedded at the edges within the carbon layer for GO, and the reduced form(rGO) the absence of oxygen-carrying functional groups and high surface area make a promising tool for adsorption (Bustos-ramirez et al., 2015; Zhao et al., 2011).

GNS can suspend well in water and hence form colloidal suspension due to the electrostatic repulsion originating by the presence of carboxylic and hydroxyl groups on the GO sheets, necessitating to examine the colloidal stability and its environmental transport to evaluate its fate and health risk (Li et al., 2009). Once GO releases into the environment, their adsorption of organic contaminants further influences the fate and transport of both, which could enhance the mobility of adsorbed ECs on GO

nanomaterials causing an environmental risk, leading for its evaluation in the aquatic environment. The structure and properties of ECs such as the pKa, aromatic ring substitution, and solubility will affect its interaction with GO surface. Therefore, the adsorption of organic compounds by GO nanoflakes is required to understand the fate of these organic pollutants in water.

In the present study, we aim to examine the adsorption of ECs on GNS we synthesized in water and the adsorption mechanism. Some common phenolic contaminants were chosen to compare their adsorption behaviors. Phenol, 4-chlorophenol (4-CP), 2,4-dichlorophenol (2, 4-DCP), 2,4,6-trichlorophenol (2,4,6-TCP), bisphenol A(BPA), 4-nonylphenol (4-NP), and tetrabromobisphenol (TBBPA) were chosen as adsorbates to study their interaction mechanism on GNS. Debromination was observed during the adsorption of TBBPA on GNS due to the formation of additional peaks. Interaction of TBBPA with GO and rGO was examined using batch experiments, surface properties, and reaction mechanisms. The reaction products were identified as the by-products of TBBPA. Figure 1.1 shows the interaction of GNS with emerging contaminants and the stability in aqueous solution.

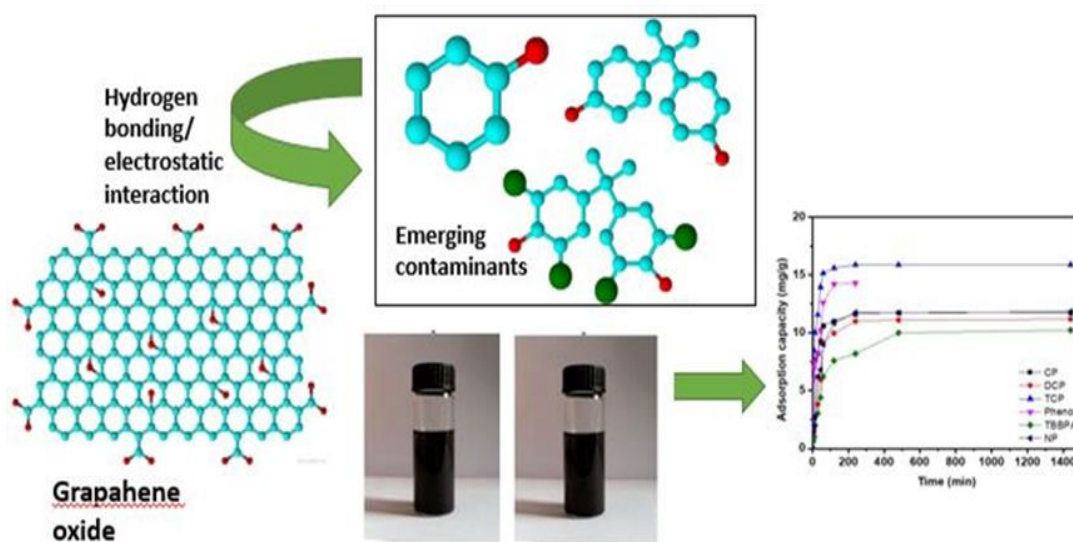


Figure 1. 1 Removal of Emerging contaminants using GNS

1.2 Primary Objectives

- To study the interaction of GO NPs with emerging contaminants and some common phenolic compounds in a water matrix.
- To study the reactivity of Graphene Oxide and Reduced Graphene Oxide toward Tetrabromobisphenol A, Bisphenol A, and Phenol from Water.
- To investigate the debromination of TBBPA by graphene-based materials

1.3 Organization of Thesis

The thesis consists of five chapters the details are listed below

Chapter 1

This chapter provides the introduction to emerging contaminants, their effects on the environment and the treatment techniques such as conventional and advanced treatment methods, significance, and objective of the research.

Chapter 2

It gathers information about research work conducted recently for the removal treatment especially adsorption of ECs (bisphenol A, nonylphenol and tetrabromobisphenol A) various nanomaterials used as adsorbents, the stability of nanomaterials (graphene oxide and reduced graphene oxide) in the environment and degradation techniques (metal-based) employed for complete degradation of tetrabromobisphenol A are discussed in detail.

Chapter 3

It gives details about the sampling, materials, experimental methodology, analytical techniques, and tools used for the characterization of nanomaterials.

Chapter 4

This chapter deals with the results and discussion on the adsorption of phenolic compounds on graphene oxide (GO), surface interaction of graphene oxide and reduced graphene oxide on phenol, bisphenol A and tetrabromobisphenol A and debromination

of tetrabromobisphenol A by graphene-based nanomaterials and its reusability for 5 cycles.

Chapter 5

It gives information about the summary of the present study, conclusions drawn based on the experimental results. The recommendations and scope for future work were also presented.

CHAPTER 2

LITERATURE REVIEW

Literature review on the classification of engineered nanomaterials (ENMs), emerging contaminants its stability in aqueous solution, various treatment technologies used for the removal of the emerging contaminants and its ability for debromination of flame retardants are discussed in detail in this section.

2.1 Engineered Nanomaterial's (ENM)

Nanomaterials are particles that ENMs are manufactured particles with one dimension to be below (100nm) or even lesser. They have various shapes and can be either single, aggregated, spherical or even irregular. ENMs are described to be the emerging class of contaminants that poses a risk to both human health and the environment. They are directly released in the environment during their manufacture and disposal (Kumar et al., 2014). They are classified as

- Fullerenes (carbon nanotubes and graphene)
- Metal ENM (e.g. elemental Ag, Au)
- Oxides (TiO₂, Fe-oxides)
- Complex compound
- Quantum dots

ENMs are likely to become hazardous in the near future that will affect the human health and the environment, currently, there is a lot of attention paid to its effect on human health but very few data on its release into the environment and the effects. The risk of this substance is determined on its release and exposure and the knowledge about its environmental exposure is not fully understood. Figure 2.1 shows the wide range of applications of nanomaterials. The recent development in the wide range of engineering applications and commercial products have led to the widespread emergence of NPs, this nanoscale material was produced decades back, but its application in the industries started in the recent years.

The unique properties of nanomaterials are due to the nanoscale dimension leading to its usage as a novel technology and also increase the usage of existing processes (Perreault et al., 2015a, 2015b). These materials possess multiple applications in water treatment, energy production, and contaminant sensing, this widespread use of this material will lead to its discharge into the environmental compartments (air, soil, and water) triggering the increased interest in this study.

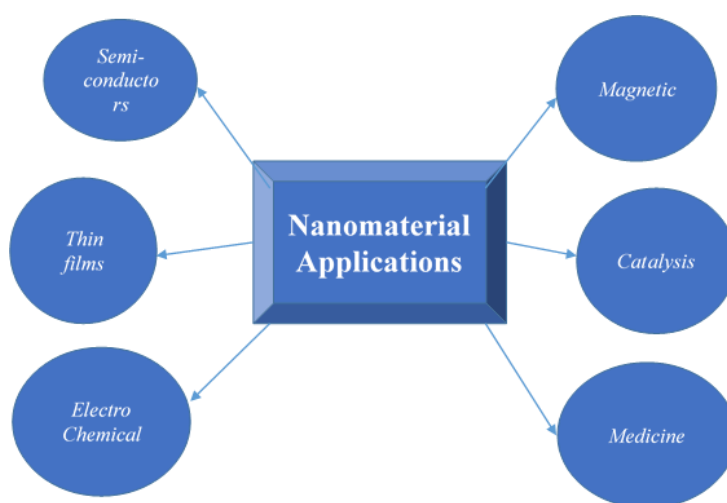


Figure2. 1:General applications of nanomaterials

2.2 Graphene-Based Nanomaterials (GNS)

Graphene-based nanomaterials (GNs) consist of four forms that include graphene, graphene oxide (oxidized form), reduced graphene oxide (reduced form) and graphene-quantum dots (size less than 20nm) (Ghosal et al., 2018). The various types of carbonaceous materials are shown in Fig. 2.2. Among the various GNS being used GO and rGO are considered as novel material, has gained recent attention among researchers due to its unique physicochemical properties that include high surface area, thermal, electrical mobility and mechanical strength leading to the extensive use in various fields of nanotechnology (Bhagobaty et al., 2007). In the field of environment, these materials are used as an adsorbent, photocatalysis (Li et al., 2009) for environmental decontamination and electrode for contaminant removal (Wang et al., 2011).

Graphene is a two- dimensional monolayer made up of a single layer of carbon atoms of sp^2 bonding arranged in a hexagonal structure, it's flexible, clear and extremely thin.

Being highly resistant and a good conductor of electricity makes it a promising tool for a number of uses especially in the field of electronics. Graphene an allotrope of carbon in its pristine form is composed of carbon atoms of sp^2 bonded aromatic structure. The defects, wrinkles, and the flat structure covered with pi rings of the graphene nanosheet aid in faster adsorption of pollutants. It's a two-dimensional atomic layer single layer of graphene is obtained by the exfoliation.

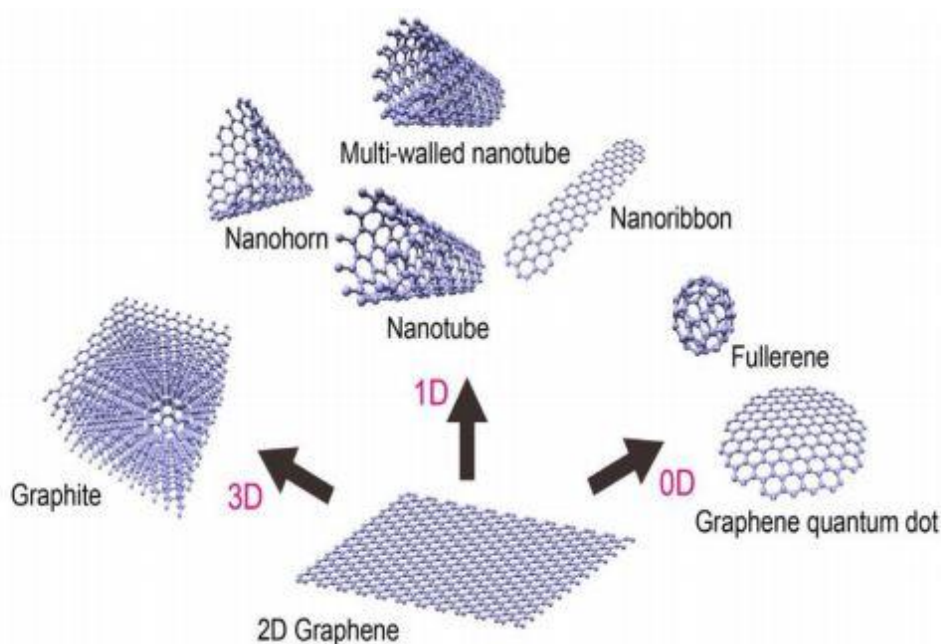


Figure2. 2: Different types of carbonaceous materials (Liao et al. 2018)

Graphene oxide (GO) a new class of carbon-based nanomaterial consisting of monolayered sheets of graphene, honeycomb in a structure that has oxygen consisting of groups like carbonyl, carboxyl, epoxide and hydroxyl (Lanphere et al., 2013). These oxygen-containing groups that include epoxy and hydroxide that acts as an anchoring site for various active species making the properties of GO more interesting and fascinating. GO is highly hydrophilic in nature and can be easily dispersed in many solvents by sonication. These excellent properties of GO increase its usage in various fields that include sensors, energy storage, biomedicine and catalysis (Sotirelis, 2016). Graphene oxide nanoparticles (GONPs) are oxidized form of graphene at the nanometer scale has also gained a lot of importance due to its wide range of mechanical and electrical properties.

The reduced form of graphene oxide (rGO) is synthesized by the use of chemical agents, thermal annealing, photoreduction or microwave assistance, GO reduction results in residual oxygen content, carbon vacancies, and clustered pentagons, heptagons carbon clusters (Meyer et al., 2010). The performance of graphene-based nanomaterial depends largely on the synergistic interaction of the properties of graphene and reduced form and also the metals attached to the graphene. Figure 2.3. shows the variation in the structure of graphene-family due to oxidation and reduction for the synthesis of GO and rGO.

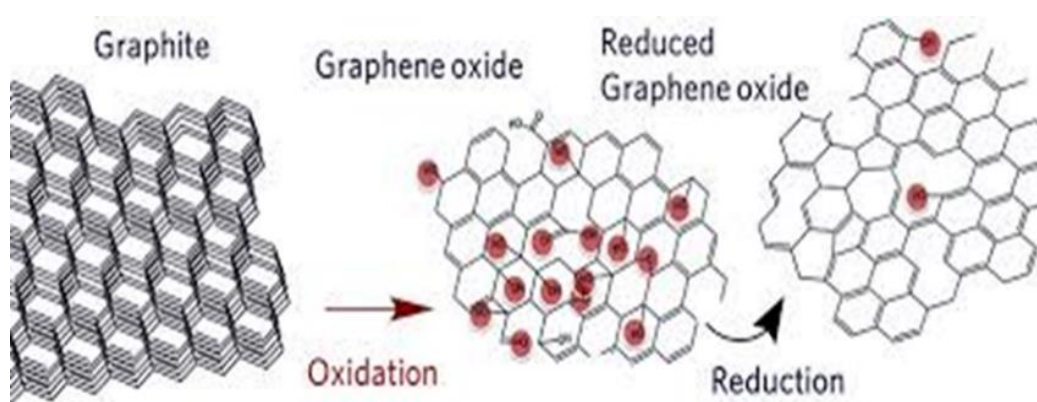


Figure2. 3: Structure of graphite, graphene oxide (GO) and reduced graphene oxide (rGO) (Khairir et al., 2015).

2.3 Emerging Contaminants (ECs)

Water is considered to be the most essential substance for human civilization, access to clean and affordable water remains to be a global challenge in this century. Water availability in recent years is threatened due to the increase in the release of anthropogenic pollutants from the industrial and non- industrial sectors. Annual report of UN estimated about 1500 km³ of wastewater to be generated on an average (UNESCO 2003). Emerging contaminants (ECs) are a new class of pollutants with increasing concern, found in environmental media due to an increase in urbanization and industrialization. The contaminants originate from various sources whose concentration ranges from ng/L to µg/L mainly dominated by pesticides, pharmaceuticals, and personal care products, hormones, food additives, and nanomaterials (Zhao et al., 2014). They are unregulated substances mostly occurring naturally or synthetically causing a suspected hazard to the surrounding and human

health (Petrie et al. 2015). EC's are generally found in industrial and municipal wastewater treatment plants cannot be easily remediated through conventional treatment technologies henceforth the requirement for newer technologies are on raise (Rivera-utrilla et al., 2013), Figure 2.4 shows the source of ECs in the environment and how they reach the water system through man-made activities.

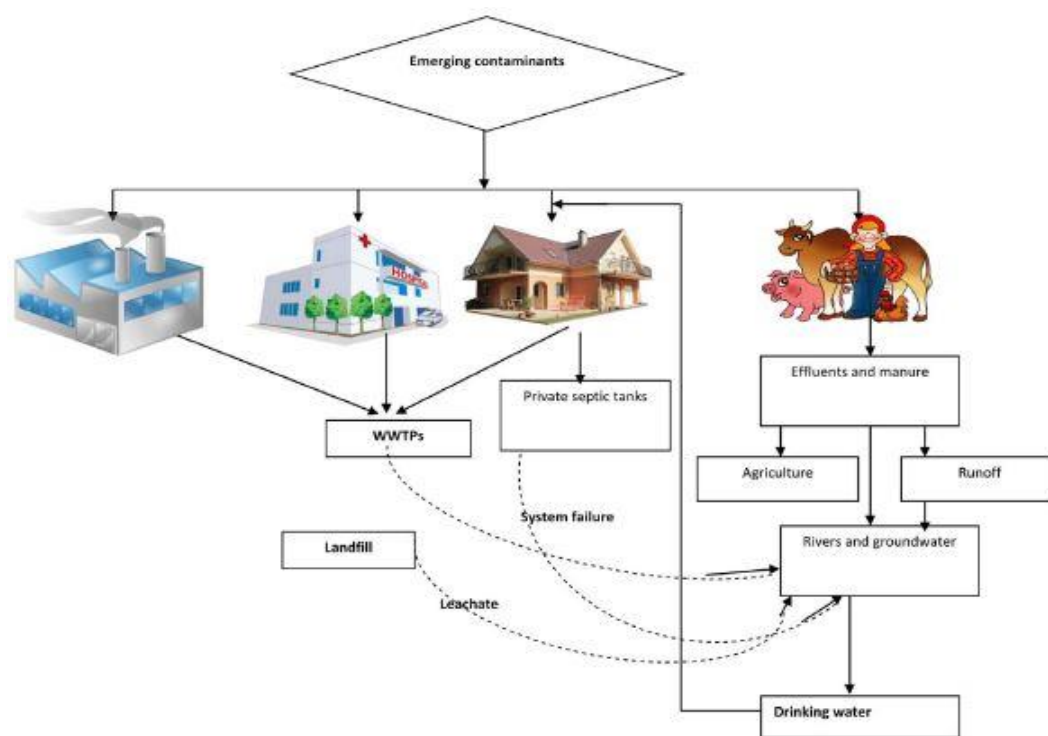


Figure2. 4: Various sources for the release of emerging contaminants into the environment

The recent advances in nanotechnology have led to the new-generation treatment process. Nanomaterials especially GNS possess great potential in the removal of ECs in lab scale studies due to high specific surface area and reactive sites. Adsorption and photocatalysis are effective treatment for the removals of ECs from water (Qu et al. 2013).

2.4 Stability of Graphene-Based Materials

The usage of graphene-based materials is on increases which will lead to the release of GNS in an aqueous environment. Recent studies on the global life cycle release of engineered nanoparticles into water are around 0.7% to 4%, and maximum release(80%) of SNPs was into the landfills causing a threat to water environment

(Keller et al. 2013). GO contains O-functionalities such as carboxyl, carbonyl, hydroxyl, and phenol groups (Gao et al., 2009; Lo et al., 2008). These functional groups evidently increase the hydrophilicity of GO, making it easily dispersible in aqueous solution and stable under common environmental conditions.

Ye et al. (2018) investigated the aggregation and stability of graphene nanoplatelets, graphene oxide, and reduced graphene oxide, under various parameters like pH, divalent ions and dissolved organic carbon for 21 days. They found that pH ranging from 6 to 9, divalent ions both Ca^{2+} and Mg^{2+} of concentrations 2.5 to 10 mM and DOC ranging from 0.5 to 2.5 mg/L significantly affected the dispersion stability in aqueous media. These results underlie the interaction of environmental factors with GNS surface thus affecting the stability (Ye et al., 2018).

Wide range of phenolic compounds and its interaction with graphene oxide and its stability in aqueous solution was studied. Considering the adsorption of phenolic compounds on GO, after adsorption GO had good stability in water in presence of common electrolytes affecting its transport with organic contaminants in the environment. These findings help in the prediction of the contaminant fate in the environment (Catherine et al., 2018).

Lu et al. (2018) (GNS) considering the implications of humic acid. GNS- water interface is important in water treatment system to evaluate its environmental impact. The desorption of phthalic acid on rGO in the presence of HA was quick, these results are important in evaluating the fate of GNS with PAEs in the environment (Lu et al., 2018).

Su et al. (2018) investigated the aggregation of ^{14}C -labeled few-layer graphene (FLG) at concentrations ranging from 2 mg/L to 10 mg/L using both dynamic light scattering and sedimentation measurements. FLG started to agglomerates at concentrations higher than 3mg/L. The presence of NOM significantly increased the agglomeration due to electrostatic and steric interaction, they also studied the bioaccumulation of larger sized FLG using Zebrafish, hence more attention should be paid in evaluating the environmental risk of FLG (Su et al., 2018).

Hou et al. (2015) studied the stability and aggregation of GO and three forms of reduced GO (varying in time) taking into account the pH, ionic strength and natural organic matter. The stability of GO decreases with an increase in the reduction of functional groups, while the environmental factors play a vital role in the stability of rGO. They concluded pH play an important role in the stability of rGO (Chowdhury et al., 2015a).

Kashyap et al. (2014) prepared graphene oxide by modified Hummers method and graphene by chemical reduction of GO colloids. They investigated the stability of both GO and graphene on account of pH varying from 4-12 with excellent stability due to its zeta potential values. These findings help in the fabrication of graphene-based composites for aqueous processing methods (Kashyap et al., 2014).

Chowdhury et al. (2013) investigated the stability of GO and its aggregation kinetics considering various parameters relevant to the environmental system (pH, ionic strength and salt types) (Chowdhury et al., 2013). These findings indicate that GO nanomaterial is highly stable in the natural aquatic environment, thus its transport in aqueous media is highly possible. Recently, it has been shown that colloidal GO nanoparticles (GONPs) can be quite mobile in porous media. An important implication is that GONPs can become an effective contaminant carrier, resulting in the enhanced transport and enhanced uptake of a range of environmental contaminants (Terzi et al. 2008; Wang et al. 2011). Figure 2.5 shows the stability of GNS in aqueous solutions in the presence of various environmental factors (pH, NOM and divalent ions). They remain stable in water for more than 50 days.

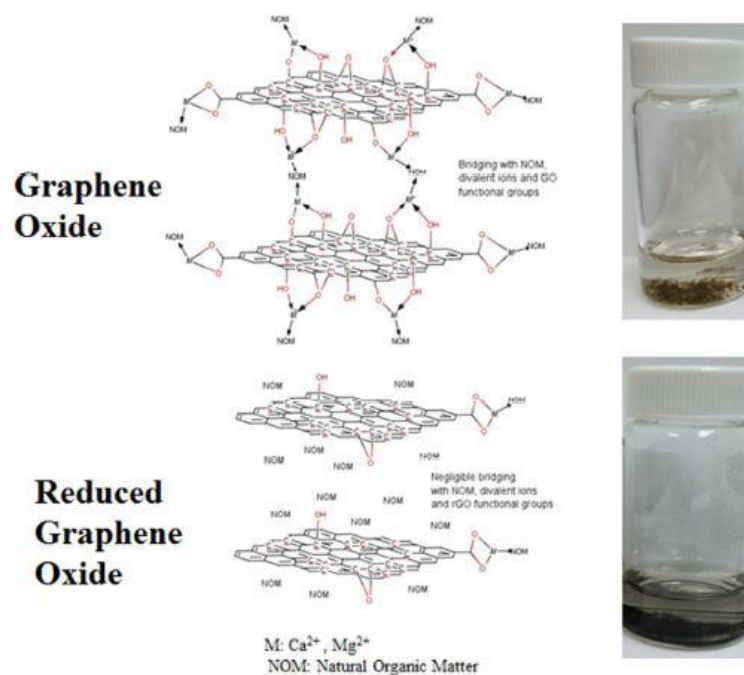


Figure 2. 5: The stability of GNS in aqueous solution Hou *et al* (2015)

2.5 Adsorbents for Removal of Emerging Contaminants

Various literature pertaining to the use of different adsorbents for wastewater organic pollutant elimination have been studied over the last decade (Hamdaoui and Naffrechoux 2009). Treatment of various ECs from water and wastewater sludge (Barceló, 2005;Grassi et al., 2012), paper mill wastewaters (Latorre et al., 2005), sediments and soil (Taha et al., 2011), fragrance materials, pesticides (Monarrez et al., 2008), human pharmaceuticals from environment have been investigated.

2.5. 1 Carbon nanotubes (CNTs)

Various nanomaterials have been used as effective adsorbents for the sorption of ECs from effluents (Maiti et al., 2018). CNTs is a promising adsorbent for the removal of many ECs due to their relatively high surface area, small size, large porosity, (Cai et al., 2014; Yu et al., 2017b; Yuan,Yu,Li, et al., 2014). CNTs are extensively used adsorbent materials for the removal of organic pollutants from wastewater. However, there are some existing problems for the treatment of ECs such as separation from the

aqueous phase; reduced dispersibility; and small particle size. Hence, researchers have chemically modified CNTs (Yang et al. 2012) for being employed as an adsorbent

Multi-walled carbon nanotubes (MWCNTs) with different oxygen contents for the adsorption of tetracycline (TC) from aqueous solutions was studied (Yu et al., 2014b). The maximum adsorption capacities Q_{\max} was calculated by the Langmuir model were 217.8, 269.25, 217.56, and 210.43 mg g^{-1} for carbon nanotubes with 2.0%, 3.2%, 4.7% and 5.9% of oxygen, respectively. Yu et al., 2016, continued to verify the effect of oxygen content ranging from 2.0% to 5.9% of oxygen on the sorption capacity of carbon nanotubes removal of ciprofloxacin antibiotic from aqueous solution. Based on the Langmuir isotherm model, the values of Q_{\max} obtained were 150.6, 178.9, 206.0, and 181.2 mg g^{-1} for carbon nanotubes with 2.0%, 3.2%, 4.7% and 5.9% of oxygen, respectively (Yu et al., 2016).

SWCNT for adsorption of bisphenol A (BPA) and 17 α -ethynylestradiol (EE2) from landfill leachate study was performed (Joseph et al., 2011). Different leachate solutions were prepared by altering the pH, ionic strength, and dissolved organic carbon (DOC) in the solutions to mimic the varying water conditions that occur in leachate during the various stages of waste decomposition. Based on the Langmuir isotherm model, the Q_{\max} values obtained were 44.8 and 120 mg g^{-1} for BPA and EE2, respectively.

2.5.2 Graphene

Graphene is a carbon allotrope having defined features favorable for various environmental applications. The carbon nanomaterial-graphene oxide is produced by the oxidation of graphite through a chemical process. The significance of graphene is due to its chemical, thermal, electrical and mechanical properties, inimitable morphology, and high specific surface area. Due to its strong binding of delocalized π -electrons with toxic pollutants, graphene has been used as a rapid adsorbent for pollutant removal (Apul et al. 2013). The process of adsorption by the graphene oxide (GO) becomes influenced by the occurrence of active functional groups on its surface (Santhosh et al., 2017).

Xu et al. (2012) studied the sorption of bisphenol A (BPA) using graphene. The adsorption capacity obtained from Langmuir isotherm of graphene for BPA was 182

mg g⁻¹ at 302 K. This was much higher when compared to other carbonaceous materials investigated in the literature, which may be attributed to the hydrogen bonds, and π - π interactions, as well as the single layer sp²-hybridized structure.

Kwon and Lee (2015) reported the adsorption of 4-n-nonylphenol (4-n-NP) and bisphenol A (BPA) on magnetic reduced graphene oxides (rGOs) as a function of contact time, pH, ionic strength and humic acid were investigated by batch adsorption system. The maximum adsorption capacities of magnetic rGOs at pH 6.5 and 293 K were 63.96 and 48.74 mg g⁻¹ for 4-n-NP and BPA, respectively. The higher affinity of rGOs with 4-n-NP was attributed to π - π stacking and a flexible long alkyl chain of 4-n-NP, whereas adsorption of BPA on rGOs was energetically favored by a lying-down configuration due to π - π stacking and dispersion forces, which was further demonstrated by FTIR analysis.

Bele et al. (2016) studied the production of graphite oxide (GO) by different reduction degrees by using hydrazine hydrate and finally to graphene using NH₄OH. Their adsorption performance for bisphenol A (BPA) was evaluated taking into account pH, ionic strength. The adsorption capacities were increased with increasing the reduction degree of GO with the maximum adsorption capacity Q_{max} 94.06 mg g⁻¹ to be presented by graphene that was the result of the optimum reduction degree. The increase in the degree of GO reduction reduced the amount of oxygen-containing functional groups on the surface of reduced samples, resulting to the increase of the π - π interaction between adsorbent-adsorbate and to increase of adsorption capacity. Some of the literatures related to adsorption of emerging contaminants with graphene based materials are listed in Table 2.1.

2.6 Adsorption Mechanism

The process of adsorption involves the intermolecular transfer of pollutant onto the solid surface of the sorbent. The characteristics of adsorbent and adsorbate are unambiguous and adsorption depends upon their composition and chemical nature, respectively (De Gisi et al., 2016). Adsorption involves van der Waals forces of interaction, electrostatic attraction, π - π interactions, and other hydrophobic interactions. The process of adsorption is also regulated using physical interactions. In some cases, chemisorption may occur. The physical adsorption is carried out mainly

through polarity, steric interaction, π - π interaction, Van der Waals forces, hydrogen bonds, hydrophobicity, and dipole-induced dipole interactions. In contrast to physisorption, the substances that are adsorbed by chemisorption involve the development of a chemical bond by electron sharing between the adsorbent and the pollutant. Chemical adsorption is more common to occur between metallic ions and adsorbents that possess several functional groups. For organic contaminants, it is anticipated that the main mechanism of interaction would be physical (Seabra et al., 2013).

Table2. 1: Adsorption of Emerging contaminants using Graphene based materials

Material	Compound	Parameters	References
Graphene	Phenol	pH= 6.3 at 285K Q_{\max} 28.26 mg g ⁻¹	(Li et al., 2012)
Graphene	2-Chlorophenol	pH, ionic strength and temperature variation Q_{\max} 208.76 mg g ⁻¹	(Fan et al., 2017)
Graphene oxide sheets	2,4,6- trichlorophenol	pH, ionic strength, Q_{\max} 10.39 mg g ⁻¹	(Jiali Wang et al., 2014)
Graphene	2,4- dicholophenol 4- chlorophenol	pH, temperature and dosage Q_{\max} 108.87 mg g ⁻¹ Q_{\max} 114.2 mg g ⁻¹	(Yuan,Yu,Li, 2014)
Graphene	2-Chlorophenol 4-chlorophenol 2,4- dicholophenol 2,4,6- tricholophenol	Q_{\max} 88.1 mg g ⁻¹ 114.2mg/g 155.3mg/g 175.8mg/g	(Hamdaoui et al., 2009)
Graphene oxide	TBBPA	Contact time, pH, ionic strength, Q_{\max} 16.23 mg g ⁻¹	(Zhang et al., 2013)

The π - π interaction occurred amongst the aromatic rings of paracetamol and the syringyl group of lignin. The hydrogen bonds of guaiacyl moieties of grape stalk were also responsible for the sorption of paracetamol. In a solid-liquid sorption system, the removal of solute molecules is mainly explained using diffusion layer and intra-particle diffusion. The sorption regulating step could involve external or intra-particle diffusion process. In order to elucidate the mechanism of sorption, researchers have used Boyd's and intra-particle diffusion equation. Electrostatic interactions, acid-base interactions, p-complexation, and H-bonding have been proposed to describe the adsorption of organics onto metal-organic frameworks (Hasan and Jung 2015; Khan et al. 2013). Recently, H-bonding (Seo et al. 2016) has been regarded as an important mechanism to explain the adsorption of polar organics on functionalized metal-organic frameworks.

2.7 Debromination of TBBPA

The debromination of TBBPA has by reactive materials have gained immense attention among researchers in the recent years, widespread research has been reported on the effective debromination of TBBPA using reactive bimetallic nZVI powder, such as Ni/Fe and Pd/Fe, Au/Fe@biocarbon.

(Lin et al., 2009) used Birnessite (δ -MnO₂) a naturally occurring soil component to study the dissipation of TBBPA. Dissipation of 50% of TBBPA occurred in less than 5 min in a system (pH 4.5) containing 625 μ M MnO₂ and 3.50 μ M TBBPA at 21 °C, and the removal further increased to as high as 90% when the reaction was prolonged to 60 min. First order model was found to closely fit the reaction kinetics. The reaction rates increased with a decrease in pH. The pathway of the reaction with MnO₂ and TBBPA was also proposed.

s-Fe/Cu bimetallic particles synthesized could degrade TBBPA in aqueous effectively (Yu et al., 2017a) . The optimum TBBPA was 95.9 %, on the increase of Cu mass loading from 0 wt% to 6 wt%, 4 wt% mass loading was the best; with TBBPA initial concentration increased from 5 mg/L to 30 mg/L, TBBPA removal efficiency decreased from 91.2% to 73.0%; also, when dosage increased from 10 g/L to 30 g/L, removal efficiency increased from 58.1% to 95.9%; pH 6.5 was beneficial to degrading TBBPA.

Zerovalent iron nanoparticles (nZVI) demonstrated the excellent capacity to debrominate TBBPA to tri- bromobisphenol-A (TBBPA), di-bromobisphenol-A (DBBPA), bromobisphenol A and bisphenol-A (Lin et al., 2012) . The influencing factors like the initial pH, TBBPA concentrations, initial pH and the effect of co-solutes were studied in detail. The pathway and its intermediate products were also identified. More than 86% was debrominated in 16h at pH of 7.5. The debromination of TBBPA by nZVI followed pseudo-first-order decay model, the higher dosage in the acidic condition favored the process and presence of Ca^{2+} and Na^{2+} species inhibited the reaction.

UV/Fenton reaction catalyzed by titanomagnetite ($\text{Fe}_{3-x}\text{Ti}_x\text{O}_4$) to degrade TBBPA. In the system with 0.125 g L^{-1} of $\text{Fe}_{2.02}\text{Ti}_{0.98}\text{O}_4$ and 10 m mol L^{-1} of H_2O_2 , almost complete degradation of TBBPA (20 mg L^{-1}) was accomplished within 240 min UV irradiation at pH 6.5 (Zhong et al., 2012) . The presence of Ti^{+4} improved the catalytic activity of magnetite, also the degradation pathway was proposed and the complete degradation of TBBPA was obtained. Literature related to debromination of TBBPA using metal catalyst are listed in Table 2.2.

Table2. 2: Debromination of TBBPA using metal based nanomaterials

Material	Compound	Parameters	References
s-Fe/Cu	pH= 6.5, dosage varied from 10 to 30g/L ,95% removal.	First order	(Yu, Hung et al 2017)
Au/Fe@biocarbon	debromination efficiency 98 to 99 %, within 100 min at pH= 5	First order	(Kang et al., 2018)
Fe-Ni bimetallic	pH= 4.5 less than 5 hours, 90 % removal.	First order	(Peng et al 2017)
Ni/nZVI (nickel nanoscale zero-valent iron)	pH= 5 to 6 120 min 93% degradation	Psedu-first order	(Hung et al 2016)
Sulfidated nano zero valent iron	90% removal of 20 ppm TBBPA within 24 hrs.	First order	(Peng et al 2016)

Zerivalent iron nanoparticles (nZVI)	pH= 7.5, 16hours debrominated	86%	Pseudo-first order	(Hung et al 2013)
--------------------------------------	-------------------------------	-----	--------------------	-------------------

2.8 Risk of Environmental nanomaterials(ENM) and its applications in water treatments

ENMs are likely to become hazardous in the near future that will affect the human health and the environment, currently, there is a lot of attention paid to its effect on human health but very few data on its release into the environment and the effects. The risk of this substance is determined on its release and exposure and the knowledge about its environmental exposure is not fully understood. Compared with the toxicological examination of ENMs, few data are available about their actual release. In terms of release, Ag-ENM is again the most studied ENM so far. From a regulatory point of view, data on ENM environmental release and exposure are required to estimate the associated risk. Regardless of whether new or established ENMs are examined, models of exposure and their combination with toxicological data can contribute to a prospective risk assessment according to the precautionary principle. Recent indications on the toxicity of already established ENMs reveal that widespread use of a substance should not be mistaken for evidence that the substance does no harm. Recently, it has been observed that graphene and its compounds (graphite nanoplatelets) have interesting physicochemical properties and can be used for water treatment. The graphene and its compounds are gaining importance in water treatment due to their unique properties (Zhao et al. 2011a). The future of water treatment seems to be quite bright because of the development of different types of graphene materials (Ali et al., 2018).

2.9 Summary of Literature

GNS are novel engineered nanomaterial that is being widely used for various environmental application exfoliated by oxidizing agents to produce layers of graphene, that is present in the environment due to its various applications and commercial development. The large scale production and use of carbon-based nanomaterials have to lead to the release into the environment necessitating its evaluation. On its release, it

is highly toxic to both environment and humans its become essential to evaluate its ecological risk. Due to the electrostatic repulsion, originating from the presence of oxygen-containing functional groups on the structure of GNS, they can suspend well in water for months. The structure and properties of ECs such as the pKa, aromatic ring substitution, and solubility will affect its interaction with GO surface. The release of GO into the environment along with adsorbed contaminants causes higher environmental risk and toxicity to aquatic organisms due to their higher solubility and enhanced mobility, leading to the significance of the study. The two dimensional graphene-based materials (GBMs) are highly attractive carbocatalysts for various environmental applications due to its versatile volume-surface ratio, rich in surface chemistry, and strong carbon-carbon bond along the xy plane with good compatibility. GBMs that include graphene oxide (GO) and reduced graphene oxide (rGO) with different carbon oxygen ratio contain a variety of oxygen-carrying functional groups that are chemically reactive. The promising properties with ease of synthesis and process ability make GBMs an ideal material for the reduction of most commonly used brominated flame retardant, tetrabromobisphenol A (TBBPA). Metal free carbon based materials have the potential to generate wide range of organic transformations. However, the mechanism of their action is still ill-defined. Herein we also explore the metal free GO and rGO for the complete debromination of TBBPA from aqueous Carbon based nanomaterials are engineered nanomaterial present in the environment. Research on NM fate, transformation, and toxicity is gaining attention to facilitate risk assessment and management. GO and rGO have potential application in the removal of emerging contaminants that contain benzene ring even at lower concentration due to the strong π - π interaction media. GO releases into the environment, their adsorption of organic contaminants further influences the fate and transport of both, and enhance the mobility of adsorbed ECs on nanomaterial's causing an environmental risk. NPs fate and transport in the environment are largely dependent on material properties such as surface chemistry, and particle size in environmental media

2.10 Scope of Study

GNS have potential application in the removal of emerging contaminants that contain benzene ring even at lower concentration due to the strong π - π interaction between the

benzene ring of the contaminant and that of both GO and rGO. ECs and conventional phenolic compounds are an important class of pollutants mostly found in industrial wastewater. GNS have good stability in water adsorption once GNS releases into the environment, their adsorption of organic contaminants further influences the fate and transport of both, which could enhance the mobility of adsorbed ECs on GNS causing an environmental risk. The surface properties and reaction mechanisms of graphene materials are important to be studied for the potential environmental application. ECs such as TBBPA, BPA, 4-NP and common conventional compounds like 4-CP, 2,4-DCP, 2,4,6-TCP and phenol, were chosen to study its kinetics, isotherm and thermodynamic effect towards GNS. However understanding the mechanism governing its interaction with GNS will further facilitate its prediction of the contaminant fate in the environment, causing environmental risk to humans and aquatic organisms. GNS due to the presence of oxygen functional groups on its surface facilitates the debromination process of TBBPA to less brominated and toxic compounds.

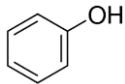
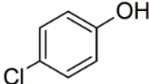
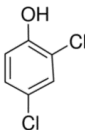
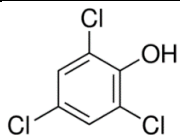
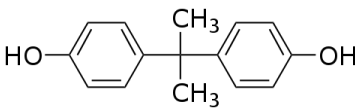
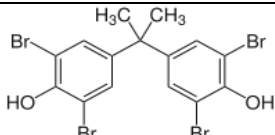
CHAPTER 3

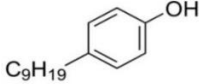
METHODOLOGY

3.1 General

The detail properties (both physical and chemical) of selected halogenated compounds (Phenol, 4-CP, 2, 4-DCP, 2,4,6 -TCP, BPA, 4-NP, and TBBPA) are shown in Table 3.1. The various techniques used for the characterization of nanomaterials are listed. The detailed experimental methodology and analytical procedures are explained below.

Table3. 1: Molecular structure and chemical properties of phenolic compounds

Compound	Structure	Kow	pKa	Solubility (g/L)
Phenol		1.16	10	86.6
4-chlorophenol		2.39	9.41	27
2,4-dichlorophenol		3.17	7.89	4.5
2,4,6-trichlorophenol		3.7	6.23	0.9
BPA		3.36	9.6	0.03
TBBPA		5.90	7.5	0.00416

4- nonylphenol		5.76	10.37	0.005
----------------	---	------	-------	-------

3.2 Materials

Graphite flakes (<20 mm) and potassium permanganate (KMnO₄) were purchased from Sigma-Aldrich. Hydrochloric acid (HCl, 37%) and sulfuric acid (H₂SO₄, 98%) with Grade AR were purchased from Merck. Phenol, 4-CP, 2, 4-DCP, 2,4,6-TCP, BPA, 4-NP, and TBBPA were obtained from Acros chemical company. Hydrogen peroxide (30–32%) Grade AR was purchased from Acros chemical company. All solutions were prepared using deionized (DI) water (Millipore, Temecula, CA, USA).

3.3 Characterization of Graphene Oxide

The properties of GO were characterized by using Fourier-transform infrared spectroscopy (FTIR), Raman spectroscopy, and X-ray diffraction (XRD). All were performed at different beamlines in the National Synchrotron Radiation Research Center (Taiwan). The surface elemental composition was also accomplished by using X-ray photoelectron spectroscopy (XPS). The morphological characterization was performed using SEM and TEM.

3.3.1 Fourier Transform Infrared Spectroscopy (FTIR)

FTIR spectra analysis was performed to investigate the structure and functional groups of the materials. FTIR was performed by using KBr pellets because it is transparent in the IR region of the electromagnetic spectrum. The IR spectra were recorded on the FT-IR 8300 Shimadzu instrument using pressed KBr disks (10 mg sample and 200 mg KBr). The spectral resolution was 4 cm⁻¹, and each spectrum was obtained after acquiring 90 spectra. The 10 mg of each sample plus 200 mg of KBr were weighed and ground in an agate mortar with a pestle until a homogeneous mixture was obtained. Disc pellets were prepared and the spectra were recorded from 4000 cm⁻¹ to 600 cm⁻¹. The Beer-Lambert law (or Beer's law) is the linear relationship between absorbance and concentration of an absorbing species, used to calculate the concentration of a sample given its absorbance using the following formula Eq.1

$$A = a(\lambda) \cdot b \cdot c \quad (1)$$

A is the measured absorbance,

$a(\lambda)$ is a wavelength – dependent absorptivity coefficient; b is the path length, and c is the analyst concentration

3.3.2 X-Ray Diffraction (XRD)

The crystalline structures of the materials were identified by X-ray diffractometer (MAC SCIENCE, MXP18) using Cu K α irradiation ($\lambda=1.54056$ Å) and operating at accelerating voltage of 30kV and an emission current of 20mA. The X-ray patterns were acquired from 10 $^{\circ}$ to 60 $^{\circ}$ at a sampling width of 0.02 $^{\circ}$ and a scanning speed of 4deg/min. Moreover, the crystallite size was estimated by using the Scherer equation which is useful when crystals are smaller than 1000Å in size using Eq 2

$$d = 0.89 \lambda / B \cos \theta \quad (2)$$

3.3.3 X-ray Photoelectron Spectroscopy (XPS)

XPS is a surface-sensitive quantitative spectroscopic technique that measures the chemical states of elements were determined using an X-ray photoelectron spectrometer (XPS, Ulvac-PHI 1600 photoelectron spectrometer) with an Al K α X-ray source at 1486.6 ± 0.2 eV. To eliminate the chemical shifts resulting from the charge effects, the binding energies of the photoelectrons were calibrated by fixing the C1s from the carbonaceous contaminants at 284.5 eV. XPS measurements to determine the chemical states of elements were determined using (XPS, ESCA PHI 1600).

3.3.4 Identification of Bromide Ion

To quantify the formation of Br $^{-}$ during the reaction, 5-mL samples were withdrawn and passed through a Whatman 0.22- μ m poly (vinylidene fluoride) membrane filter (Whatman, Florham Park, NJ, USA). The concentration of Br $^{-}$ was determined using an ICS-2000 ion chromatograph (Dionex, Sunnyvale, CA, USA). An IonPac AS19 analytical column (250 \times 4.0 mm, Dionex) was employed for the separation. The conductivity detector temperature was 35 $^{\circ}$ C. The eluent was 10 mM KOH solution with a flow rate of 1.0 mL/min. The injection volume was 25 μ L. Under these conditions, the typical retention time for Br $^{-}$ was 7.5 min.

For product or intermediate identification, 50 mL of reaction solution containing 2.0 mg/L TBBPA and 3.0 g/L of rGO were reacted in pH 7.5 solution (methanol/H₂O, 50/50, v/v). At 2, 4, 8, 12, and 16 h, the reaction solution was collected and consecutively extracted three times with 20 mL of methylene chloride. The organic phases were collected and combined, dehydrated by passing through a filter paper filled with anhydrous sodium sulfate, and concentrated to near dryness on a vacuum rotary evaporator. The residue was evaporated to dryness under nitrogen flow and redissolved in 1.0 mL of acetone-hexane (1:1). The extract was then divided into two equal parts, from which one part was analyzed directly and the other part was derivatized before analysis. For derivatization, the extract was evaporated to dryness under nitrogen, and 150 μ L of BSTFA + TMCS was added to silylate the polar products. Immediately after the addition of the silylation reagent, the vial was crimped with a cap with Teflon-lined septum and kept at 60 °C for 2 h.

The silylated products were redissolved in 0.5 mL of hexane. Aliquots (2 μ L) of the silylated and nonsilylated extracts were injected into an Agilent Model 7890A gas chromatograph (GC) coupled with an Agilent Model 5975C mass spectrometer (MS) (Agilent Technologies, Wilmington, DE, USA) for chemical structural elucidation. A Hewlett–Packard Model HP-5MS column (30 m \times 0.25 mm \times 0.25 μ m; Agilent) was used for separation. The inlet temperature was 260 °C, and the detector temperature was 320 °C. The oven temperature was initiated at 80 °C and held for 3 min, then increased to 300 at 3 °C/min and held for 30 min. The flow rate of the carrier gas (helium) was 1.0 mL/min. The injection of 2 μ L sample was carried out by an Agilent Model 7693 autosampler in the pulsed splitless mode turning on after 1.0 min. The temperatures of the transfer line, ion source, and MS detector were 280, 230, and 150 °C, respectively. The MS detector was operated in the electron impact mode at 70 eV, and the mass spectra were acquired in the full scan mode with m/z ranging from 50 am to 1000 am.

3.4 Synthesis of Graphene Oxide (GO) and Reduced Graphene oxide (rGO)

GO was synthesized by following the Improved Hummers method (Park et al., 2009; Sahu et al., 2017). In brief, 2.0 g of graphite flakes were added to a mixture of 225 mL of sulfuric acid and 25 mL phosphoric acid maintained at a temperature of 35°C. 5.0 g

of potassium permanganate was gradually added to the solution that was maintained at 35°C and stirred continuously for 10 hrs. The resultant mixture was cooled in an ice bath, diluted with 225 mL of deionized (DI) water, then 3 mL of 30% hydrogen peroxide was added to the mixture to remove the residual permanganate. A large number of bubbles will be released and the solution color will be changed to brilliant yellow. The suspension was centrifuged several times and washed with 0.1 N hydrochloric acid and phosphate buffer to remove extra manganese ion. The final solution was washed with DI water to lower the pH value to around 5-7 and then dried in rotary vapor at 45°C. The GO suspension was prepared by sonication GO sheets in DI water for 2 hrs.

The thermal reduction of GO was performed in a quartz tube in which GO was placed in an aluminum boat placed inside the quartz tube in the presence of argon gas at 400 °C for 8hrs. The graphene oxide was thermally expanded and reduced within 2hrs to obtain reduced graphene oxide (rGO), powder form(McAllister et al. 2007). Shown in Fig 3.1.

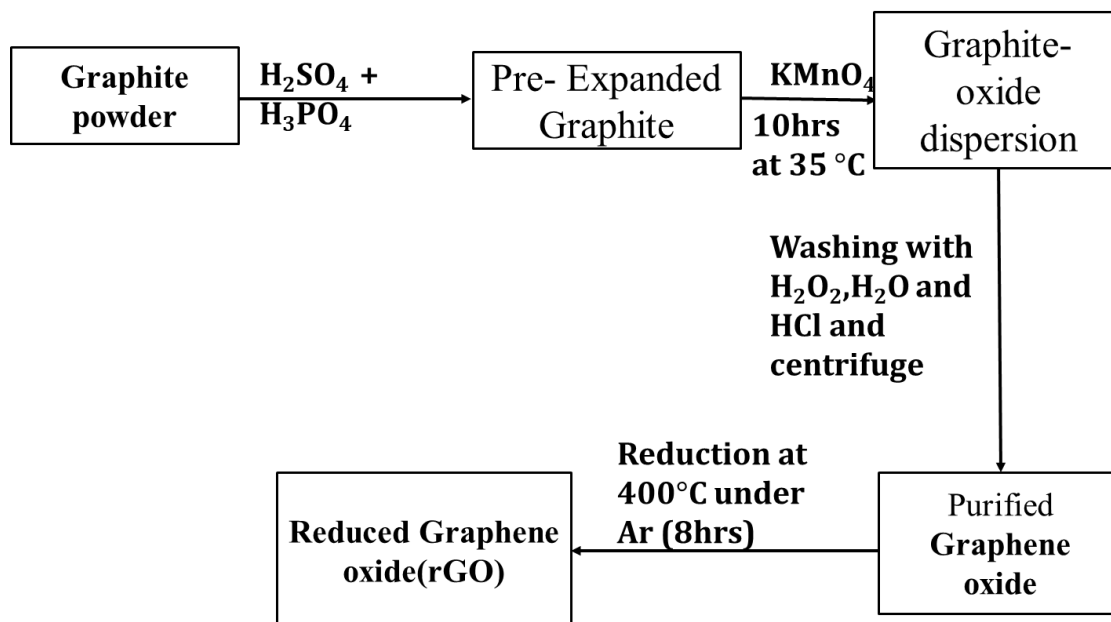


Figure3. 1: Synthesis of GO and rGO

3.5 Experimental Methodology

3.5.1 Adsorption experiments

The stock solutions (100 mg/L of phenol, 4-CP, 2,4 –DCP, 2,4,6-TCP, TBBPA, BPA, and 4-NP) was prepared in deionized (DI) water for phenol, 4-CP, 2,4-DCP ,2,4,6 –TCP and BPA, while for TBBPA and 4-NP the stock solution was prepared in a mixture of methanol (less than 2%) and water. Sorption batch experiments of phenol, 4-CP, 2,4-DCP, 2,4,6-TCP, 4-NP, BPA and TBBPA were all performed in a shaker at 150 rpm at 25 °C in the dark. 4 mL amber vials with PTFE screw cap were added one sorbate and the background solution containing 0.01 M CaCl₂ in DI water and 200 mg/L NaN₃ as bio inhibitor (Zhou et al., 2015). Table 3.1, the physiochemical properties of the pollutants considered in our study are listed. The kinetic studies were performed by using 20 mg/L sorbate and 5 mg GBMs was used to determine the equilibrium time for each sorbate. For isotherms, the vials were prepared as the above by adding various concentrations of sorbate (Table 3.2) and shaking for more than 48 hrs. All were repeated at least three times.

Table 3. 2 Reaction conditions for the removal of emerging contaminants using GBMs

Adsorbent	Initial concentration (ppm)	Reaction conditions
Phenol	1,2,5,10,15,20,30 and50	150 rpm at 25 °C adsorbates concentration of 5mg (for adsorption) and15mg/L(debromination) in the dark.
4-chlorophenol	1,2,5,10,15,20,30 and50	
2,4-dichlorophenol	1,2,5,10,15,20,30 and50	
2,4,6-trichlorophenol	1,2,5,10,15,20,30 and50	
BPA	1,2,5,10,15,20,30 and50	
TBBPA	1,2,5,10,15,20,30 and50	

4- nonylphenol	1,2,5,10,15,20,30 and50	
----------------	-------------------------	--

The vials were centrifuged at a speed of 6000 rpm for 10 mins and then the supernatants were analyzed by Agilent 1200 HPLC equipped with an UV/Vis detector for phenol (275 nm), 4-CP (286 nm), 2,4-DCP (285 nm), 2,4,6-TCP (284 nm), and TBBPA (280 nm), as well as with a fluorescence detector for BPA and 4-NP (excitation at 220 nm and 315 emissions at 315 nm). The HPLC conditions used are listed in Table 3.3. The adsorption amount was determined by the difference of the concentration measured before and after sorption from Eq 3.

$$q_e = (C_0 - C_e) V/m \quad (3)$$

q_e , mg/g is the adsorption capacity, C_0 and C_e are the initial and final concentration of the compound is the volume (mL) and m is the mass of the adsorbent (mg).

Table 3. 3 HPLC Conditions of phenolic compounds

Compounds	Temperature of column	Wavelength	Flow rate (ml/min)	Mobile phase ratio
Phenol	30	275	0.80	60:40
4-chlorophenol	30	286	0.80	60:40
2,4-dichlorophenol	30	285	1.00	60:40
2,4,6- trichlorophenol	30	284	1.00	60:40
TBBPA	30	280	0.80	70:30
BPA	30	220 315	0.80	70:30
4- nonylphenol	30	220 315	0.80	70:30

3.5.2 Thermodynamic Studies

Adsorption isotherm is the relationship between the quantity of adsorbate per unit of adsorbent and equilibrium solution concentration at a constant temperature. The

adsorption isotherms of phenol, BPA and TBBPA on the graphene-based materials at 15, 25 and 35°C were studied. Thermodynamic considerations are essential to conclude whether the adsorption process is spontaneous or not. The Gibbs free energy change (ΔG , kJ/mol) of the adsorption process is the fundamental criteria to determine the spontaneity, is related to the equilibrium constant (K_c). The value of ΔG° at any selected temperature is obtained by the equation by the van't Hoff equation (Eqs 6 and 7) (where R is the universal gas constant and the value is 8.314 J/mol K)

3.5.3 Debromination and regeneration experiments

The debromination experiments were performed by mixing 15 ppm of GBMS containing 10 ppm of TBBPA in 4mL screw-capped glass bottles under ambient conditions. TBBPA stock solution was prepared with mixture of water and methanol (less than 2%). Quantitative adsorbent and TBBPA were dissolved in background solution (0.01 M CaCl_2 in DI water and 200 mg/L NaN_3) to maintain the ionic strength and inhibit the biological activity. The vials were placed in a shaker at 150 rpm in dark and pH 6 was maintained throughout the experiments. All the experiments were carried out in triplicate and the standard error was less than 5%. The glass vials were shaken the suspension was centrifuged at 6000rpm for 10mins and the supernatant was analysed further.

To investigate into the recyclability and reusability of our iron oxide NPs, experiments of phenol, 4-CP, 2,4-DCP, 2,4,6-TCP, 4-NP, BPA and TBBPA removal by GBMs were performed in five cycles. For the first cycle, 5 mg/L of the pollutant solutions were removed from 15 mg/L GBMs after 20 min. After each cycle of removal reaction, GBMs were separated and recycled from the solution. The adsorbents adsorbed on the GBMs was extracted by 0.05 M NaOH, and then the aqueous pH of the vials including the GBMs was adjusted to between 3 and 4 by titrating with 0.01 M HCl. The resulting GBMs were used in the succeeding cycles.

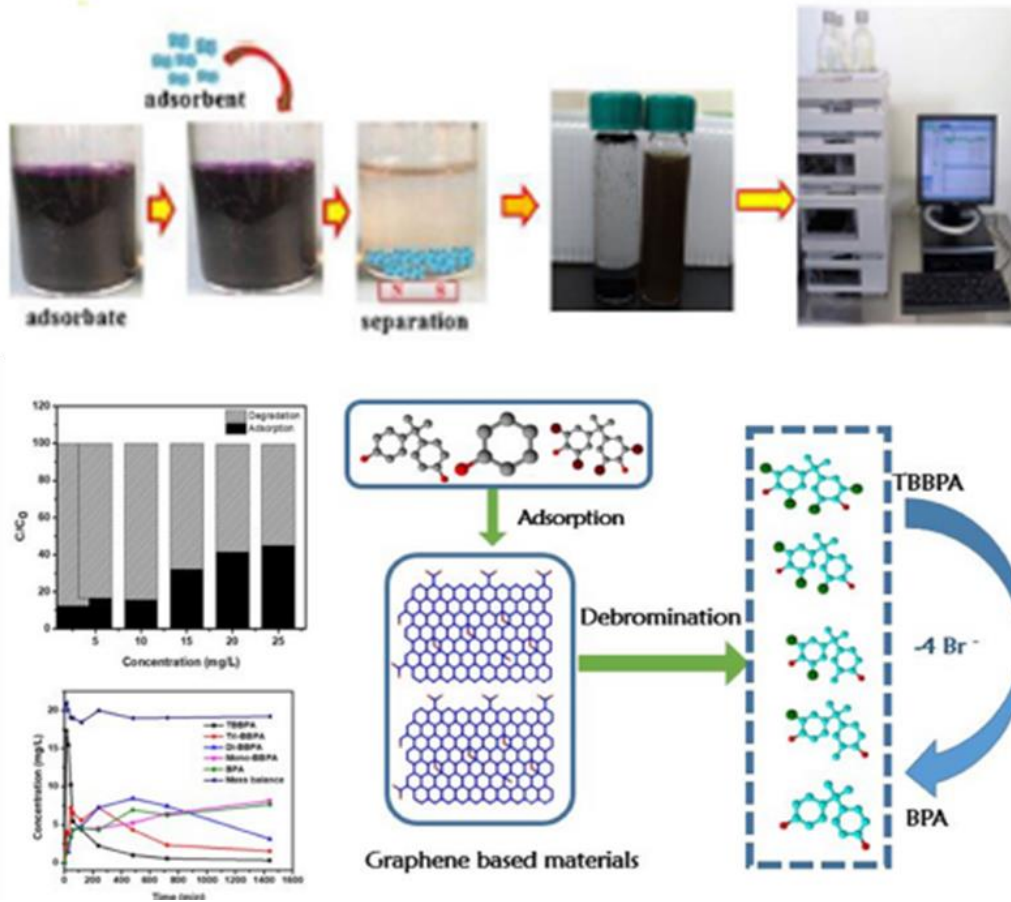


Figure3. 2: Schematic of work performed

3.5.4 Data Analysis

Pseudo-first-order and pseudo-second-order kinetic models were used to analyze the adsorption kinetics of these phenolic compounds on two graphene-based materials in equation (2) and (3)

$$\ln(Q_e - Q_t) = \ln Q_e - k_1 t \quad (2)$$

where Q_t (mg/g) is the adsorbed amount of sorbate onto the adsorbent with time, k_1 (min^{-1}) is the pseudo-first-order rate constant, and t (min) is time. The values of k_1 and Q_e were calculated from the linear plots of $\ln(Q_e - Q_t)$ versus t . The pseudo-second-order model can be expressed as

$$\frac{t}{Q_t} = \frac{1}{k_2 Q_e^2} + \frac{1}{Q_e} t \quad (3)$$

where k_2 (g/mg min^{-1}) is the pseudo-second-order rate constant.

Two nonlinear models, Langmuir and Freundlich equations, were utilized to describe the fitting of the adsorption isotherm of the three chemicals on graphene-based materials equation (3) and (4)

$$Q_e = \frac{bq_m C_e}{1+bC_e} \quad (4)$$

$$Q_e = K_f C_e^{1/n} \quad (5)$$

where C_e (mg/L) is the equilibrium concentrations of sorbate in the solution, b (L/mg) is a coefficient in Langmuir equation, q_m (mg/g) is the Langmuir monolayer adsorption capacity, K_f is Freundlich adsorption constant, and n is exponential Freundlich coefficient.

The Gibbs free energy change (ΔG , kJ/mol) was calculated by the van't Hoff equation (where R is the universal gas constant and the value is 8.314 J/mol K) shown in equation (6):

$$\Delta G = -R T \ln (K_c) \quad (6)$$

where T is the temperature (K), the equilibrium constant (K_c) equals Q_e/C_e at a specific temperature.

Information on the inherent energetic changes related to adsorption is also provided by the further thermodynamic analysis. As Gibbs-Helmholtz equation (7), the change in enthalpy (ΔH , kJ/mol) and the change in entropy, (ΔS , kJ/mol K) at a constant temperature.

$$\Delta G = \Delta H - T \Delta S \quad (7)$$

The values of ΔH and ΔS were calculated from the slope and intercept of the plot between $\ln (K_c)$ versus $(1/T)$.

CHAPTER 4

RESULTS AND DISCUSSION

4.1 General

We have divided the results and discussion chapter into three division based on the objectives of our study, and the results are discussed under each objective listed below.

4.2 Interaction of Graphene nanoflakes with emerging contaminants and some common phenolic compounds in a water matrix

4.2.1 Characterization of Graphene nanoflakes

The SEM and TEM images displayed the wrinkles distributed on the edge of GO nanoflakes (Figure 4. 1a and 1b) and also showed larger and flat structure thus creating a potential adsorption site. These wrinkled sheets are due to the presence of oxygen-containing groups (J. Wang et al., 2014; Zhao et al., 2012). From the XRD patterns for GO nanoflakes and graphite (Figure 4. 1c), the diffraction peak of graphite appeared at 26.82° and that of GO at 9.72° , which confirmed GO we synthesized. The results show that graphite was completely oxidized to GO. The increase in the distance is due to the introduction of oxygen-carrying functional groups on the edge of the layer (Dimiev et al., 2014).

The functional groups of GO nanoflakes shown in the FTIR spectra (Figure 4. 1d) have a strong peak at 3320 cm^{-1} due to the O-H stretching, the other main peaks at 1760, 1620, 1420 and 1048 cm^{-1} due to vibration of C=O, aromatic stretching of C=C, benzene ring C=C stretching and alkoxy C-O stretching vibration, respectively. The peak at 1760 cm^{-1} ascribes the stretching vibrations due to C=O in the carbonyl group of GO after oxidation from graphite (Yu et al., 2014a). For graphite, the peaks at 1574, 1739 and 1240 cm^{-1} correspond to the benzene ring C=C stretching vibrations, carboxyl C=O, and epoxy C-O vibrations. The presence of broadened peaks of an oxygenated functional group on GO explains the successful oxidation of GO from graphite (Thirumal et al., 2016).

Raman spectra a nondestructive technique for characterization of the structure and quality of carbon-based materials. In Raman spectra (Figure 4.1e), two prominent spectra of GO nanoflakes have been observed at 1349 and 1582 cm^{-1} confirming to D band and G band, respectively. GO had some peak changes compared to graphite, a strong G band at 1579 cm^{-1} and a weak D band at 1360 cm^{-1} (Johra et al., 2014). The G band in GO is shifted to a wavenumber higher than graphite, due to the oxygenation of graphite, that resulted in the formation of sp^3 carbon atoms. Furthermore, the ratio of D band and G band is used to define the degree of disorder and the reduction of graphene (Perumbilavil et al. 2015). The ratio of I_D/I_G of Graphite is 0.85 and for GO is 0.99, whose difference arose due to the defects created by the aromatic structure and degree of disorders. The increase in the ratio of I_D/I_G of graphite to GO confirms the presence of oxygen-containing groups to the graphitic structure.

Zeta potential is an important factor to characterize the colloidal dispersion stability and also infer the magnitude and sign of the double layer surrounding the colloidal particle. Values of zeta potential more than +30mV or -30mV are considered to be stable due to electrostatic repulsion (Konkena et al., 2012). Zeta potential of GO samples at different pH values was measured and found that it was decreasing with increasing solution pH (Figure 4.1f). The aqueous dispersion of GO nanoflakes was found to be stable in the neutral pH, which resulted from a high negative value of zeta potential (- 50.3mV). It also confirmed the presence of negatively charged functional groups we observed on the edges of the GO surface.

To investigate the stability of prepared GO nanoflakes, UV- visible spectroscopy was used. The sedimentation curves for GO dispersed in water and the stability of GO in water along with the various concentration of BPA was plotted (Figure 4.1g). GO has special lamellar structure and good dispersion stability that improve sedimentation stability.

The surface properties or defects of GO were also analyzed, the distribution of C1s of GO (Figure 4. 1h) shows the highest intensity binding energy at 287.8 belonging to the carbonyl functional group, whereas the other peak at 286.7 corresponds to C=C/C-C in aromatic rings. The distribution of O1s spectra of GO (Fig.1i) was also analyzed using XPS, the peak at 533.2 correspond to -C-O and -OH groups. The BET surface area of GO was 0.727 m^2/g .

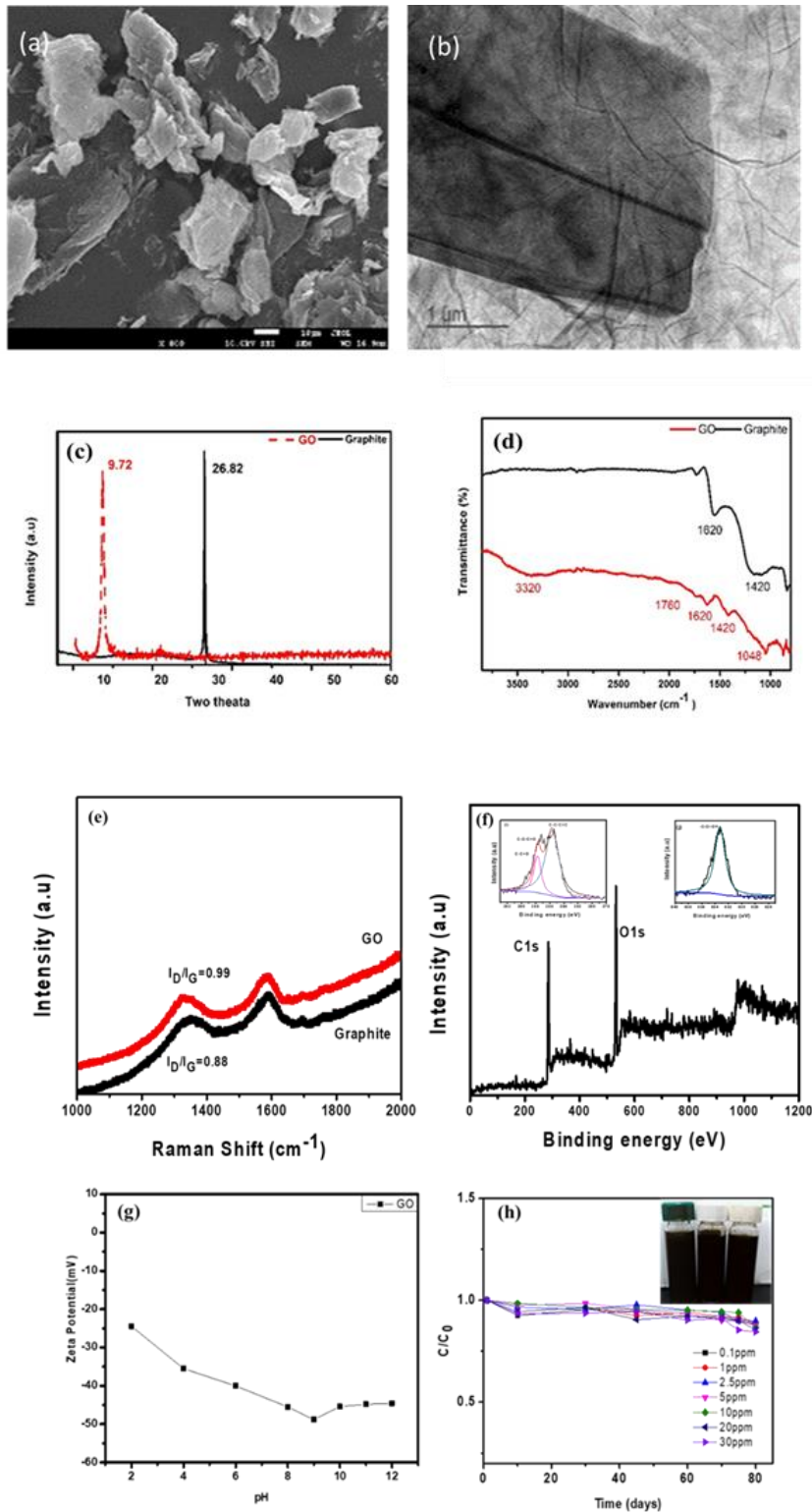


Figure4. 1: (a) SEM and (b) TEM of GO. (c) XRD, (d) FTIR, and (e) Raman spectra of graphite and GO (f) carbon (C1s) peaks of GO and Oxygen(O1s) peaks (g) Zeta

potential of GO samples as a function of pH (h) Sedimentation curve after adsorption of BPA on GO, insert a photography of aqueous dispersion of GO.

4.2.2 Kinetics of phenolic contaminants on graphene oxide

The adsorption kinetics of phenolic compounds on GO was investigated at 298K. For these seven chemicals, the rapid sorption occurred during the first 30 min of the reaction time, thereafter followed a slow rate for 120-400 mins, and attain the saturation in 480 min for all compounds. Figure 4. 2 shows that the rate of adsorption increases with the increase in time, similar kinetics pattern was also observed by (Xu et al. 2012), indicating that graphene-based materials possess fast adsorption. The adsorption kinetics of PCs on GO nanoflakes is divided into three stages, the first stage of film diffusion (fast diffusion), the second stage of intraparticle diffusion (slow sorption), and the final stage of dynamic equilibrium (Phatthanakittiphong and Seo 2016). The correlation coefficient (R^2) was relatively high for the pseudo-second-order model as compared to the first-order Table 4.1. Adsorption of organic compounds on GO also followed the second-order model providing a good fit J. Wang et al. (2014); (Jiali Wang et al., 2014).

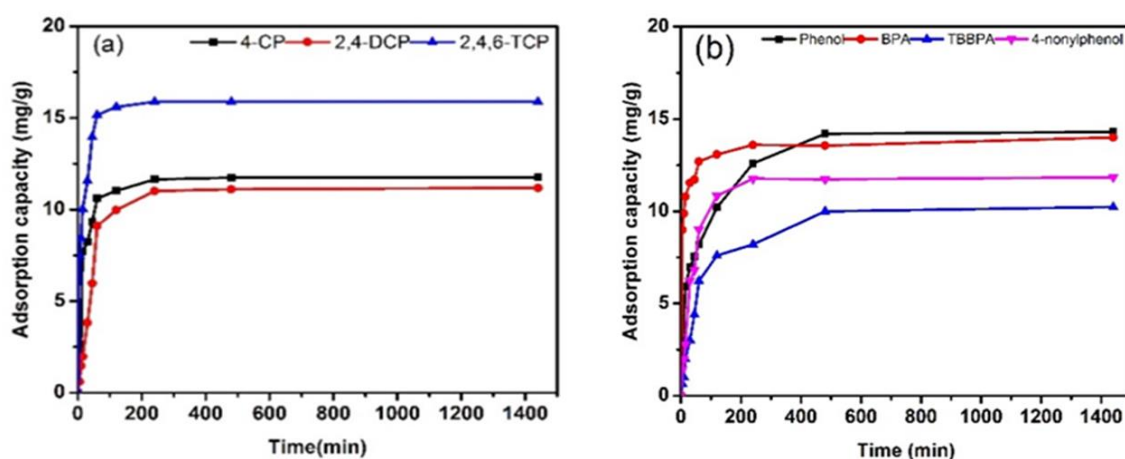


Figure4. 2: (a) Adsorption kinetics of 4-chlorophenol, 2,4-dichlorophenol, 2,4,6-trichlorophenol (b) phenol, BPA, 4- nonylphenol and TBBPA on GO.

Table4. 1: kinetics constant for adsorption of PCs on GO.

	Pseudo-first-order			Pseudo-second-order		
	k_1	q_e (mg/g)	R^2	k_2 (g/mg min) (10^{-3})	q_e (mg/g)	R^2
Phenol	0.012	13.45	0.86	2.17	8.641	0.992
4-chlorophenol	0.044	10.09	0.922	6.35	8.904	0.963
2,4-dichlorophenol	0.051	10.22	0.812	2.044	8.57	0.944
2,4,6-trichlorophenol	0.087	14.56	0.823	11.01	8.97	0.954
BPA	0.064	13.67	0.87	11.01	8.025	0.98
TBBPA	0.056	9.56	0.913	1.589	14.706	0.972
4- nonylphenol	0.032	11.54	0.943	3.066	8.212	0.99

4.2.3 Adsorption isotherms of phenolic compounds onto graphene oxide

The adsorption of PCs by GO did not increase in a linear pattern with the increase of the concentration of PCs (Figure 4.3). For phenol, 4-CP, and DCP, the adsorption reached a plateau when the equilibrium aqueous concentration was around 10 mg/L. As 2,4,6-TCP and BPA was around 20 to 30 mg/L, the adsorption of them on GO seemed saturation. However, for 4-NP and TBBPA, the adsorption increased with the aqueous concentration in the range we studied.

Table 4. 2: Isotherm constants for adsorption of PCs on GO

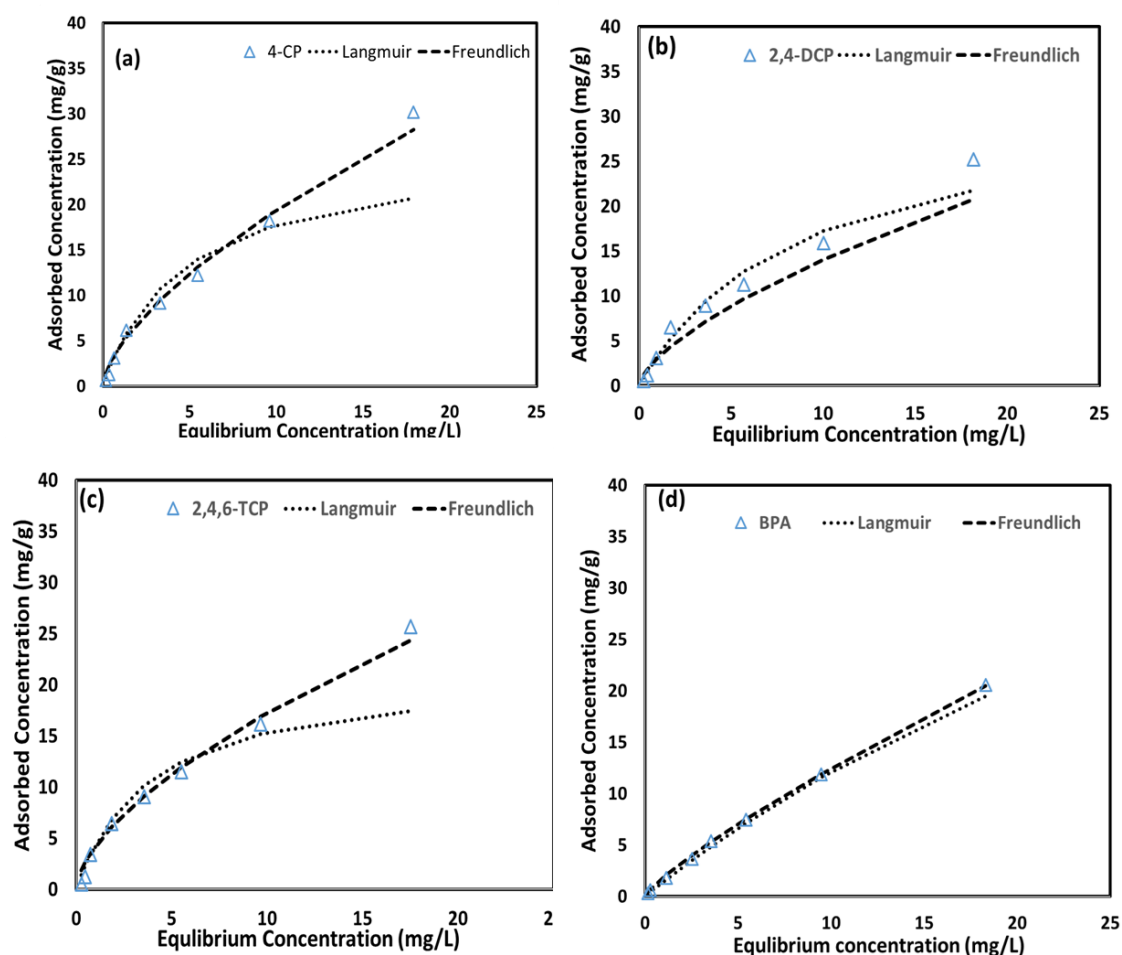
Compound	Langmuir			Freundlich			q_m/SA (mg/m^2)
	q_m	b	R^2	K_f	$1/n$	R^2	
Phenol	29.25	0.48	0.92	3.43	0.72	0.94	38.60
4-chlorophenol	19.70	0.23	0.98	2.98	0.67	0.79	27.09
2,4-dichlorophenol	18.75	0.15	0.75	4.55	0.56	0.90	26.52
2,4,6-trichlorophenol	21.92	0.20	0.88	4.27	0.61	0.91	30.15
BPA	20.80	0.19	0.95	3.16	0.77	0.72	28.61
4-nonylphenol	22.06	0.21	0.98	1.85	0.99	0.89	30.34
TBBPA	22.95	0.35	0.95	3.04	0.71	0.91	31.56

Figure 4.3 also presented these fitting data by two isotherms for phenolic compounds and their relative parameters were listed in Table 4. 2. In Table 4.2, the Langmuir model fitted the sorption isotherms better than the Freundlich model, suggesting the possible single layer adsorption on GO. The adsorption isotherms were normalized according to the surface area of the adsorbent (q_m/SA) it signifies the differences in the adsorption affinities the original sorption isotherms than in the surface area (include in thesis) normalization sorption isotherms. This outcome indicates that the higher adsorption affinity of GO for emerging contaminants that of the original ones can be largely attributed to their larger surface area and mesoporous volume, and further confirms the pore-filling effect as the main sorption mechanism for adsorption mechanism.

Compared to the maximum adsorption capacity values obtained in this study to those in other literature. The synchronized occurrence of monolayer adsorption could happen on the presence of a flat structure of GO surface confirmed by its SEM image (Figure 4. 1b). Our measured q_m value of 2,4,6-TCP adsorption on GO was twice to that of

(Wang et al. 2013) (J. Wang et al., 2014), which could result from the surface properties of our GO and may contribute to more risk due to its high adsorption ability.

GO exhibited a similar type of adsorption affinities to six compounds including phenol, 4-CP, 2,4-DCP, 2,4,6-TCP, BPA, and 4-NP, while the highest adsorption capacity of TBBPA was observed. Due to the formation of hydrogen bonds between the phenolic molecules and the oxygen-carrying functional groups on GO surface (Kalita et al. 2016), polar PCs could have similar adsorption ability as more nonpolar PCs such as chlorinated ones. Furthermore, with the highest K_{ow} value of TBBPA and two benzene rings, TBBPA exhibited a stronger π - π interaction and its bromination could also enhance its hydrophobic interaction with GO.



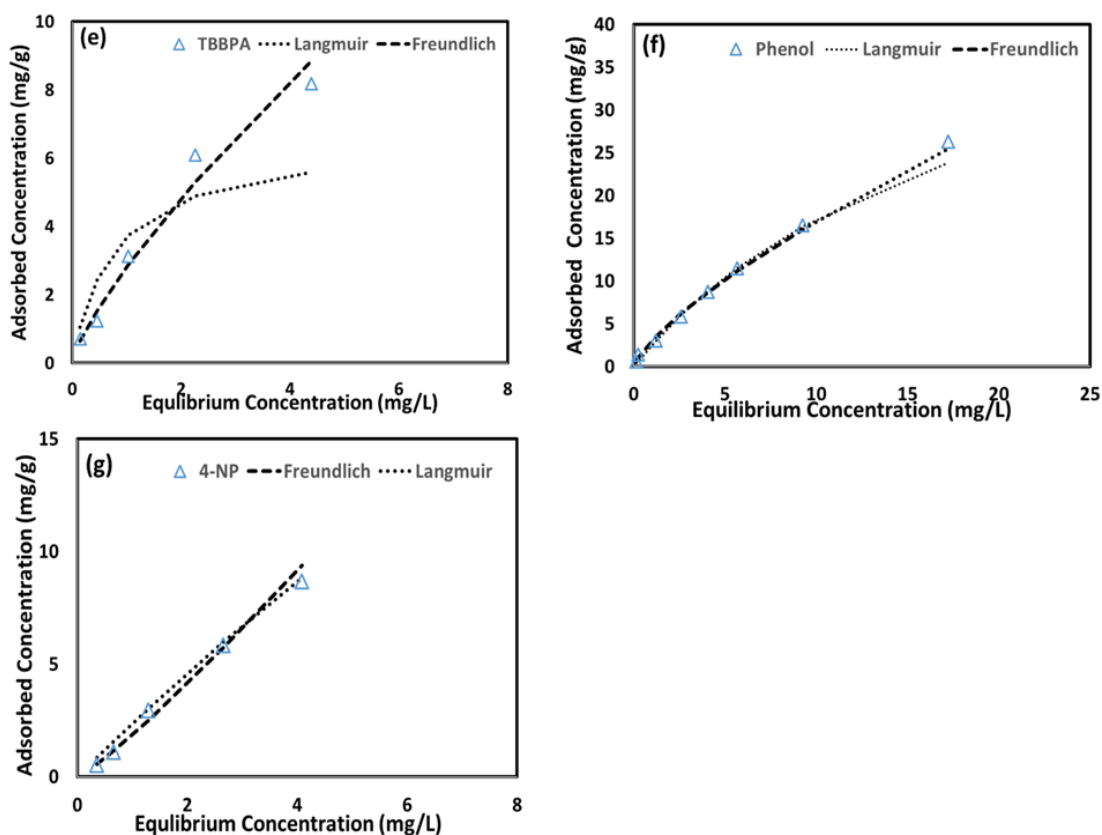


Figure 4. 3: Adsorption isotherms of (a) 4-CP, (b) 2,4-DCP, (c) 2,4,6-TCP, (d) phenol, (e) 4-NP (f) BPA and (g) TBBPA on GO. The dotted line represents the Freundlich model and the dashed line represents the Langmuir model

4.2.4 Adsorption mechanism of phenolic compounds onto graphene oxide

The adsorption mechanisms of organic contaminants on graphene-based materials at the molecular level are dependent on the structure of the adsorbates. The π - π interaction, hydrophobic effect, hydrogen bonding, and electrostatic interaction are commonly used to demonstrate the adsorption mechanism of organic chemicals on GO. GO as an adsorbent have probable application in the effective removal of contaminants with benzene rings at lower concentration due to strong π - π interaction. In the present study, adsorption affinities for the three chlorinated compound followed a similar trend, with a small difference in the order of TCP>DCP>CP, the small difference is due to the π - π electron donor-acceptor (EDA) interaction with graphene oxide. The adsorption of PCs on graphene oxide occurred in the order of and TBBPA > phenol > 4-NP > 2,4,6-TCP > BPA > 4-CP > 2,4-DCP, which generally followed the same trend of chemicals'

K_{ow} except for phenol. Since these PCs have a similar affinity toward GO, adsorption mechanism was mainly dominated by Van der Waals force. The main mechanism governing the interaction could also be due to the π - π interaction as each carbon atom of GO has a π -electron perpendicular to the GO surface Apul et al. (2013); Zhang et al. (2013). Furthermore, the availability of adsorptive sites on GO for the adsorption of PCs is provided by the surface properties and defects such as oxygen moieties. The interaction of hydrogen-bond donor and acceptor (HDA) also contributed the adsorption. Since GO nanoflakes had oxygen carrying functional groups, PCs, OH-containing compounds, have a strong HDA ability thus exhibiting HAD interaction with GO surface. The greater interactions between TBBPA with GO could result from its highest hydrophobicity and stronger π - π interaction because of its two fused benzene rings whereas the chlorinated PCs have just one benzene ring (Wang et al. 2014a).

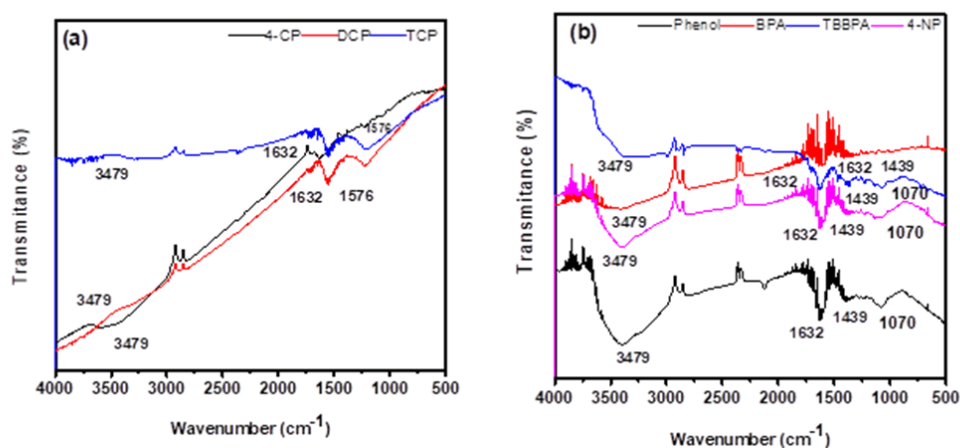


Figure 4. FTIR spectra after adsorption of (a) 4- Chlorophenol, 2,4- dichlorophenol and 2,4,6 trichlorophenol and (b) bisphenol- A, phenol, TBBPA and 4- nonylphenol on GO.

After adsorption of PCs onto GO, the peak intensities were modified in the whole range of the interaction between PCs and GO (Fig.4.4 a and b). The interaction between PCs and the oxygen-carrying functional group was confirmed by the presence of peaks at 3479 cm^{-1} , 1632 and 1070 cm^{-1} respectively, these peaks confirm the adsorption of PCs were held on GO due to the hydrogen bonding. The FTIR spectra of PBA, phenol, TBBPA, and 4-NP on GO exhibit bands at 1439 cm^{-1} due to the stretching vibrations

of aromatic rings, while the peak at 3479 cm^{-1} is due to -OH stretching (Lin et al., 2012) (Lin and Xing 2008). A small shift in the region between $1500\text{-}1700\text{ cm}^{-1}$ were observed after adsorption, (Zhou et al., 2017b) observed that the -OH bond of single-walled carbon nanotubes after adsorption from 3320 to 3479 for phenol and aniline. (Phatthanakittiphong et al., 2016) observed the shift in peak intensity from 1620 cm^{-1} to 1632 cm^{-1} , confirming the π - π interaction to be the main governing mechanism for adsorption of BPA on GO, similar to our study. The π – π interaction, hydrophobic effect, and hydrogen bonding are commonly used to interpret the adsorption mechanism of organic pollutants on carbon-based materials. PAH was demonstrated to adsorb on graphene-based material mainly due to π – π interaction (Wang and Chen 2015).

Solution pH will have an influence on the surface charge of the adsorbent and also the dissociation state of the organic compound related to its dissociation constants (pK_a). The original pH of 2,4,6- TCP solution was around 5, adding GO to the solution had no much change in the pH of the solution. In the present work, tested compounds have different pK_a values, among these 2,4,6-TCP has the lowest pK_a (6.18), and TBBPA has two proton bonding sites, carboxyl, and piperazine group with pK_a values of 7.5 and 8.5, leading to the consideration of pH effect (Zhang et al., 2013). For 2,4,6-trichlorophenol its natural form prevails at $\text{pH} < 6.18$ and anionic form at $\text{pH} > 6.18$. Adsorption capacity of 2,4,6-TCP on GO nanoflakes from Fig 4.5a the adsorption capacity values of 2,4,6-TCP showed some changes with increasing pH still it reached the pK_a value, followed by a slight decrease in the adsorption capacity. At the studied pH range of solution, TCP could not deprotonate due to its initial solution pH less than its pK_a value. Considering the properties of GO the mechanism can be explained due to the hydrogen bonding or π - π interaction. Investigating the solution pH over pH_{zpc} (Liu et al., 2014), the enhancement could result from its hydrophobic interaction with GO and also HDA interaction by the hydrogen-bond donor of protonated TCP. In case of TBBPA, its uptake decreased with decrease of TBBPA molecular, main adsorption mechanism is due to π - π electron and hydrophobic interaction, in the range of $\text{pH} > 7$, TBBPA adsorption declined and then increased due to the anionic form being less hydrophobic than the molecular form (Gao et al., 2012).

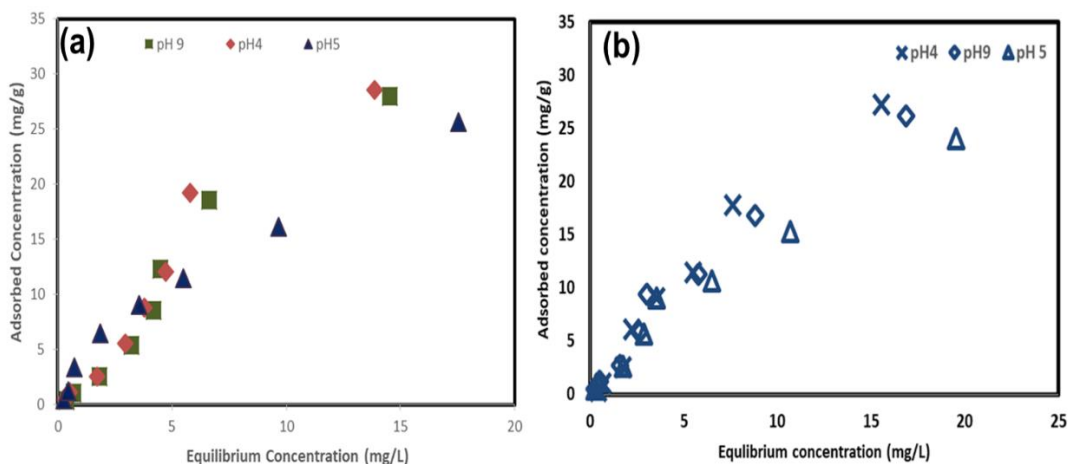


Figure 4.5: (a) The effect of pH on adsorption isotherms of 2,4,6-TCP (b) The effect of pH on adsorption isotherms of TBBPA on GO

$\pi - \pi$ electron donor-acceptor interactions have been widely used to address the adsorption of organic compounds on the graphene surface, a hydroxyl group (-OH) a strong electron- rich group can result in electron conjugation with the benzene rings making them electron rich. The electron-rich benzene ring can interact with the positively charged groups of rGO, leading to high adsorption capacity for rGO (Yu et al. 2016b). (Chen et al., 2015) reported that $\pi - \pi$ EDA interactions would lead to stronger adsorption of hydroxyl and amino-substituted compounds on carbon nanotubes, and they also reported that there are more defects in rGO compared to GO and graphene resulting in higher adsorption. The trend with the carbon-based materials showed higher adsorption for rGO than GO, which was found to be in correlation with SSA as rGO ($227.82 \text{ m}^2/\text{g}$) was 10 times higher than GO ($2.02 \text{ m}^2/\text{g}$). Elimination of oxygen molecules on graphene-based material can enhance the interaction between $\pi - \pi$ system of rGO and with that of the organic compound. In the present study the adsorption of phenol, BPA and TBBPA on graphene-based materials occurred in the order of TBBPA > BPA > phenol, which followed the same trend of chemicals' K_{ow} . As the chemicals follow the trend of K_{ow} , the main mechanism governing the adsorption process may be due to hydrophobic interaction. The adsorption mechanism of graphene materials at molecular level are dependent on the structure of the adsorbate, and the surface of the carbon based material due to its heterogeneity. The incorporation of

oxygen carrying functional groups will induce hydrogen bonding between the pollutant and the surface of GO, while the absence of O- functional groups will lead the possibility of π interaction. Adsorption of TBBPA on graphene-based materials displaced higher adsorption capacity towards rGO than GO. $\pi - \pi$ interaction, hydrophobic effect, and hydrogen bonding are commonly used to interpret the adsorption mechanism of organic pollutants on carbon-based materials.

4.3 Reactivity of Graphene Oxide and Reduced Graphene Oxide toward Tetrabromobisphenol A, Bisphenol A, and Phenol from Water.

4.3.1 Characterization of GNS

Selected chemical properties of the two adsorbents are listed in Table 4.3. The C/O is used to indicate the polarity and hydrophobicity of adsorbents. The morphology of GO and rGO are illustrated in SEM and TEM images (Figure 4.6.a, b,c,and d). XRD spectra (Figure 4. 7a) is an important tool for characterization of GO and rGO, the intense peak of graphite (26.5), rGO (24.6) and GO (10.1), clearly indicating the confirmation of the material we synthesized, which are in good agreement with the supporting data (Mishra et al. 2014). In Raman spectra (Fig. 4.7c) two prominent spectra are seen in G band (1597, 1607 and 1595 cm^{-1}) and D band (1365, 1363 and 1354 cm^{-1}) for graphite, GO and rGO. There is a shift in G band for GO to a higher wave number due to oxygenation of graphite resulting in the formation of sp^3 carbon atoms, whereas the broadened D band is due to the reduction in the size of the sp^2 domain. The ID/IG ratio is higher for GO due to the formation of oxygen-carrying functional groups, in case of rGO due to the formation of sp^2 domains that are newly formed during the reduction (Perumbilavil et al., 2015).

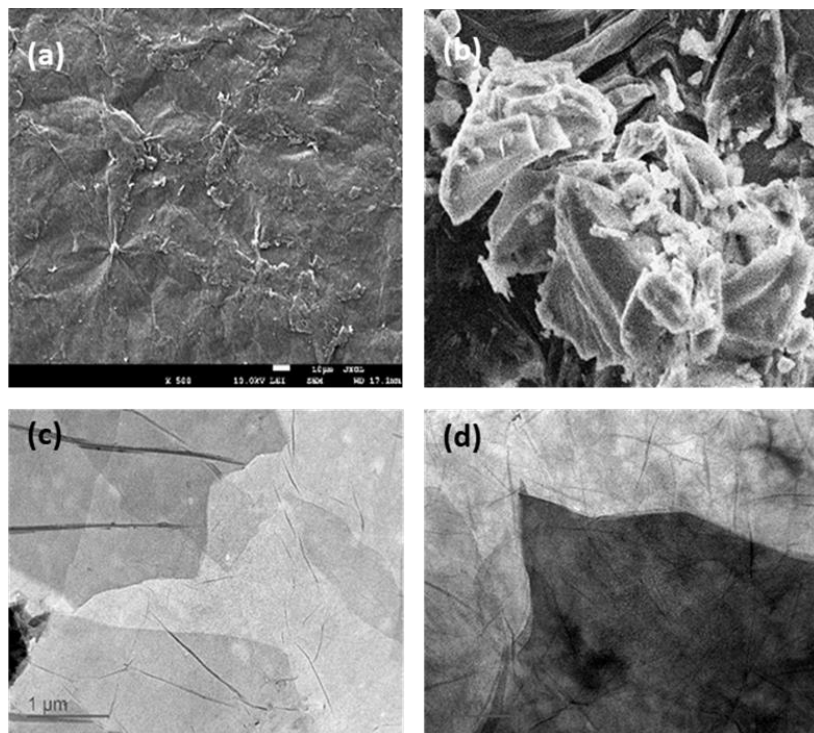


Figure4. 6: (a) SEM and (b) TEM of rGO. (c) SEM and (d) TEM of GO

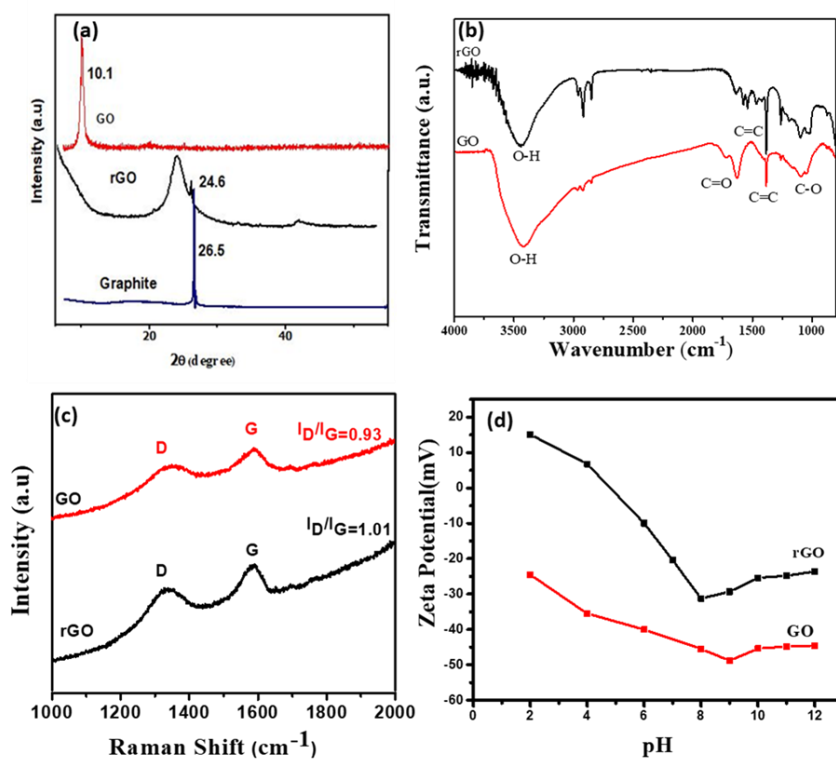


Figure4. 7: (a)XRD of graphite, rGO and GO, (b) FTIR, (c) Raman spectra and (d) Zeta potentials of GO and rGO

Table 4.3 Selected physicochemical properties of carbonaceous materials.

Carbonaceous materials	Elemental composition ^a			SSA(m ² /g) ^b	I _D /I _G ^c
	C	O	O/C		
GO	53	42	0.79	2.02	0.93
rGO	80	16	0.2	227.82	1.01

^a Analyzed using Energy-dispersive X-ray spectroscopy

^b Specific Surface Area measured using the Brunauer–Emmett–Teller (BET) method

^c Intensity at D to intensity at G band analyzed with Raman spectrometry.

4.3.1 Adsorption kinetics of TBBPA, BPA, and phenol on GNS

The adsorption kinetics of TBBPA, BPA, and phenol on GO and rGO was shown in Figure 4.8. The adsorption of these chemicals on GO showed rapid adsorption in the first 60 mins, then followed a slow pattern of up to 200 mins, finally reached equilibrium at 480 mins. As shown in Fig 4.8 b for rGO, adsorption was rapidly increased in the first 5 min and adsorption equilibrium was reached in 120 min, which is similar to other researches (Wang et al. 2014c). A slight higher adsorption amount of these compounds was observed for rGO compared to GO, which could be due to the large surface area of rGO and its sheet-like structure mentioned in the literature (Chen and Chen 2015a).

The kinetic results were fitted to two models, pseudo- first- order and second order rate kinetics. The correlation coefficient (R^2), and the rate constants for each chemical were estimated (Table S2). The good regressions of R^2 (0.88-0.99) were observed using both pseudo-first-order and pseudo-second-order kinetic models, but a better fit was observed for the pseudo-second-order kinetic model, suggesting that the sorption of TBBPA, BPA, and phenol onto these adsorbents depends on the amount of the solute adsorbed on the surface of adsorbent and the amount adsorbed at equilibrium (Bele et al. 2016). The adsorption capacities estimated using pseudo-second-order kinetic model $q_{e, cal}$, also matched with the $q_{e, exp}$, the adsorption kinetic constant for rGO (11.7, 10.5, 12.2 g/mg min⁻¹ for phenol, BPA, and TBBPA, respectively) was higher than GO (

2.22, 9.87, 5.64 g/mg min⁻¹) thus confirming that rGO exhibited faster adsorption kinetics than GO (Kwon et al., 2015). The fast adsorption may be due to the hydrophobic layers of graphene on rGO as the hydrophobic surface can induce faster adsorption (Xu et al., 2012).

Similar adsorption kinetics was observed for phenol (Zhou et al., 2017a)(Yu et al. 2017a), where the phenol was adsorbed on the rGO surface easily, indicating the fast sorption kinetics of graphene-based materials. In the case of BPA, faster sorption within 5 mins was observed, which could result from the difference in the synthesis procedure of rGO and their low dosage. On the other hand, (Konicki et al., 2017) studied the sorption of dyes on GO and indicated that the boundary layer effect resulted from the intraparticle diffusion (Kamila Mijowska, 2017). In the graphene-based materials we synthesized, the fast adsorption of these phenolic compounds in accordance with the adsorption kinetic studies of aromatic compounds on graphene indicated the efficiency of the carbon-based materials in the adsorption.

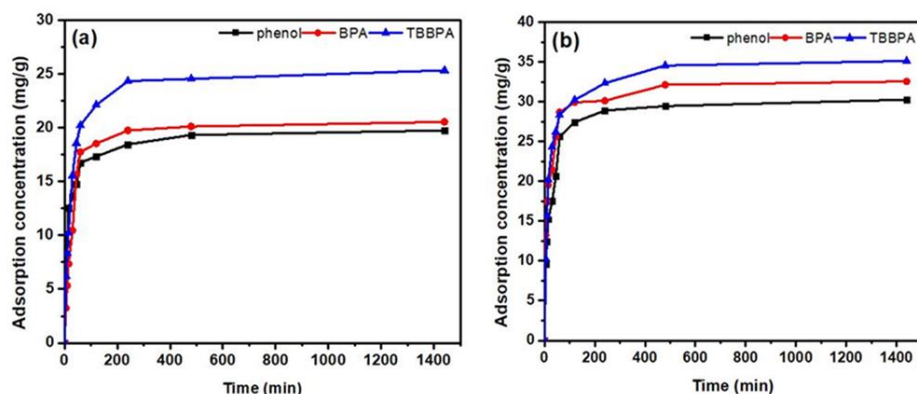


Figure 4. 8: (a) Adsorption kinetics of phenol, BPA and TBBPA on GO and (b) that of phenol, BPA and TBBPA on rGO.

4.3.2 Adsorption isotherms of TBBPA, BPA, and phenol on GNS

The adsorption of the three single compounds on rGO or GO were studied with various initial concentrations at 288K. In Figure 4.9, when the aqueous concentration was around 8 mg/L at 288K, the adsorption of BPA on both GO and rGO reached a plateau at 8 mg/g and then raised around 10 mg/g with the increase in the equilibrium aqueous concentration. Adsorption isotherms of phenol and TBBPA on GO and rGO had a similar pattern. Obviously, the uptake of TBBPA, BPA, and phenol on GO and rGO

increases with the increase in their aqueous concentration and then reach equilibrium, this is due to that higher the concentration with a more strength driving force can provide to overcome the mass transfer resistances of actives sites where did not reach equilibrium. These kinds of non-linear adsorption isotherms were generally found for the adsorption of chemicals from solutions on a solid surface.

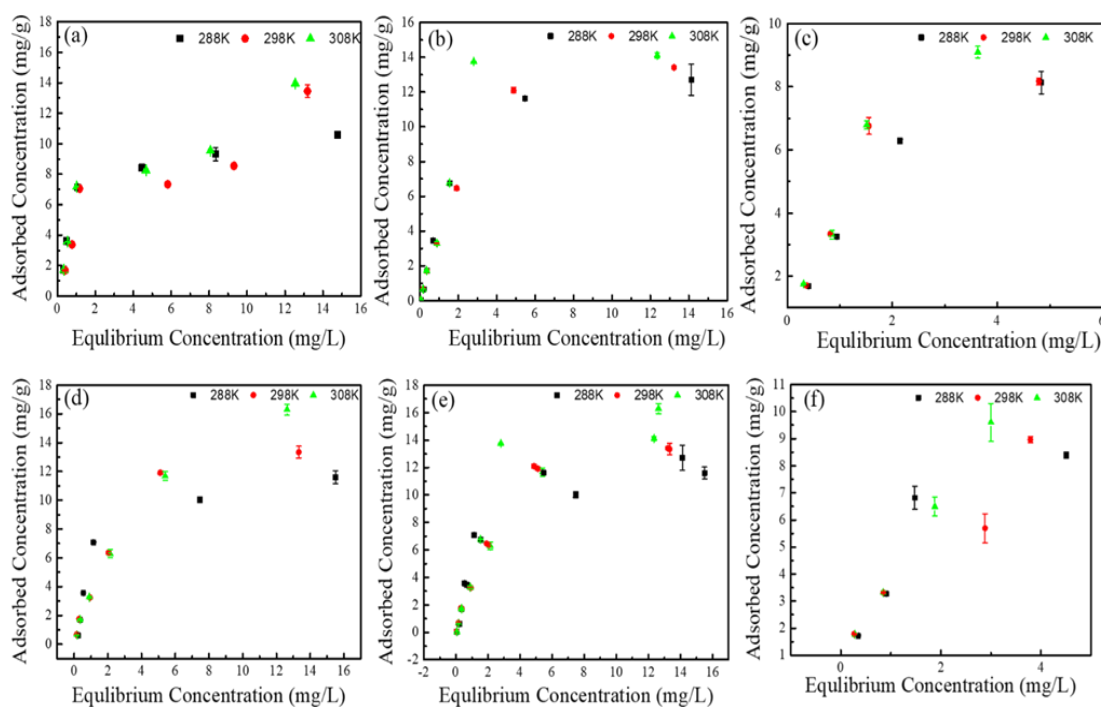


Figure4.9: Adsorption isotherms of (a) phenol, (b) BPA (c) TBBPA on GO and (d) phenol, (e) BPA, (f) TBBPA on rGO under different temperature conditions.

4.3.3 Effect of temperature on adsorption isotherms

Thermodynamic parameters provide information about the energy changes associated with adsorption. The constants listed in Table 4.5 were determined through linearized data as shown in Figure 4.10. From Table 4.5, the negative values of ΔG indicate the feasibility in the process and also the spontaneous nature of adsorption (Yu et al. 2014). At the same interval, Gibbs free energy was close with the increase from 288 to 308K proving temperature of the solution on the adsorption was insignificant. This was similar to the result obtained for the adsorption of TBBPA with reduced-graphene aerogel and GO. The decrease in negative value with an increase in temperature implies

the spontaneous nature of adsorption of TBBPA, BPA, and phenol on GO/rGO. Yu *et al.* observed the similar sorption pattern inversely proportional to temperature for phenol adsorption on rGO, demonstrating higher temperature was effective for removal of phenol.

The adsorption enthalpies of phenol, BPA, and TBBPA on GO were 6.09, 5.82 and 11.84 kJ/mol, respectively (Table 4.5). The adsorption enthalpies of phenol, BPA, and TBBPA on rGO were 2.25, 4.19 and 1.09 kJ/mol, respectively (Table 4.5). The adsorption enthalpies of these compounds on GO were higher than those on rGO, indicating more adsorption energy was needed to GO than rGO. Overall, the ΔH values in the present work lie between 0 and 20 kJ mol⁻¹, stating the dominance of physisorption, which was also observed by Wang *et al.* Furthermore, the positive values of our ΔH indicate that the adsorption process is endothermic in nature (Kyzas *et al.*, 2013). The adsorbate would displace more water molecules from the surface resulting in the endothermic reaction, thus ΔH° would be positive. Positive values of ΔS indicate the stability in the adsorption process, with minimal structural change at the solid-liquid boundary. The low positive values of ΔS demonstrate that the randomness is moderately increased during the adsorption process, also relating to the degree of freedom of the adsorbed (Zhang *et al.* 2013). The positive change in enthalpy for a positive change in entropy was observed for the adsorption of rGO on phenolic compounds which was also observed (Young Ku, 2000). Different surface properties of GO and rGO could account for different sorption mechanisms (Li *et al.* 2018)

Table 4.4. Isotherm constants for adsorption of phenol, BPA and TBBPA on GNS

Compound	Sorbate	Temperature	Langmuir			Freundlich		
			q_m (mg/g)	b	R^2	K_f	$1/n$	R^2
Phenol	GO	308	19.24	0.45	0.97	3.23	0.65	0.97
		298	16.63	0.30	0.98	3.71	0.62	0.89
		288	16.00	0.34	0.99	4.08	0.70	0.95
BPA		308	20.98	0.08	0.95	4.27	0.85	0.91
		298	18.68	0.10	0.98	5.30	0.83	0.97
		288	16.68	0.23	0.97	3.47	0.62	0.96
TBBPA		308	13.91	0.32	0.88	4.28	0.38	0.73
		298	17.26	0.29	0.91	3.75	0.46	0.67
		288	13.55	0.42	0.87	4.26	0.46	0.75
Phenol	rGO	308	16.06	0.65	0.97	3.75	0.64	0.89
		298	12.74	1.01	0.97	3.66	0.56	0.96
		288	13.31	0.37	0.97	4.15	0.71	0.98
BPA		308	23.20	0.02	0.95	3.24	0.65	0.91
		298	17.30	0.09	0.98	2.56	0.92	0.97
		288	17.07	0.03	0.95	3.47	0.73	0.91
TBBPA		308	11.18	0.01	0.98	3.50	0.43	0.97
		298	8.22	0.18	0.96	3.63	0.80	0.96
		288	14.77	0.13	0.92	6.83	0.76	0.95

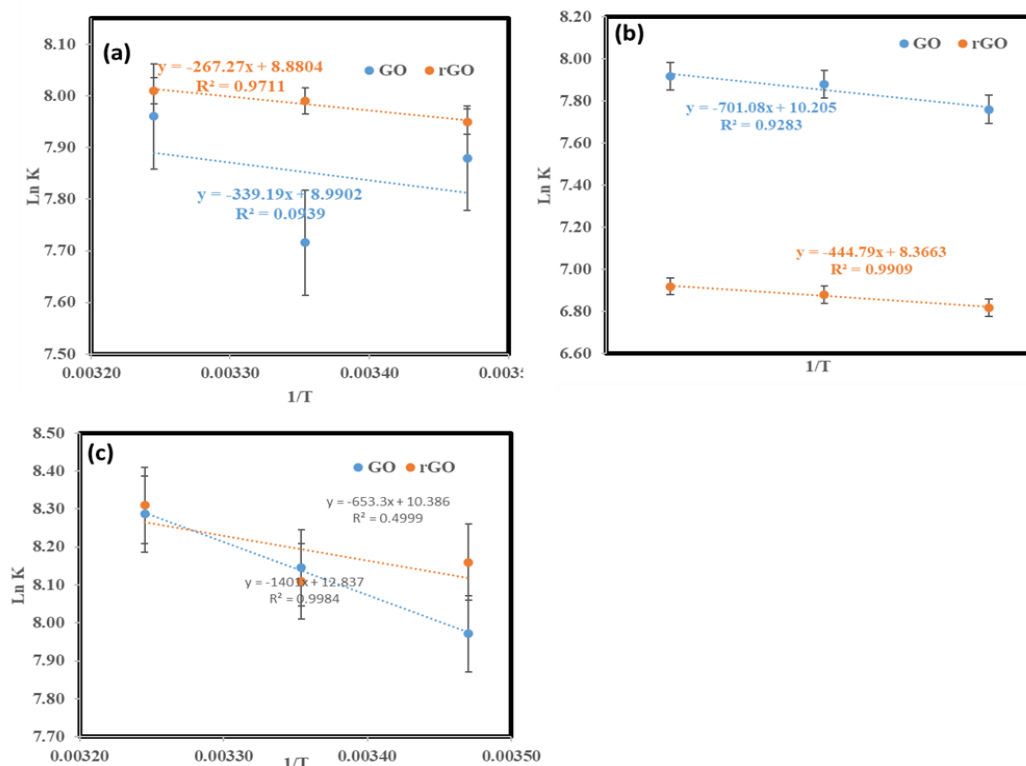


Figure 4. 10: Plots of $\ln K$ versus $1/T$ for adsorption of (a) phenol, (b) BPA and (c) TBBPA on GO and rGO.

Table 4. 5. Adsorption thermodynamic parameters for phenol, BPA and TBBPA on rGO and GO

Adsorbent	Compound	ΔG (kJ/mol)			ΔH (kJ/mol)	ΔS (J/(K mol))
		288 K	298 K	308 K		
GO	Phenol	-18.86	-19.11	-20.38	2.82	0.07
	BPA	-18.58	-18.86	-18.95	5.82	0.08
	TBBPA	-19.08	-20.18	-21.21	11.84	0.10
rGO	Phenol	-19.03	-19.78	-20.51	2.25	0.07
	BPA	-18.66	-18.83	-18.93	4.19	0.07
	TBBPA	-19.54	-20.08	-21.28	5.35	0.08

4.3.4 Possible Adsorption mechanism

The adsorption mechanism of graphene materials at molecular level are dependent on the structure of the adsorbates, and the surface of the carbon based material due to its heterogeneity. The incorporation of oxygen-carrying functional groups will induce hydrogen bonding between the pollutant and the surface of GO, while the absence of O- functional groups will lead to the possibility of π interaction. Adsorption of TBBPA on graphene-based materials displaced higher adsorption capacity towards rGO than GO. $\pi - \pi$ interaction, hydrophobic effect, and hydrogen bonding are commonly used to interpret the adsorption mechanism of organic pollutants on carbon-based materials. The strength of $\pi - \pi$ interaction, hydrophobic interaction and hydrogen bonding depend on octane-water distribution coefficient (K_{ow}), hydrogen-bonding acceptor ability (β_m) and π -polarity ability (π^*), the values for TBBPA ($\log K_{ow} = 0.81$, $\pi^* = 0.28$ $\beta_m = 0.33$) 31. The hydrogen bond interactions between TBBPA and oxygen-carrying functional groups of rGO, left the benzene ring to face the water molecular in the system. Oxygen carrying functional groups on GO can lead to the formation of hydrogen bonding with the water molecule, thus making GO more hydrophilic and decreasing the adsorption capacity 32 compared to rGO.

PAH was demonstrated to adsorb on graphene-based material mainly due to $\pi - \pi$ interaction. Chen et al also reported that $\pi - \pi$ EDA interactions would lead to stronger adsorption of hydroxyl and amino-substituted compounds on carbon nanotubes, and also reported that there are more defects in rGO compared to GO and graphene resulting in higher adsorption. π electron rich regions present on the graphene layers interact with electron acceptor substance by $\pi - \pi$ interactions, have been widely used to address the adsorption of organic compounds on the graphene surface. The hydroxyl group (-OH) a strong electron- rich group can result in electron conjugation with the benzene rings making them electron rich. The adsorptive sites available on graphene based materials are measured by the surface properties, the edges and surface of GO have abundant oxygen – carrying functional groups that include O-H/C-O, C=O and C(O) O, that make the surface highly hydrophilic and hinder the $\pi - \pi$ interaction. The trend with the carbon-based materials showed higher adsorption for rGO than GO, which was found to be in correlation with SSA as rGO (227.82 m²/g) was 10 times

higher than GO (2.02m²/g). Elimination of oxygen molecules on the graphene-based material can enhance the interaction between π - a system of rGO and with that of the organic compound.

4.4 Investigate the debromination of TBBPA by graphene-based materials

4.4.1 Removal of TBBPA by GO and rGO

A series of systematic experiments were performed to evaluate the removal capacities of TBBPA by GO and rGO. After the batch experiments, we found additional peaks along with the parent compound, which were confirmed to be the by-products of TBBPA. The release of bromide ion was confirmed by IC analysis, which further confirms the debromination of TBBPA. The adsorption kinetics were carried out to understanding the rate processes that occur in the aqueous solution. The effect of initial concentration on the adsorption capacity for TBBPA on GO showed rapid adsorption in the first 60 mins, then followed a slow pattern up to 200 mins, finally attain equilibrium at 480 mins. As shown in Fig. 4.11 rGO adsorption was rapidly increased in the first 5 min and adsorption equilibrium was reached in 120 min giving maximum adsorption capacity (Wang et al. 2014c). Similar results were obtained for the adsorption of phenol on rGO during the initial state and lower adsorption rate at later stage with the increase in time 20. Increase in the adsorption capacity was observed for rGO compared to GO, due to the large surface area, and sheet-like structure (Yu et al. 2017a).

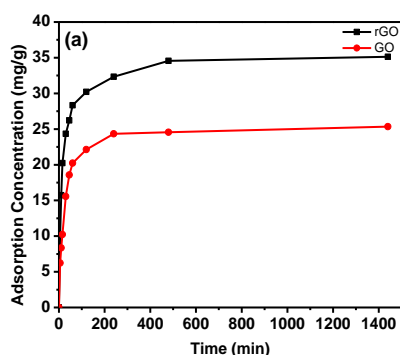


Figure4. 11: Adsorption kinetics of TBBPA on rGO and GO.

Table 4.6 Kinetics constant for adsorption of TBBPA on rGO and GO.

Carbonaceous material	Pseudo-first-order			Pseudo-second-order		
	k1 (min ⁻¹)	q _e (mg/g)	R ²	k ₂ (g/mg min) (10 ⁻³)	q _e (mg/g)	R ²
rGO	0.044	35.60	0.95	2.52	24.70	0.96
GO	0.059	25.57	0.92	5.64	22.83	0.94

The results were fitted to both the models, the correlation coefficient (R^2) and the rate constants for each chemical was found Table 4.6. The kinetic parameters were calculated and fitted using pseudo- first- order and second order rate kinetic models, good linear fit R^2 of (0.88-0.99) were observed using both pseudo-first-order and pseudo-second-order kinetic models, but a better fit was observed for the pseudo-second-order kinetic model. Adsorption isotherm is used to describe the relationship between the quantity of adsorbate per unit of adsorbent at a constant temperature. The adsorption isotherms of TBBPA onto GO and rGO were studied at pH 5.5, under different temperature (288K, 298K, and 303K) with various initial concentrations. In Figure 4 the uptake of TBBPA on GO and rGO increases with the increase in the concentration and then reach equilibrium, this is due to, higher the concentration more strength driving force will provide to overcome the mass transfer resistances of actives sites not reach equilibrium (Wu et al., 2016).

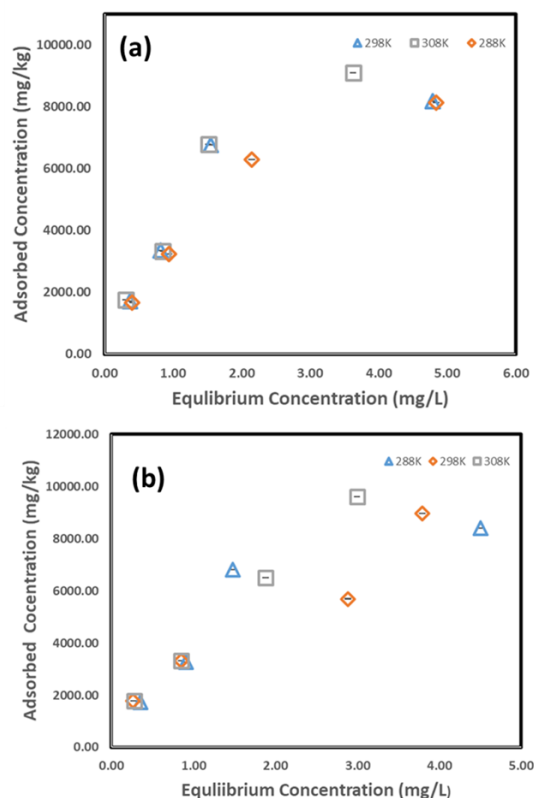


Figure4.12: Adsorption isotherms of TBBPA on (a) GO and (b) rGO under different temperature conditions

Langmuir and Freundlich models were employed to gain insight into the adsorption thermodynamic behaviour. From (Table 4.7 and Fig 4.12), the Langmuir model fitted the sorption isotherms better than the Freundlich model, and the maximum (Q_{max}) adsorption capacity was similar to the experimental data at 288,298 and 308K. The adsorption process suggests that adsorption behaviour is governed by monolayer adsorption on the homogenous surface.

On the basis of Fig. 4. 12 it is found that adsorption capacity followed the order $GO < rGO$ indicating the heterogeneous adsorption sites is higher for rGO compared to graphene materials (Chen and Chen 2015b). rGO displayed slightly higher adsorption capability towards TBBPA compared to GO, the saturated adsorption amounts (q_m) of rGO from Langmuir model are 14716.91 mg/kg towards TBBPA higher than GO 13550.39 mg/kg as shown in (SI Table S7). $\pi - \pi$ interaction between the aromatic structure of the compound and sp^2 regions of rGO, and also the electrostatic

interactions between the charged compound and the oxygen-containing groups of rGO are the main governing mechanisms to shows a higher adsorption capacity than GO.

Table 4.7 Isotherm constants for adsorption of TBBPA on rGO and GO

Adsorbent	Temperature	Langmuir			Freundlich			q_m/SA (Kg/m ²)
		q_m (mg/kg) R^2	b		K_f	1/ n	R^2	
GO	308	13910.17	0.45	0.97	4080.722	0.70	0.95	6.88
	298	17260.60	0.30	0.98	3718.55	0.622	0.89	8.54
	288	13550.39	0.34	0.99	3263.13	0.65	0.97	6.70
rGO	308	11189.50	0.65	0.97	4155.98	0.71	0.98	0.049
	298	8227.22	1.01	0.97	3669.93	0.56	0.96	0.036
	288	14716.91	0.37	0.97	3751.87	0.64	0.89	0.064

Thermodynamic parameters provide information about the energy changes associated with adsorption. The adsorption capacity increased with increase in temperature, indicating high temperature is suitable for the adsorption of TBBPA. The projected constants are listed in Table 4.8. The negative value of ΔG° , indicates the feasibility in the process and also the spontaneous nature of adsorption (Ren et al., 2015). At the same interval, Gibbs free energy was close with the increase from 288 to 308K proving temperature of solution on the removal was insignificant. This was similar to the result obtained for the adsorption of TBBPA with sodium bisulfite reduced- graphene aerogel and on graphene oxide (Zhang et al., 2018; Zhang et al., 2013).

Table 4.8. Adsorption thermodynamic parameters for TBBPA on rGO and GO

Temperature (K)	GO			rGO		
	ΔG (kJ/mol)	ΔH (kJ/mol)	ΔS (kJ/mol K)	ΔG (kJ/mol)	ΔH (kJ/mol)	ΔS (kJ/mol K)
308	-19953			-20352		
298	-20925	11.28	0.10	-21827	9.56	0.10
288	-22124			-22419		

4.4.2 Products and pathways of TBBPA transformation by GO and rGO

Transformation of TBBPA by GNS nanoparticles involves heterogeneous reaction, during which the TBBPA molecule is adsorbed on the surface of the nanoparticle and undergo a subsequent reductive transformation. Four TBBPA transformation by-products were identified in the system when the reaction of TBBPA with GO and rGO after 2-h (tribromobisphenol-A (tri-BBPA), di-bromobisphenol A (di-BBPA), mono-bromobisphenol A (mono-BBPA) and bisphenol A) using HPLC system as shown in (Figure 4.13(a)). The time-dependent concentration of the intermediate and final products at pH 5.5 and concentration of GO and rGO was 15 mg. During the reaction, tri-BBPA, di-BBPA, mono-BBPA, and BPA were observed followed by the removal of TBBPA. The concentration of the intermediates increased first to maxima in sequence and then decreased with time. As mono-BBPA, di-BBPA, and tri-BBPA are not commercially available, their concentrations in the aqueous phase were determined on the mass basis with compensation for the number of bromide ion based on the standard curve of TBBPA and BPA (Li et al., 2016). According to Figure 4.13, the mass balance was the sum of all residual TBBPA, tri-BBPA, di-BBPA, mono-BBPA, and BPA remained during the degradation experiments.

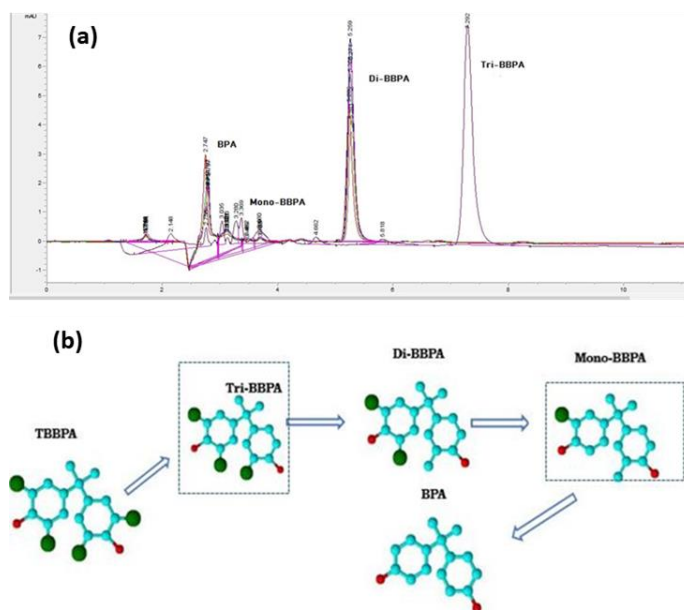


Table 4. 9. Distribution of the intermediates and the final products at a reaction time of 240min

Adsorbent	GO (%)	rGO(%)
TBBPA	10.3	10.2
Tri-TBBPA	8.4	5.97
Di-BBPA	41.5	38.47
Mono-BBPA	25.2	26.1
BPA	12.6	13.9

Similar debromination pathways have also been proposed previously for the transformation of TBBPA by the use of iron-based nanomaterials (Li et al., 2016; Zhang et al., 2012). In this study, the TBBPA and its brominated intermediates are easily adsorbed on the surface of GO and rGO where the C-Br bond is broken and the Br atom is replaced by hydrogen releasing the Br⁻ ion. However, combined debromination of TBBPA and its intermediates was not predictable as all the intermediates were detected shortly (Li et al., 2012). To disclose the degradation mechanism of TBBPA with GO and rGO bromide ion concentration (Br⁻) was recorded using ion chromatography Figure 4.14. In the present study the concentration of Br⁻ was increasing with the increase in the concentration, and the control concentration of Bromide was also recorded showing that 95% of TBBPA was brominated.

4.4.3 Time dependent quantification of by-products

A series of catalysis experiments were performed under dark and ambient condition. The conditions are catalyst dosage 15 ppm, pH 5.5 and TBBPA concentration of 10ppm at room temperature. The same conditions are incorporated throughout the study unless otherwise stated. Graphite, GO and rGO were introduced to evaluate the TBBPA removal efficiency in aqueous solution represented in Figure 4.14a Graphite exhibits negligible TBBPA removal in 4hrs reaction time. No by-products were identified

during the reaction. The removal can be considered as adsorption on the surface of graphite as bromide ions were not detected using IC analysis. TBBPA concentration was markedly degraded with an increase in time, about 85% and 90% and BPA was identified as an end product. LC-MS system was used to identify TBBPA intermediates in the GBMs system. Figure 4.14b-d constitute the m/z values of tri-, di-, and mono-BBPA. The formation of various intermediates was observed at specific retention times using HPLC VWD. Rapid formation of BPA must be considered as an advantage, as BPA is less toxic and readily degradable than the brominated BPA. Overall three by-products as di-bromobisphenol A and bisphenol A were identified using LC-MS system Fig 4.14.

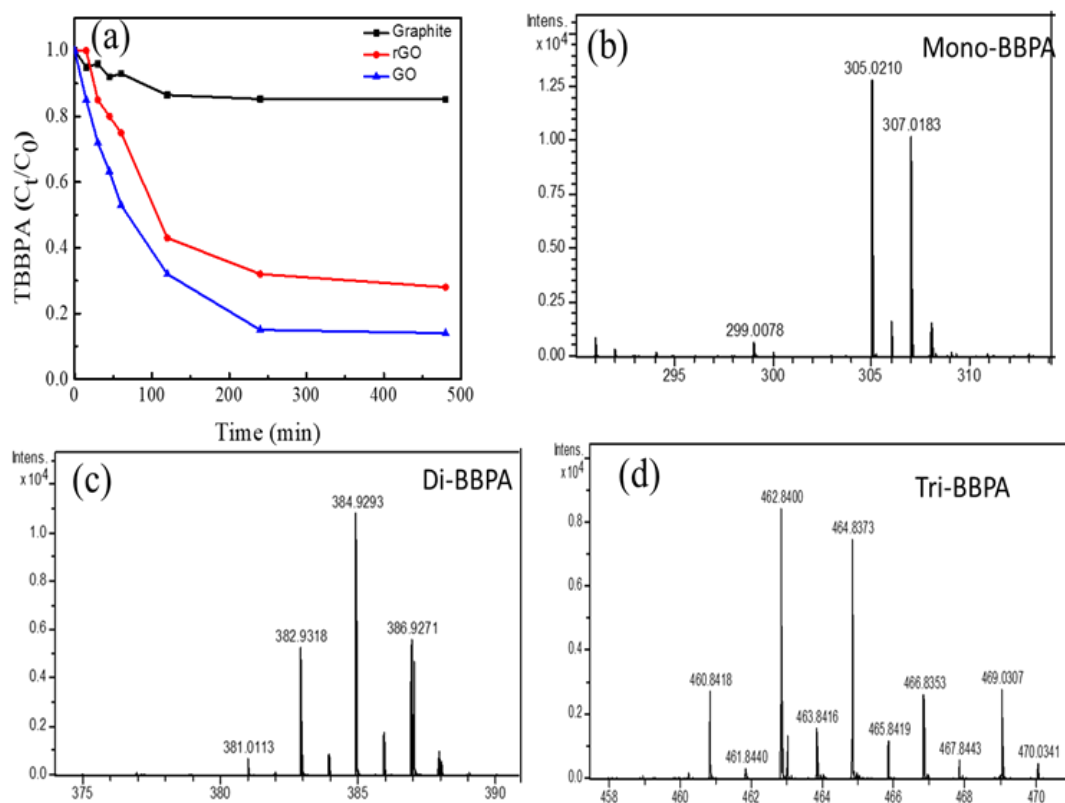


Figure 4.14: TBBPA degradation (a) using graphite, GO and rGO and intermediates m/z profile from LC-MS (b) Mono-BBPA (c) Di-BBPA, and (d) Tri-BBPA.

The time-dependent concentration profile of the final product and the intermediates were detected by LC shown in Figure 4.15a. GO exhibited slightly higher catalytic activity compared to rGO, indicating its major role in the transformation and fate of

TBBPA in environment. Figure 4.15a shows the time-dependent concentration profile of the final product and the intermediates by LC. During the reaction, tri-BBPA, di-BBPA, mono-BBPA, and BPA were observed followed by the removal of TBBPA. The concentration of the intermediates increased first to maxima in sequence and then decreased with time. After 240 mins the concentrations of TBBPA degradation 90% with the formation of tri, di, mono, and BPA was identified as the final product. Furthermore, the detection of bromine ions in solution confirmed the debromination process, the released Br⁻ anions were identified by ion chromatography. In Figure 4.15b we observe that after 480 mins of reaction the concentration of bromide ion in the solution reaches 67 μmol/L while TBBPA concentration reduced to 2 μmol/L under experimental condition. Peng et al observed increase in the bromide concentration and reached around 55 μmol/L showing around 80% degradation in the initial 60 mins, suggesting the debromination phenomenon similar to our findings (Peng et al., 2017). The distribution of the reactant, intermediate and final product varied for GO and rGO, it was observed that maximum percentage of TBBPA was transformed to mono-BBPA, di-BBPA and BPA for both GO and rGO at pH 5.5 within 240 min as reported by (Li et al., 2016), acidic pH revealed the complete and rapid debromination of TBBPA. After 480 mins only 10.3% of TBBPA remained in the solution showing maximum transformation to mono, di-BBPA and finally BPA. Typical catalytic activity was also observed when rGO was introduced into the system. Results are shown in Supporting information. For rGO we observe similar degradation process with slight variation in the formation of BPA and less efficiency compared to GO.

4.4.4 Plausible mechanism for the debromination activity

The presence of oxygen functional groups on GBMs has influence on the production of reactive oxygen species (ROS). To clarify the catalytic mechanism electron spin resonance (ESR) with spin trapping technique DMPO was employed as a tool for identification ROS generated during the reaction system (He et al., 2014). ESR-DMPO was used to detect Superoxide and hydroxide radicles produced on the surface of the catalyst during the reaction. While Superoxide and singlet oxygen were identified and has been proposed as the plausible mechanism for the degradation activity of TBBPA. The ESR using DMPO as a spin trap is shown in Figure 4.16 a, in case of DMPO one

spin adducts were generated by GO system, the four characteristic peaks (1:1:1:1) correspond to the DMPO-OOH duct at room temperature (Maliyekkal et al., 2013). While the solid GO exhibited two curves the narrow signal signify the sigma electron defects, while the broad signal represents the aromatic graphene structure (Kempiński et al., 2017). There are 6 classical peaks generated to the signal of DMPO-OOH with GO and the corresponding g values are 2.0162, 2.0113, 2.0083, 2.0035, 2.0004 & 1.9957. In addition, we also observe C-related dangling bonds at g value of 2.0029 and within the signals range between 2.0022 and 2.0035. In this g range ESR signals form spins in the oxygenated functional groups such as carboxylic, carbonyl and epoxide groups found in GO. After the chemical reduction the functional groups were removed resulting in the reduced spin state density in the quenched ESR signal for rGO shown. While the peak at $g = 2.002$ for rGO represents the super oxygen anion radical ($rGO-OO^-$), formed by the interaction of oxygen molecule and carbon atom of the adjacent carbonyl group at the rGO surface, leading to the activation of oxygen then converting adsorbed O_2 to $rGO-OO^-$. Superoxide radical is short-lived and was not clearly detected by DMPO due to rapid reaction with the H^+ or due to the scavenging by the graphene surface (Figure 4.16b) (Qiu et al., 2014).

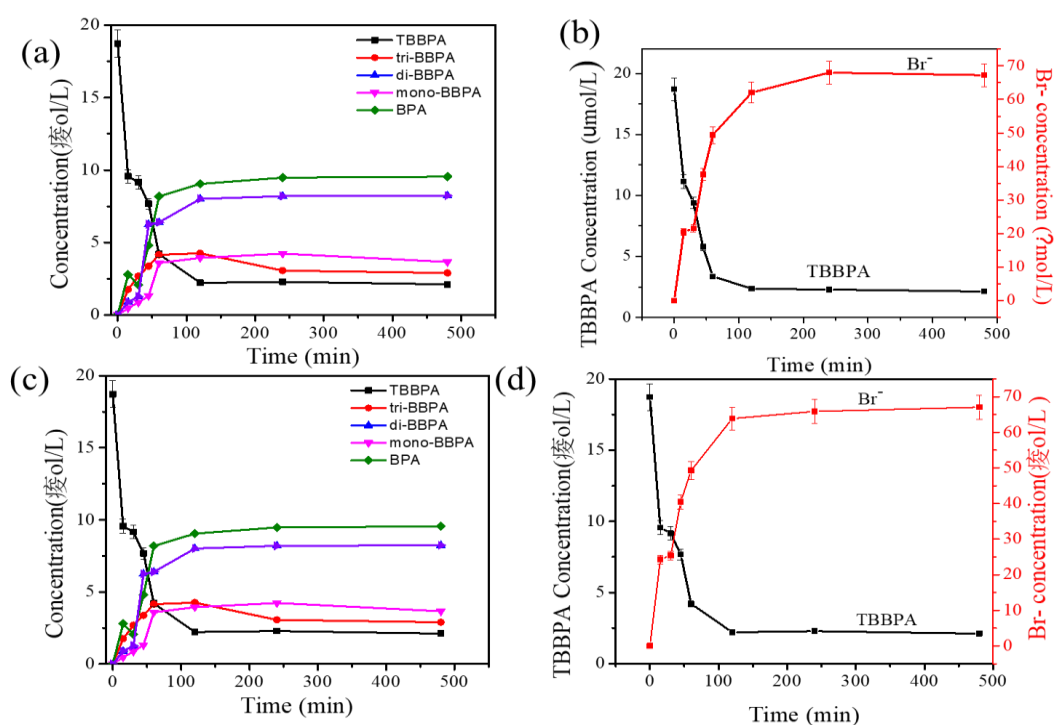


Figure 4.15: (a) Time-dependent profile of TBBPA degradation and (b) evolution of bromide

ion concentration, at pH 5.5, GO and (c) and (d) for rGO, dose 15 ppm, 10 ppm TBBPA.

To explore if $^1\text{O}_2$ was produced during TBBPA debromination, degradation of furfuryl alcohol (FFA) as $^1\text{O}_2$ indicator was examined. $^1\text{O}_2$ steady-state concentration was calculated by testing the degradation of FFA in GBMS using HPLC-UV detector details in SI (Oliva-Teles et al., 2005). The concentration of GBMs used was 15 mg/L with a known concentration of FFA. As shown in Figure 4.16 c we observed that sorption on graphite had no noticeable decay in FFA concentration, but both rGO and GO oxidized FFA to some extent. However, GO show higher decomposition of FFA in the dark compared to rGO due to the presence of oxygen-carrying function groups on the plane. reduction in the consumption of FFA resulting in the release of singlet oxygen. As observed in GBMs system, FFA decomposition in the dark was higher for GO when compared to rGO due to the presence of oxygen-carrying function groups on the plane and no reduction was observed for graphite. This demonstrates that the electron-donating capacity of GO is higher compared to rGO, the lower electron-donating ability will lead to lower reactivity towards TBBPA.

Total Polyphenolic substances (TPC) in GBMs was measured according to the Folin-Ciocalteu (F-C) method. This method measures all form of phenols including monophenols, polyphenols, and lignin phenols (Lv et al., 2018). TPC activity represents the total phenolic composition in GBMs samples. The FC method measures the reduction of the reagent by phenolic compounds that will give rise to the formation blue complex measured at 750 nm against gallic acid as a standard. The FCS reagent forms a blue color with an OH group in the phenolic ring. From Figure 4.16d, we observe total phenols values for GO and rGO and a higher value for Graphite, implicating that these materials possess both free radical scavenging activity and oxidant reducing power (Song et al., 2010).

The active scavengers (O_2^\bullet and O_2) attack the target compound and degrade the pollutants. The reductive transformation of TBBPA is revealed in the debromination process. Dissolved oxygen can react with the defective sites of graphene oxide to produce ROS, primarily O_2^\bullet (Liang et al., 2012). Compared to other ROS O_2^\bullet has high reactivity, and in this study, it can attack C-Br bonds and bromine is released into the solution, these radicles then occupy the position belonging to bromide ions (Zhang et

al., 2019). Subsequent substitution reaction occurs as these products are completely converted to BPA.

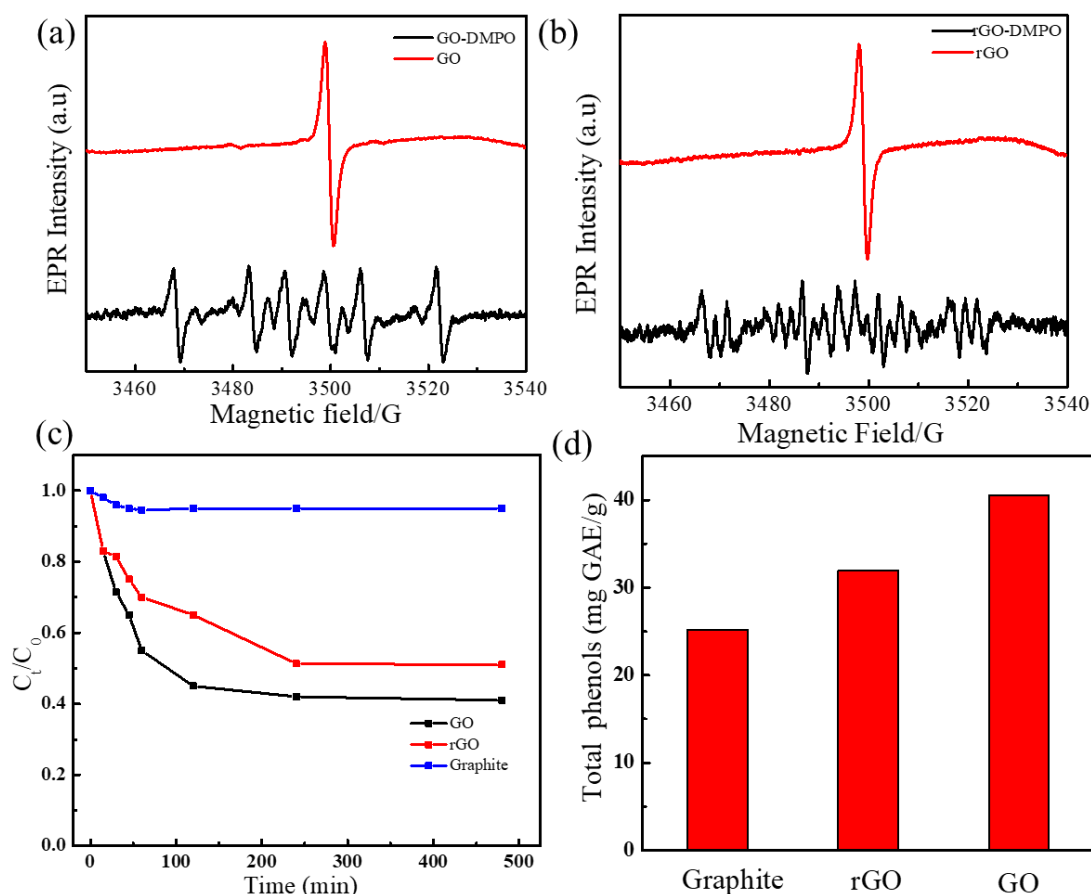


Figure 4.16: ESR signal using DMPO as a spin duct for (a) rGO, (b) GO; FFA analysis with time for (c) GBMs; Total phenols concentration for (d) GBMs

The fraction of adsorption and degradation of TBBPA using GO and rGO is shown in (Figure 4.17), as the concentration of TBBPA increased the adsorption amount on both GO and rGO also increased. The maximum percentage was degradation of about 80 % and 20 % adsorption at different temperatures. Both GO and rGO were favorable for the degradation of TBBPA due to the presence of sp^2 carbon atoms and also π orbitals that help in the formation of delocalized electron network (Fang et al., 2019).

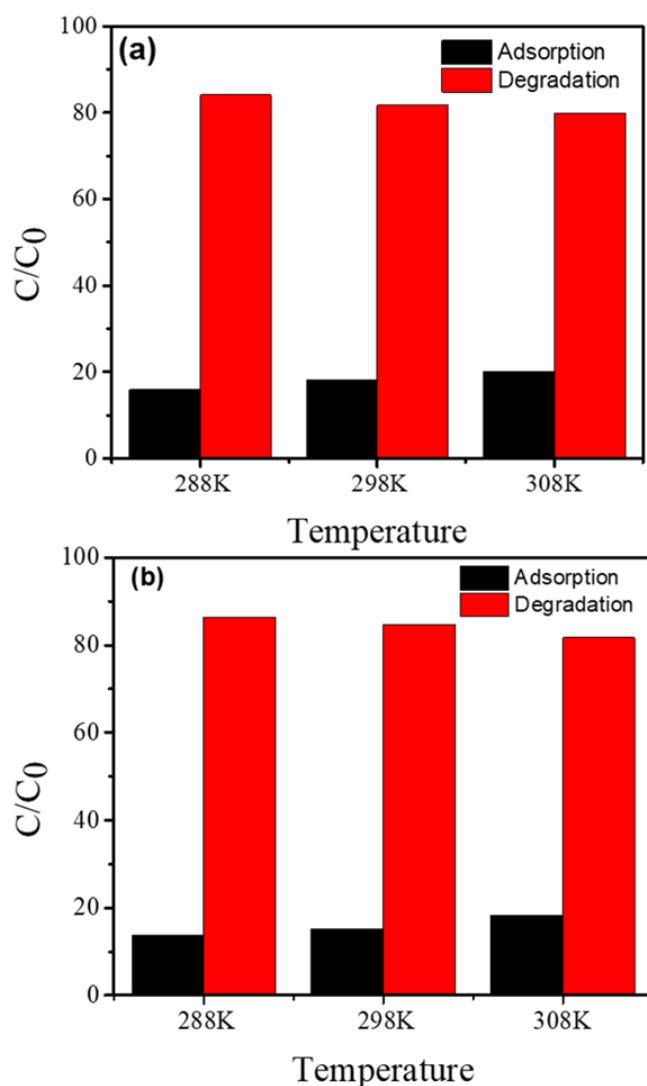


Figure 4.17: Degradation and adsorption of TBBPA reacted with (a) GO and (b) rGO

4.4.5 Reusability of recycled GBMs nanoparticles

The graphene based nanoparticles were separated and reused for ten successive removal cycles of all the pollutants (Fig. 4.18). After each experimental cycle, the samples were analyzed using HPLC to assess degradation. The reusability studies revealed that adsorbent reusability was >93% of its activity up to 5 cycles. The loss was negligible during recovery of GBMs; the adsorbates removal efficiency still retained more 90% even in the fifth cycle. The results indicated that graphene based nanomaterials showed great reusability. The results indicated that the complex was reusable before losing its degradation efficiency and activity. The loss of activity might be due to repeated

washing. The graphene based nanoparticles prepared in the present study removes all adsorbates at a much faster rate and can be effectively used for transformation of phenolic and emerging compounds at industrial scale (M. D et al., 2018).

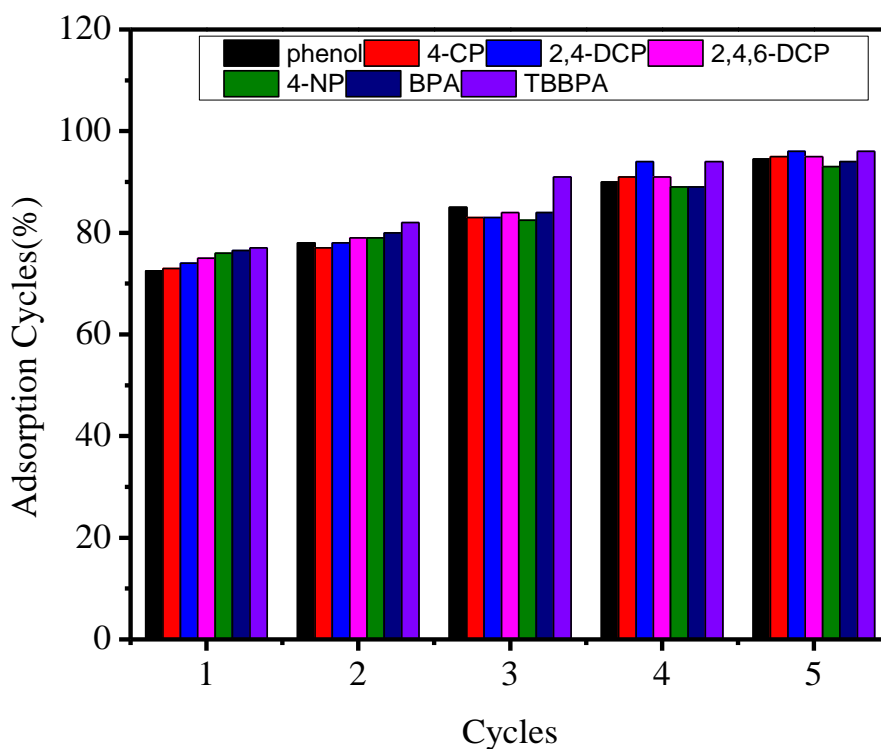


Figure4.18: Cycling experiments with recycled graphene based nanoparticles.

CHAPTER 5

SUMMARY AND CONCLUSIONS

5.1 Summary

The present study was conducted to investigate the use of synthesized GNS for adsorption of selected halogenated compounds and emerging contaminants from water. GNS that we synthesized can suspend very well in water for months. The debromination process was observed for the brominated compound using GNS. The main objective of the present work was to understand the adsorption of halogenated compounds at GNS-water interface is important to assess the potential of GNS as an adsorbent in the water system to analyze its environmental impact. TBBPA is considered as a major environmental emerging contaminant due to its parent compound and its transformation products causing impacts on the ecosystem and human health, in this study we reveal the reducing activity of GNS for the debromination of TBBPA and its effect on adsorption capacity. We have studied a wide range of halogenated compounds and its adsorption capacity towards GNS, considering the kinetics, isotherms (Langmuir and Freundlich) and thermodynamic activity (15,25 and 35°C). These findings emphasize that when graphene-based nanomaterials are used for sorption studies of halogenated compounds more attention should be considered on estimating the adsorption capacity.

5.2 Conclusions

5.2.1 Interaction of GO NPs with emerging contaminants and some common phenolic compounds in a water matrix

- The adsorption kinetics of these seven PCs including emerging and conventional contaminants on GO in aqueous solutions was described by the second-order model better than the first-order one.
- It also indicated the equilibrium time around 5-10 hrs. The maximum adsorption capacity of these seven PCs on GO nanoflakes was around 19-23 mg/g in our studied concentration range, which was around twice that measurements in the literature.

- Adsorption isotherms of these PCs on GO were fitted by Langmuir model well. Adsorption mechanism of PCs on GO was mainly dominated by Van der Waals force and π - π interaction. The interaction of hydrogen-bond donor and acceptor (HDA) also contributed the adsorption since GO had oxygen-carrying functional groups.
- Due to these specific and non-specific interaction forces, the equilibrium adsorption amount was similar to expect TBBPA. TBBPA has the highest hydrophobicity, strong π - π interaction, and HDA ability from its two hydroxyl functional groups.
- Since the high stability of GO nanoflakes in water could increase the hazardous potential once organic contaminants such as ECs adsorbed on them, these better understandings of their adsorption behaviors can facilitate the fate prediction of organic contaminants in the aquatic environment. Finally, we compared the results of our study with the others stated in the literature for the removal of phenolic compounds, which was satisfactory with the conditions and operating system.

5.2.2 The reactivity of Graphene Oxide and Reduced Graphene Oxide toward Tetrabromobisphenol A, Bisphenol A, and Phenol from Water.

- GO nanoflakes and reduced graphene oxide that varied in C/O were successfully synthesized via a modified Hummers method and a thermal method.
- The adsorption kinetics of phenol, BPA, and TBBPA onto GO and rGO in aqueous solutions was described pseudo-second-order model better than pseudo-first-order one.
- The equilibrium time only needed around 5-10 hrs. The maximum adsorption capacity on GO nanoflakes was around 10-15 mg/g and rGO was around 8-18 mg/g in our studied concentration range.
- Adsorption isotherms of these organic contaminants on GO and rGO were fitted by the Langmuir model well. The slight more adsorption of phenol, BPA and TBBPA on rGO than GO was observed.
- The adsorption of these three phenolic compounds on GO and rGO slight

increased with the temperature.

- Thermodynamic parameters such as the Gibbs free energy around -18.6~21.3 kJ/mol indicated the spontaneous adsorption process with a small change in entropy. From the heat of adsorption, we studied around 2.3~11.8 kJ/mol, endothermic reactions of physical adsorption for three compounds were found for both GO and rGO.
- The main mechanisms governing the adsorption uptakes are the hydrogen bonding and the $\pi - \pi$ interaction between emerging contaminants. These better understandings of the adsorption of these emerging contaminants on graphene-based materials can facilitate the prediction of the fate of these chemicals in the environment and the design for their treatments.

5.2.3 Investigate the debromination of TBBPA by graphene-based materials

- Graphene family nanomaterials are gaining potential application as a novel material for various environmental applications due to its exceptional properties. Graphene based nanomaterials are found to possess catalytic activity in the natural environment.
- Both graphene oxide and reduced graphene oxide showed the dechlorination of 1,1,2,2-tetrachloroethane in water. In addition, both GO and rGO have been identified to show debromination activity towards TBBPA. The catalytic reaction will undoubtedly alter the environmental toxicity and fate of the pollutant and affect the risk of both graphene based material and the pollutant.
- To the best of our knowledge, this is the first work reporting the use of graphene based nanoparticles without doping of metal for complete debromination to obtain BPA. The results obtained in this study open a new possibility that degradation fraction must also be considered along with adsorption.
- Graphene based nanomaterials are found to possess catalytic activity in the natural environment. The present study demonstrates the role of novel GO and rGO as redox indicator for the complete debromination of TBBPA. It

was found that both GO and rGO increased the reduction rate of TBBPA under aerobic conditions.

- The catalytic reaction also opens up a new avenue for the development of carbon-based material as a metal-free catalyst for TBBPA debromination. The optimal removal conditions were explored as pH-5.5, catalyst dose: 15mg/L. Under this optimal condition, TBBPA were almost removed within 240min
- It was confirmed that the debromination activity of TBBPA was due to the presence of radical scavengers on the surface of GBMs. The results presented in this study will open a new possibility to consider degradation fraction along with adsorption. Furthermore, this study also provides an alternative for the efficient degradation of halogenated organic compounds.
- Furthermore, graphene based nanoparticles could be recycled, reused, and retained 90% removal efficiency after five cycles, suggesting their great potential for use in pollution treatments.

5.3 Scope for Future Research

The present work focuses on the adsorption of selected halogenated compounds on graphene nanomaterials in aqueous media. In the future, this work can be extended in considering the various environmental factors and also studying the debromination effect on similar brominated compounds.

- Desorption of the halogenated compounds considering various environmental factors such as pH, ionic strength and natural organic matter.
- Debromination behavior of graphene-based nanomaterials towards brominated compounds under dark and light conditions (2-bromophenol, 4-bromophenol, and chlorophenol)
- Toxicity studies

REFERENCES

- Ali, Alharbi, Tkachev, Galunin, Burakov, & Grachev. (2018). "Water treatment by new-generation graphene materials: hope for bright future". *Environmental Science and Pollution Research*, 25(8), 7315-7329.
- Apul, Wang, Zhou, & Karanfil. (2013). "Adsorption of aromatic organic contaminants by graphene nanosheets: comparison with carbon nanotubes and activated carbon". *Water Research*, 47(4), 1648-1654.
- Bele, Samanidou, & Deliyanni. (2016). "Effect of the reduction degree of graphene oxide on the adsorption of Bisphenol A". *Chemical Engineering Research and Design*, 109(9), 573-585.
- Bhagobaty, & Malik. (2007). "Microbial Degradation of Organophosphorous Pesticide : Chlorpyrifos ". *Internet Journal of Microbiology*, 4(1), 1-13.
- Bustos-ramirez, Barrera-diaz, Icaza, Martínez-hernández, & Velasco-santos. (2015). "Photocatalytic Activity in Phenol Removal of Water from Graphite and Graphene Oxides : Effect of Degassing and Chemical Oxidation in the Synthesis Process". *Journal of Chemistry*, 8(1), 1-10.
- Cai, & Larese-casanova. (2014). "Sorption of carbamazepine by commercial graphene oxides : A comparative study with granular activated carbon and multiwalled carbon nanotubes". *Journal of Colloid and Interface Science*, 426(5), 152-161.
- Catherine, Ou, Manu, & Shih. (2018). "Adsorption mechanism of emerging and conventional phenolic compounds on graphene oxide nanoflakes in water". *Science of The Total Environment*, 635(10), 629-638.
- Chen, & Chen. (2015). "Macroscopic and Spectroscopic Investigations of the Adsorption of Nitroaromatic Compounds on Graphene Oxide, Reduced Graphene Oxide, and Graphene Nanosheets". *Environmental Science and Technology*, 49(10), 6181-6189.
- Chowdhury, Duch, Mansukhani, Hersam, & Bouchard. (2013). "Colloidal properties and stability of graphene oxide nanomaterials in the aquatic environment". *Environmental Science & Technology*, 47(12), 6288-6296.
- Chowdhury, Mansukhani, Guiney, Hersam, & Bouchard. (2015a). "Aggregation and Stability of Reduced Graphene Oxide : Complex Roles of Divalent Cations , pH , and Natural Organic Matter". *Environmental Science and Technology*, 49(11), 10886-10893.
- Chowdhury, Mansukhani, Guiney, Hersam, & Bouchard. (2015b). "Aggregation and Stability of Reduced Graphene Oxide : Complex Roles of Divalent Cations , pH , and Natural Organic Matter". *Environmental Science & Technology*, 49(11), 10886-10893.

- De Gisi, Lofrano, Grassi, & Notarnicola. (2016). "Characteristics and adsorption capacities of low-cost sorbents for wastewater treatment: A review". *Sustainable Materials and Technologies*, 3(9), 10-40.
- Dimiev, & Tour. (2014). "Mechanism of Graphene Oxide Formation". *ACS Nano*, 8(3), 3060-3068.
- Fan, Zhao, Liu, & Shen. (2017). "Adsorption Characteristics of Chlorophenols from Aqueous Solution onto Graphene". *Journal of Chemical Engineering Data*, 10(62), 1099–1105.
- Fang, Liu, Xu, Li, Huang, & Li. (2019). "Enhanced debromination of tetrabromobisphenol a by zero-valent copper-nanoparticle-modified green rusts". *Environmental Science Nano*, 6(3), 970-980.
- Gao, Alemany, Ci, & Ajayan. (2009). "New insights into the structure and reduction of graphite oxide". *Nature Chemistry*, 1(5), 403-408.
- Gao, Li, Zhang, Huang, Hu, Shah, & Su. (2012). "Adsorption and removal of tetracycline antibiotics from aqueous solution by graphene oxide". *Journal of Colloid Interface Science*, 368(1), 540-546.
- Ghosal, & Sarkar. (2018). "Biomedical Applications of Graphene Nanomaterials and Beyond". *ACS Biomaterials Science & Engineering*, 4(8), 2653-2703.
- Gogoi, Mazumder, Tyagi, Tushara Chaminda, An, & Kumar. (2018). "Occurrence and fate of emerging contaminants in water environment: A review". *Groundwater for Sustainable Development*, 6(3), 169-180.
- Hamdaoui, & Naffrechoux. (2009). "Adsorption kinetics of 4-chlorophenol onto granular activated carbon in the presence of high frequency ultrasound". *Ultrasonics Sonochemistry*, 16(1), 15-22.
- He, Kim, Wamer, Melka, Callahan, & Yin. (2014). "Photogenerated charge carriers and reactive oxygen species in ZnO/Au hybrid nanostructures with enhanced photocatalytic and antibacterial activity". *Journal of American Chemical Society*, 136(2), 750-757.
- Jackson, Jacobsen, Baun, Birkedal, Kühnel, Jensen & Wallin. (2013). "Bioaccumulation and ecotoxicity of carbon nanotubes". *Chemistry Central*, 154(1), 1-21.
- Jiang, Liu, Zeng, Liu, Hu, Zhou & Wen. (2018). "Adsorption of estrogen contaminants (17B-estradiol and 17A-ethynylestradiol) by graphene nanosheets from water: Effects of graphene characteristics and solution chemistry". *Chemical Engineering Journal*, 2(1), 1231-1240.
- Johra, Lee, & Jung. (2014). "Facile and safe graphene preparation on solution based platform". *Journal of Industrial and Engineering Chemistry*, 20(5), 2883-2887.

- Joseph, Zaib, Khan, Berge, Park, Saleh, & Yoon. (2011). "Removal of bisphenol A and 17 α -ethinyl estradiol from landfill leachate using single-walled carbon nanotubes". *Water Research*, 45(13), 4056-4068.
- Kamila Mijowska. (2017). "Rootstock effects on polyphenol content in grapes of 'Regent' cultivated under cool climate condition". *Journal of Applied Botany and Food Quality*, 90(2), 158-174.
- Kang, Zhu, Guo, Shi, Wu, & Wei. (2018). "Efficient debromination of Tetrabromobisphenol A (TBBPA) by Au/Fe@biocarbon derived from bioreduction precious metals". *Chemical Engineering Journal*, 334(2), 99-107.
- Kashyap, Mishra, & Behera. (2014). "Aqueous Colloidal Stability of Graphene Oxide and Chemically Converted Graphene". *Journal of Nanoparticles*, 665(8), 1-6.
- Khairir, Hussin, Nasir, Uz-Zaman, Abdullah, & Sabirin Zoofakar. (2015). "Study of Reduced Graphene Oxide for Trench Schottky Diode". *IOP Conference Series: Materials Science and Engineering*, 99 (6), 1-8.
- Kempiński, Łoś, Florczak, Kempinski, & Jurga. (2017). "EPR and Impedance Measurements of Graphene Oxide and Reduced Graphene Oxide". *Acta Physica Polonica A*, 132(1), 81-85.
- Konicki, Aleksandrak, Moszynski, & Mijowska. (2017). "Adsorption of anionic azo-dyes from aqueous solutions onto graphene oxide: Equilibrium, kinetic and thermodynamic studies". *Journal of Colloid and Interface Science*, 496(2), 188-200.
- Konkena, & Vasudevan. (2012). "Understanding Aqueous Dispersibility of Graphene Oxide and Reduced Graphene Oxide through pKa Measurements". *Journal of Physical Chemistry Letters*, 3(7), 867-872.
- Kozlov, Viñes, & Görling. (2012). "On the interaction of polycyclic aromatic compounds with graphene". *Carbon*, 50(7), 2482-2492.
- Kumar, Kumar, Anandan, Fernandes, Ayoko, & Biskos. (2014). "Engineered Nanomaterials: Knowledge Gaps in Fate, Exposure, Toxicity, and Future Directions". *Journal of Nanomaterials*, 2014(2), 1-16.
- Kwon, & Lee. (2015). "Bisphenol A adsorption using reduced graphene oxide prepared by physical and chemical reduction methods". *Chemical Engineering Research and Design*, 104(3), 519-529.
- Kyzas, Travlou, Kalogirou, & Deliyanni. (2013). "Magnetic Graphene Oxide: Effect of Preparation Route on Reactive Black 5 Adsorption". *Materials*, 6(4), 1360-1376.
- Lanphere, Luth, & Walker. (2013). "Effects of Solution Chemistry on the Transport of Graphene Oxide in Saturated Porous Media". *Environmental Science & Technology*, 47(9), 4255-4261.

- Li, Chen, Zhang, Li, Wang, & Chen. (2016). "Enhanced dehydrochlorination of 1,1,2,2-tetrachloroethane by graphene-based nanomaterials". *Environmental Pollution*, 214(3), 341-348.
- Li, Du, Liu, Sun, Jiao, Xia & Wu. (2012). "Equilibrium, kinetic and thermodynamic studies on the adsorption of phenol onto graphene". *Materials Research Bulletin*, 47(8), 1898-1904.
- Li, Wang, Allinson, Li, & Xiong. (2009). "Risk assessment of heavy metals in soil previously irrigated with industrial wastewater in Shenyang ,China". *Journal of Hazardous Materials*, 161(1), 516-521.
- Liang, Jiao, Jaroniec, & Qiao. (2012). "Sulfur and nitrogen dual-doped mesoporous graphene electrocatalyst for oxygen reduction with synergistically enhanced performance". *Angewandte Chemie*, 51(46), 11496-11500.
- Lin, Ding, & Huang. (2012). "Debromination of Tetrabromobisphenol A by Nanoscale Zerovalent Iron: Kinetics, Influencing Factors, and Pathways". *Industrial & Engineering Chemistry Research*, 51(25), 8378-8385.
- Lin, Liu, & Gan. (2009). "Reaction of Tetrabromobisphenol A (TBBPA) with Manganese Dioxide: Kinetics, Products, and Pathways". *Environmental Science & Technology*, 43(12), 4480-4486.
- Liu, Zhao, Wang, Du, & Xing. (2014). "Effects of solution chemistry on adsorption of selected pharmaceuticals and personal care products (PPCPs) by graphenes and carbon nanotubes". *Environmental Science & Technology*, 48(22), 13197-13206.
- Lo, Martí, Arias-este, Mejuto, & García. (2008). "The mobility and degradation of pesticides in soils and the pollution of groundwater resources". *Agricultural, Ecosystem & Environment*, 123(4), 247-260.
- Lu, Wang, & Chen. (2018). "Adsorption and desorption of phthalic acid esters on graphene oxide and reduced graphene oxide as affected by humic acid". *Environmental Pollution*, 232(2), 505-513.
- Lv, Han, Huang, Luo, Cao, & Zhang. (2018). "Relationship between Molecular Components and Reducing Capacities of Humic Substances". *ACS Earth and Space Chemistry*, 2(4), 330-339.
- M. D, S, & Gnanamani. (2018). "Preparation, characterization and reusability efficacy of amine-functionalized graphene oxide-polyphenol oxidase complex for removal of phenol from aqueous phase". *RSC Advances*, 8(67), 38416-38424.
- Maiti, Tong, Mou, & Yang. (2018). "Carbon-Based Nanomaterials for Biomedical Applications: A Recent Study". *Frontiers in Pharmacology*, 9(5), 1401-1416.
- Maliyekkal, Sreeprasad, & Krishnan. (2013). "Graphene : A Reusable Substrate for Unprecedented Adsorption of Pesticides". *Small*, 23(1), 273-283.

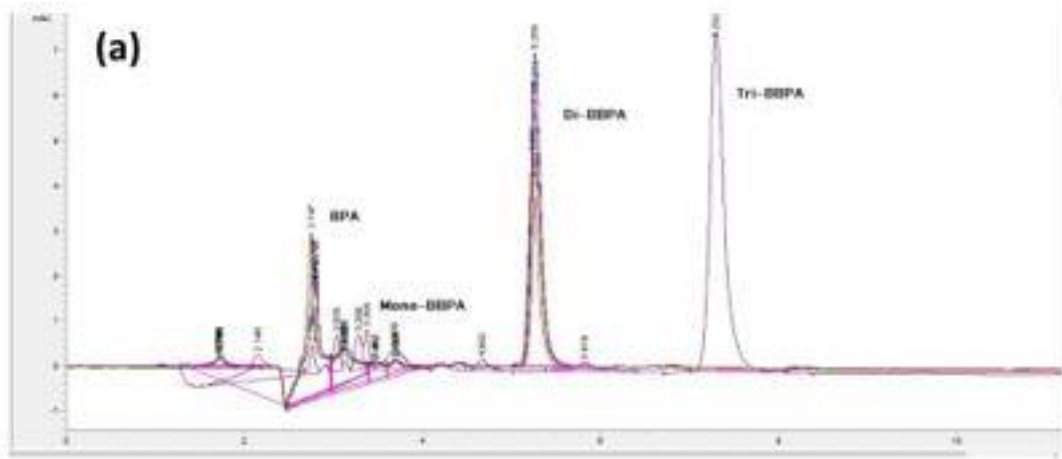
- Meyer, Sundaram, Chuvilin, Kurasch, Burghard, Kern, & Kaiser. (2010). "Atomic Structure of Reduced Graphene Oxide Cristina Go". *Nano Letters*, 10(4), 1144-1148.
- Oliva-Teles, Delerue-Matos, & Alvim-Ferraz. (2005). "Determination of free furfuryl alcohol in foundry resins by chromatographic techniques". *Analytica Chimica Acta*, 537(1-2), 47-51.
- Park, & Ruoff. (2009). "Chemical methods for the production of graphenes". *Nature Nanotechnology*, 4(3), 45-47.
- Peng, Tian, Liu, & Jia. (2017). "Degradation of TBBPA and BPA from aqueous solution using organo-montmorillonite supported nanoscale zero-valent iron". *Chemical Engineering Journal*, 309(2), 717-724.
- Perreault, Faria, & Elimelech. (2015a). "Environmental applications of graphene-based nanomaterials". *Chemical Society Review* 10(8), 1-12.
- Perreault, Faria, & Elimelech. (2015b). "Environmental applications of graphene-based nanomaterials". *Chemical Society Review* 8(12), 1-12.
- Perumbilavil, Sankar, Priya Rose, & Philip. (2015). "White light Z-scan measurements of ultrafast optical nonlinearity in reduced graphene oxide nanosheets in the 400–700 nm region". *Applied Physics Letters*, 107(5), 1-13.
- Phatthanakittiphong, & Seo. (2016). "Characteristic Evaluation of Graphene Oxide for Bisphenol A Adsorption in Aqueous Solution". *Nanomaterials*, 6(128), 2-17.
- Qiu, Wang, Owens, Kulaots, Chen, Kane, & Hurt. (2014). "Antioxidant chemistry of graphene-based materials and its role in oxidation protection technology". *Nanoscale*, 6(20), 11744-11755.
- Ramesha, Kumara, Muralidhara, & Sampath. (2011). "Graphene and graphene oxide as effective adsorbents toward anionic and cationic dyes". *Journal of Colloid And Interface Science*, 361(1), 270-277.
- Ratola, Cincinelli, Alves, & Katsoyiannis. (2012). "Occurrence of organic microcontaminants in the wastewater treatment process. A mini review". *Journal of Hazardous Materials*, 239-240(7), 1-18.
- Ren, Ren, Teng, Li, & Li. (2015). "Time-dependent effect of graphene on the structure, abundance, and function of the soil bacterial community". *Journal of Hazardous Materials*, 297(5), 286-294.
- Richardson, & Ternes. (2018). "Water Analysis: Emerging Contaminants and Current Issues". *Analytical Chemistry*, 90(1), 398-428.
- Rivera-utrilla, Sánchez-polo, Ferro-garcía, & Prados-joya. (2013). "Pharmaceuticals as emerging contaminants and their removal from water. A review". *Chemosphere* 93(7), 1268-1287.

- Sahu, Bindumadhavan, & Doong. (2017). "Boron-doped reduced graphene oxide-based bimetallic Ni/Fe nanohybrids for the rapid dechlorination of trichloroethylene". *Environmental Science: Nano*, 4(3), 565-576.
- Santhosh, Nivetha, Kollu, Srivastava, Sillanpaa, Grace, & Bhatnagar. (2017). "Removal of cationic and anionic heavy metals from water by 1D and 2D-carbon structures decorated with magnetic nanoparticles". *Scientific Reports*, 7(1), 14107-14112.
- Seabra, Rai, & Durán. (2013). "Nano carriers for nitric oxide delivery and its potential applications in plant physiological process: A mini review". *Journal of Plant Biochemistry and Biotechnology*, 23(1), 1-10.
- Song, Gan, Zhang, Xiao, Kuang, & Li. (2010). "Total phenolic contents and antioxidant capacities of selected chinese medicinal plants". *International Journal of Molecular Science*, 11(6), 2362-2372.
- Sotirelis & Constantinos V. Chrysikopoulos (2016). "Heteroaggregation of graphene oxide nanoparticles and kaolinite colloids Heteroaggregation of graphene oxide nanoparticles and kaolinite colloids". *Science of the Total Environment*, 579(5), 736-744.
- Su, Tong, Huang, Chen, Liu, Gao & Xing. (2018). "Green Algae as Carriers Enhance the Bioavailability of (14)C-Labeled Few-Layer Graphene to Freshwater Snails". *Environmental Science & Technology*, 52(3), 1591-1601.
- Taha, Gupta, Khoiroh, & Lee. (2011). "Interactions of Biological Buffers with Macromolecules: The Ubiquitous "Smart" Polymer PNIPAM and the Biological Buffers MES, MOPS, and MOPSO". *Macromolecules*, 44(21), 8575-8589.
- Terzić, Senta, Ahel, Gros, Petrović, Barcelo & Jabučar. (2008). "Occurrence and fate of emerging wastewater contaminants in Western Balkan Region". *Science of The Total Environment*, 399(1), 66-77.
- Thirumal, Pandurangan, Jayavel, & Ilangovan. (2016). "Synthesis and characterization of boron doped graphene nanosheets for supercapacitor applications". *Synthetic Metals*, 220(6), 524-532.
- Wang, Chang, & Zhi. (2011). "High yield production of graphene and its improved property in detecting heavy metal ions". *New Carbon Materials*, 26(1), 31-35.
- Wang, Chen, & Chen. (2014). "Adsorption of polycyclic aromatic hydrocarbons by graphene and graphene oxide nanosheets". *Environmental Science & Technology*, 48(9), 4817-4825.
- Wang, Gao, Wang, & Gao. (2014). "Novel graphene oxide sponge synthesized by freeze-drying process for the removal of 2,4,6-trichlorophenol". *RSC Advances*, 4(101) 57476-57482.

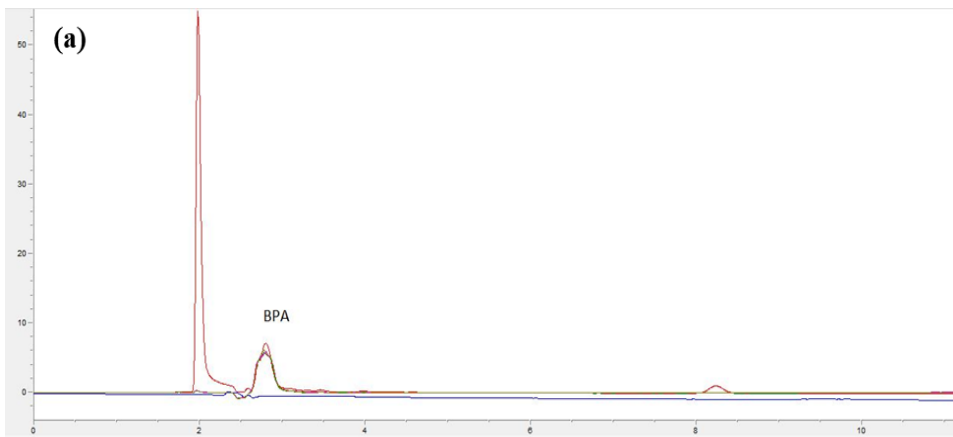
- Wu, Yuan, Zhong, Wang, & Zeng. (2016). "Enhanced adsorptive removal of p-nitrophenol from water by aluminum metal – organic framework / reduced graphene oxide composite". *Scientific Reports*, 25638 (6), 1-13.
- Wu, Zhong, Yuan, Wang, Wang, Chen & Wu. (2014). "Adsorptive removal of methylene blue by rhamnolipid-functionalized graphene oxide from wastewater". *Water Research*, 67(15), 330-334.
- Xu, Wang, & Zhu. (2012). "Decontamination of Bisphenol A from Aqueous Solution by Graphene Adsorption". *Langmuir*, 28(22), 8418-8425.
- Yang, Chen, Chang, Cao, Liu, & Wang. (2011). "Removal of methylene blue from aqueous solution by graphene oxide". *Journal of Colloid And Interface Science*, 359(1), 24-29.
- Ye, Wang, Wang, Fang, & Wang. (2018). "Aqueous aggregation and stability of graphene nanoplatelets, graphene oxide, and reduced graphene oxide in simulated natural environmental conditions: complex roles of surface and solution chemistry". *Environmental Science Pollution Research*, 25(11), 10956-10965.
- Young Ku & lee. (2000). "Removal of phenols from aqueous solution by XAD-4 resin". *Journal of Hazardous Materials*, 20(2), 58-68.
- Yu, & Han. (2014a). "Adsorption of tetracycline from aqueous solutions onto multi-walled carbon nanotubes with different oxygen contents". *Scientific Reports*, 5312(4), 1-8.
- Yu, & Han. (2014b). "Adsorption of tetracycline from aqueous solutions onto multi-walled carbon nanotubes with different oxygen contents". *Scientific Reports*, 5312(4), 1-8.
- Yu, Huang, Deng, Ju, Ren, Xiang & Li. (2017a). "Synthesis of millimeter-scale sponge Fe / Cu bimetallic particles removing TBBPA and insights of degradation mechanism". *Chemical Engineering Journal*, 325(1), 279-288.
- Yu, Huang, Deng, Ju, Ren, Xiang & Li. (2017b). "Synthesis of millimeter-scale sponge Fe/Cu bimetallic particles removing TBBPA and insights of degradation mechanism". *Chemical Engineering Journal*, 325 (1), 279-288.
- Yuan, Yu, & Li. (2014). "Effective adsorption of 2, 4-dichlorophenol on hydrogenated graphene : kinetics and isotherms". *Chinese Science Bulletin*, 59(34), 4752-4757.
- Yuan, Yu, Li, & Quan. (2014). "Effective adsorption of 2,4-dichlorophenol on hydrogenated graphene: kinetics and isotherms". *Chinese Science Bulletin*, 59(34), 4752-4757.
- Zhang, Chen, Hu, Fang, Cheng, & Chen. (2018). "Adsorption characteristics of tetrabromobisphenol A onto sodium bisulfite reduced graphene oxide aerogels ". *Colloids and Surfaces A: Physicochemical and Engineering Aspects*, 538(5), 781-788.

- Zhang, Chen, Zhou, Wu, Zhao, Lai & Li. (2019). "Efficient electrochemical degradation of tetrabromobisphenol A using MnO₂/MWCNT composites modified Ni foam as cathode: Kinetic analysis, mechanism and degradation pathway". *Journal of Hazardous Materials*, 369(4), 770-779.
- Zhang, Huang, Zhang, Yu, Deng, & Yu. (2012). "Mechanochemical degradation of tetrabromobisphenol A : Performance , products and pathway". *Journal of Hazardous Materials*, 243(9), 278-285.
- Zhang, Tang, Li, & Yu. (2013). "Sorption and removal of tetrabromobisphenol A from solution by graphene oxide". *Chemical Engineering Journal*, 222(5), 94-100.
- Zhao, Li, Ren, Chen, & Wang. (2011). "Few-Layered Graphene Oxide Nanosheets As Superior Sorbents for Heavy Metal Ion Pollution Management". *Environmental Science & Technology* 45(24), 10454-10462.
- Zhao, Wang, White, & Xing. (2014). "Graphene in the Aquatic Environment : Adsorption , Dispersion , Toxicity and Transformation Graphene in the Aquatic Environment : Adsorption , Dispersion , Toxicity and Transformation". *Environmental Science & Technology*, 48(17), 9995-10009.
- Zhao, Wen, Chen, & Wang. (2012). "Synthesis of graphene-based nanomaterials and their application in energy-related and environmental-related areas". *RSC Advances*, 2(22), 9286-9303.
- Zhong, Liang, Zhong, Zhu, & Zhu. (2012). "Heterogeneous UV / Fenton degradation of TBBPA catalyzed by titanomagnetite : Catalyst characterization, performance and degradation products". *Water Research*, 46(15), 4633-4644.
- Zhou, Apul, & Karanfil. (2015). "Adsorption of halogenated aliphatic contaminants by graphene nanomaterials". *Water Research*, 79 (25), 57-67.
- Zhou, Zhong, Zhang, Hu, Wu, Koratkar, & Shi. (2017a). "Influence of releasing graphene oxide into a clayey sand: physical and mechanical properties". *RSC Advances*, 7(29), 18060-18067.
- Zhou, Zhong, Zhang, Hu, Wu, Koratkar, & Shi. (2017b). "RSC Advances In fl uence of releasing graphene oxide into a clayey sand : physical and mechanical properties". *RSC Advances*, 7(29), 18060-18067.
- Zhu, Liu, Liu, Zeng, & Jiang. (2017). "Adsorption of emerging contaminant metformin using graphene oxide". *Chemosphere*, 179(3), 20-28.

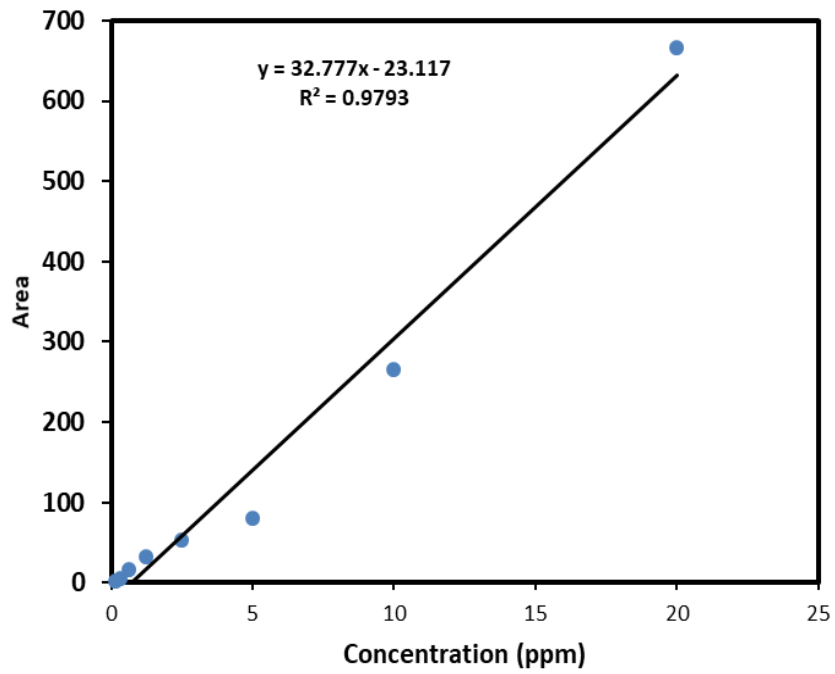
APPENDIX



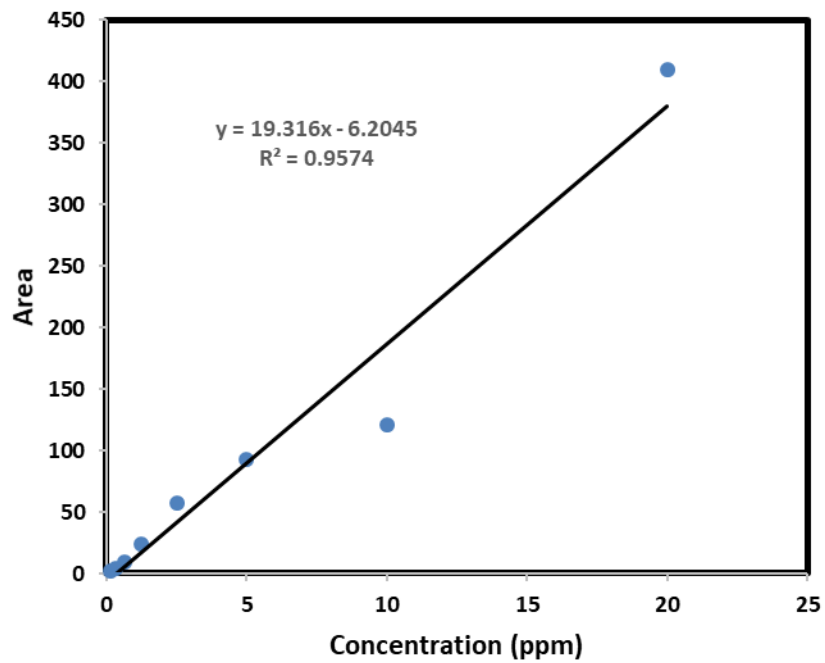
1. HPLC Chromatogram for various by-products after 4 hrs experiment



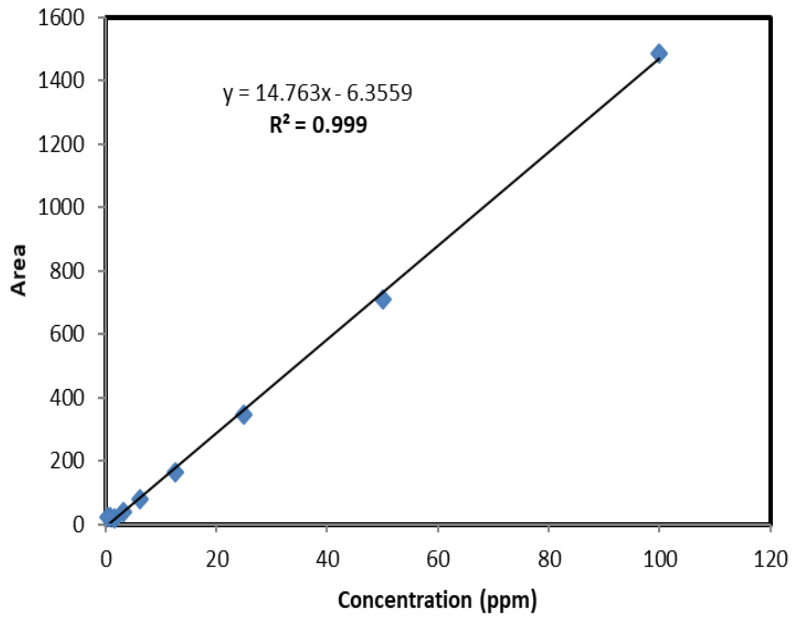
2. HPLC Chromatogram for BPA after 4 hrs experiment



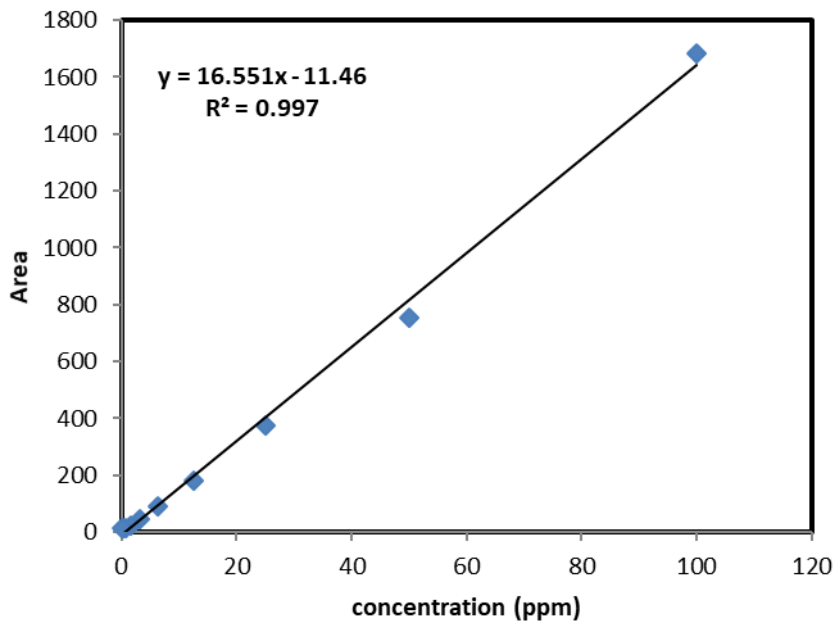
3. The plot of calibration curve for TBBPA



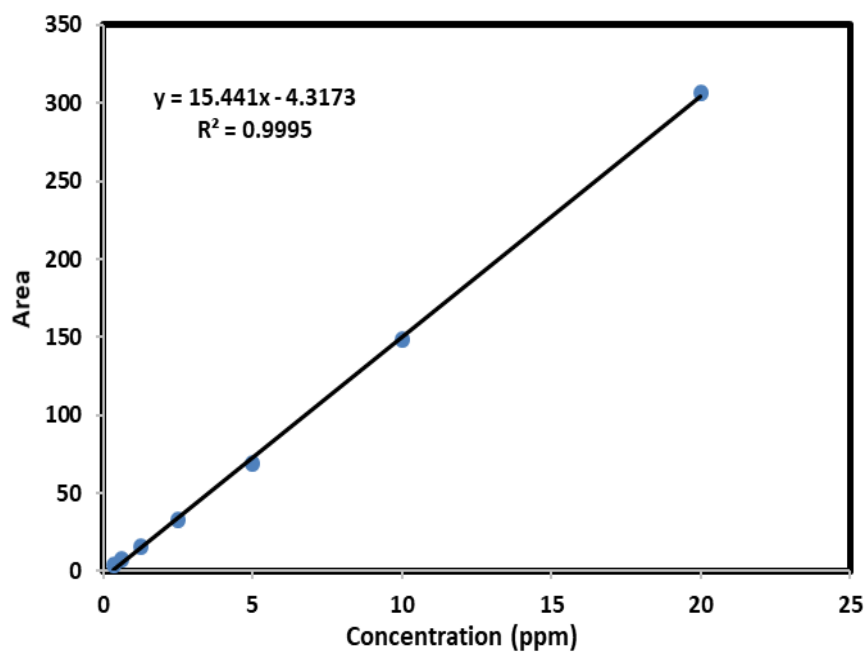
4. The plot of calibration curve for 4-NP



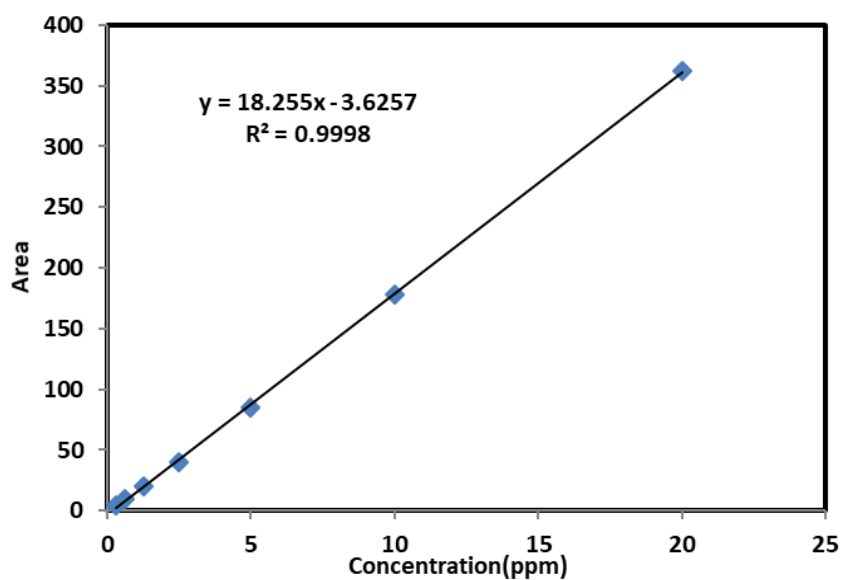
5. The plot of calibration curve for BPA



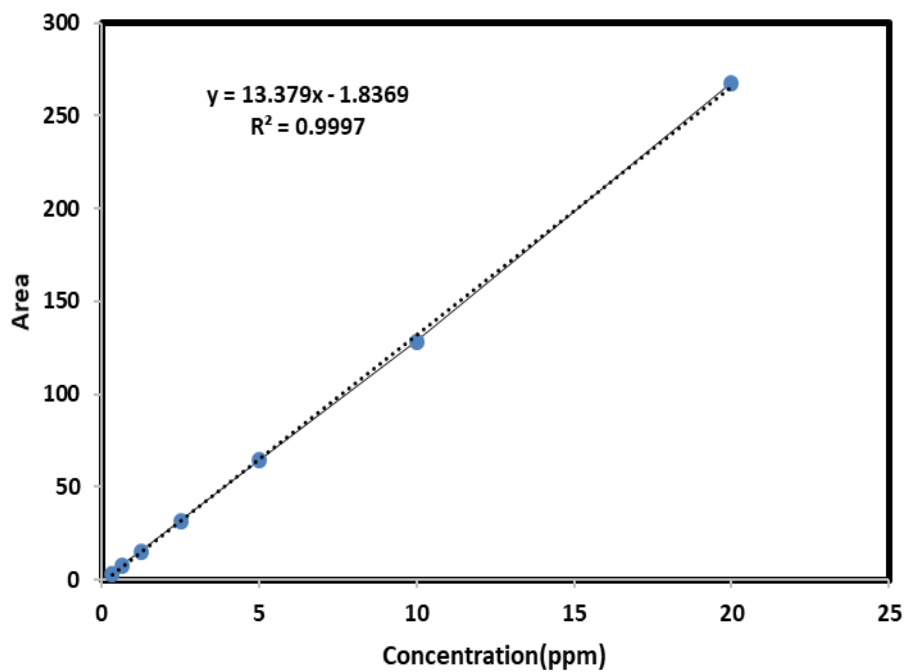
6. The plot of calibration curve for Phenol



7. The plot of calibration curve for 4-CP



8. The plot of calibration curve for 2,4-DCP



9. The plot of calibration curve for 2,4,6 -TCP

PUBLICATIONS BASED ON PRESENT WORK

Published

1. Hepsiba Catherine, Ming –Han Ou, Basavaraju Manu, and Yang-hsin Shih*, Adsorption Mechanism of Emerging and Conventional Phenolic Compounds on Graphene Oxide Nanoflakes in Water”, *Science of the Total Environment*, 2018, 635, 629-638. Environmental Sciences 22/229.

Submitted

1. Hepsiba Niruba Catherine, Ruey-an Doong, Basavaraju Manu and Yang-hsin Shih*, Surface Interaction of Tetrabromobisphenol A, Bisphenol A and phenol with Graphene-based Materials in Water: Reaction Mechanism and Thermodynamic Effects”. Submitted to *Journal of Environmental Management Under Review in Applied Nanoscience*.
2. Hepsiba Niruba Catherine, KUO Ta Fu Dave, Basavaraju Manu and Yang-hsin Shih* “Surface Interactions of Tetrabromobisphenol A with Graphene based Materials in Water: Reaction Mechanism and Thermodynamic Effects”.
Under review in Chemical Engineering Journal.

Conferences

1. Adsorption Mechanism of Emerging and Conventional Phenolic Compounds on Graphene Oxide Nanoflakes from Water Hepsiba Catherine, Basavaraju Manu, and Yang-hsin Shih, *page number:60, volume 3*. The 3rd International Conference on Emerging Contaminants.

Presentation: Oral

2. Reactivity of Graphene Oxide and Reduced Graphene Oxide toward Tetrabromobisphenol A, Bisphenol A, and Phenol from Water: Reaction Mechanism and Thermodynamic Effects Hepsiba Catherine*, Ming Chang, Ming-Han Ou, Ruey-an Doong, Basavaraj Manu and Yang-hsin Shih, *page number:77, volume*
3. The 3rd International Conference on Emerging Contaminants.

Presentation: Oral

3. Surface interactions of Tetrabromobisphenol A, Bisphenol A, and Phenol with Graphene-based materials in water: Reaction mechanism and thermodynamic effects Hepsiba Catherine, Tzu-Ho Chou, Basavaraj Manu and Yang-Hsin Shih, *page number:106, volume 10*. The 10th International Conference on Interfaces Against Pollution.

Presentation: Poster

4. Reactivity of Graphene Oxide and Reduced Graphene Oxide toward Tetrabromobisphenol A, Bisphenol A, and Phenol from Water: Reaction Mechanism and Thermodynamic Effects Hepsiba Catherine, Yi-Hsuan Lin, Yang-hsin Shih, and Basavaraj Manu , *page number: 87, volume 256*. 256th ACS National Meeting.

Presentation: Poster

Hepsiba Niruba Catherine.S

Phone: +886-933450102

E-mail: catherineenvi91@gmail.com

Education

Ph.D. (2015- 2019)

Doctorate of Philosophy(Ph.D.) in the Department of Civil Engineering at National Institute of Technology, Karnataka. India

THESIS: Evaluation of graphene oxide and reduced graphene oxide for the removal of selected halogenated phenols from water. **(GPA- 10.0/10.0)**

M.E (2012 – 2014)

Master of Environmental Engineering and Management (M.E) in Coimbatore Institute of Technology, Coimbatore, India.

THESIS: Biosorption of Nitrate from its aqueous solution onto Chrysopogon zizanioides (Vetiver). **(GPA- 8.45/10.0)**

B.E (2008 –2012)

Bachelor of Civil Engineering (B.E) in Sri Krishna Institute of Technology, Coimbatore, India.

THESIS: Experimental study of self-compacting concrete with partial replacement of cement by silica fume. **(GPA- 8.23/10.0)**

Awards

- March 2019- October 2019 – Scholarship from Ministry of Science and Technology **(MOST) Taiwan.**
- July 2015 – February 2019 - Scholarship from Ministry of Human Resources and Development **(MHRD), India**
- July 2013 - May 2014 – Scholarship from Technical Education Quality Improvement Programme **(TEQUIP), India.**

Research experience

Research Assistant: March 2019- October 2019 at the Department of agricultural chemistry NTU, Taiwan, ROC.

Advisor: Prof. Yang Hsin Shih

- New Insights into developing metal free catalyst for degradation of emerging contaminants from aqueous solution
- Photocatalytic activity in comparison with solar radiation for degradation of bisphenol A (BPA) using graphene based nanomaterials.

Proposed the novel debromination activity of tetrabromobisphenol A (TBBPA) using the metal free catalyst (graphene oxide and reduced graphene oxide) in dark and studied the mechanism for the debromination process. Performed experiments to find the best strain of microbes for diesel degradation in the soil site Taiwan.

Ph.D. student: July 2015- February 2019 at National Institute of Technology Karnataka, Surathkal, Karnataka, India.

Advisor: Dr. B. Manu

- Studied the interaction of GO NPs with emerging contaminants and some common phenolic compounds in a water matrix.
- Performed the reactivity of Graphene Oxide and Reduced Graphene Oxide toward Tetrabromobisphenol A, Bisphenol A, and Phenol from Water.
- Investigate the debromination of TBBPA by graphene-based materials.

Research Assistant: (2014 -2015) IIT Madras (IITM)

- Preparing project reports, reviewing articles and writing book chapters.
- Organized materials and writing assignments for bachelor of technology (B. Tech) students for handling a course on life cycle assessment.

Key Deliverables:

- Planned, organized, wrote and edited operational procedures and manuals.
- Used photographs, drawings, animation and charts for better understanding.

Publications

1. **Hepsiba Niruba Catherine**, Ming – Han Ou, Basavaraju Manu, and Yang-hsin Shih*, Adsorption Mechanism of Emerging and Conventional Phenolic Compounds on Graphene Oxide Nanoflakes in Water “Science of the Total Environment, 2018, 635, 629-638. **IF: 5.58.**

Submitted

1. **Hepsiba Niruba Catherine**, Rama Shankar, Yang hsin Shih, “New insights into the degradation mechanism of tetrabromobisphenol A using metal free grapheme oxide”

Status: Under Review in Chemical Engineering Journal.

2. Rama Shanker Sahu, Tzu-Ho Chou, **Hepsiba Niruba Catherine**, Yu-huei Peng Chi-Fong Ko, Chih-ping Tso, Yuh-fan Su and Yang-hsin Shih: A review of Polybrominated diphenyl ethers (PBDEs); Terrestrial contamination; Microbial treatment; Oxidative treatment pathway.

Status: Under review in Journal of Hazardous Management.

Under Submission

1. **Hepsiba Niruba Catherine**, Basavaraj Manu, Ruey-an Doong and Yang-hsin Shih, “Surface Interaction of Tetrabromobisphenol A, Bisphenol A and Phenol with Graphene based Materials in Water: Adsorption Mechanism and Thermodynamic Effects”
2. Chia-Shen Yeh, Tzu-Ho Chou, **Hepsiba Niruba Catherine** and Yang-Hsin Shih: Synthesis, characterization and evaluation of the carboxymethyl cellulose mediated CaO₂ nanoparticles for stabilized oxygen release in bioremediation of diesel.
3. **Hepsiba Niruba Catherine**, Chien-Ying Yang, Ying-Jie Chang, and Yang-hsin Shih Carbonized agricultural waste to reduce the uptake of some chlorinated contaminants into crops.
4. **Hepsiba Niruba Catherine**, Chia-Wen Hsu and Ruey-an Doong: Boron doped reduced graphene oxide for capacitive deionization applications.
5. **Hepsiba Niruba Catherine**, Yen-Tung Yang and Ruey-an Doong: Fabrication of Cu⁰/TNT/rGO composite for photoelectrocatalytic degradation of Microcystin-LR.

Work Presented in Conference

1. **October 2017–EMCON International Conference, Taiwan, Oral Presentation.**

Hepsiba Catherine, Basavaraju Manu, Ming –Han Ou and Yang-hsin Shih, “Adsorption Mechanism of Emerging and Conventional Phenolic Compounds on Graphene Oxide Nano flakes in Water”.

2. October 2017 – EMCON International Conference Taiwan, Oral presentation.

Hepsiba Catherine, Basavaraju Manu, Lin, Yi-Hsuan, Ruey-an Doong and Yang- hsin Shih, “Reactivity of Graphene Oxide and Reduced Graphene Oxide toward Tetrabromobisphenol A, Bisphenol A, and Phenol from Water: Reaction Mechanism and Thermodynamic Effects”.

3. June 2018 –IAP International Conference, France, Poster Presentation.

Hepsiba Catherine, Tzu-Ho Chou and Yang-Hsin Shih

“Surface interactions of Tetrabromobisphenol A, Bisphenol A, and Phenol with Graphene based materials in water:Reaction mechanism and thermodynamic effects ”.

4. August 2018 –ACS National meeting, Boston USA, Poster Presentation

Hepsiba Catherine, Yi-Hsuan Lin, Yang-hsin Shih and Basavaraj Manu Reactivity of Graphene Oxide and Reduced Graphene Oxide toward Tetrabromobisphenol A, Bisphenol A, and Phenol from Water: Reaction Mechanism and Thermodynamic Effects

Book Chapters

1. **Hepsiba Niruba Catherine** and Hari Mahalingam. Chapter 1: Applications of microalgae-based nanoparticles in environmental remediation. CRC press Taylor and Francis. (Accepted, in press).
2. **Hepsiba Niruba Catherine**, Rama Shanker sahu and Yang-Hsin Shih Chapter 9: Effects of nanoparticles on the biodegradation of organic materials. Elsevier (Under submission)